

**Modulation of Monocyte, Macrophages and Dendritic Cells by  
GM-CSF after Hemorrhagic Shock and during  
Polymicrobial Sepsis**

Inaugural-Dissertation

Zur

Erlangung des Doktorgrades

**Dr. rer. nat.**

des Fachbereichs

Bio- und Geowissenschaften, Landschaftsarchitektur

an der

Universität Duisburg-Essen

vorgelegt von

**Rani Meenakshi**

aus Haryana, India

August, 2006

**Modulation of Monocyte, Macrophages and Dendritic Cells by  
GM-CSF after Hemorrhagic Shock and during  
Polymicrobial Sepsis**

**Inaugural-Dissertation**

For Application for  
Doctor's Degree in natural sciences

**Dr. rer. nat.**

in the faculty of  
Biology, Geology and Landscape-architecture  
of the  
University of Duisburg-Essen

Presented by

**Rani Meenakshi**

From Haryana, India

August, 2006

Die der vorliegenden Arbeit zugrundeliegenden Experimente wurden in der AG Chirurgische Forschung-Unfallchirurgie, Klinik für Unfallchirurgie, Universität Duisburg-Essen durchgeführt.

1. Gutachter: Prof. Dr. rer. nat. Fritz Ulrich Schade

2. Gutachter: Prof. Dr. A. Ehrenhofer-Murray

Vorsitzender des Prüfungsausschusses: Prof. Dr. B. Sures

Tag der mündlichen Prüfung: 21. Feb.2007

*Dedicated*  
*to*  
*My Parents*

---

## Acknowledgements

Words are never enough to express heart-felt gratitude.

It is my privilege to express my sincere gratitude to **Priv.-Doz. Dr. Med. Sascha Flohé** and **Dr. rer. nat. Stefanie Flohé**, my immediate supervisors, for their active co-operation, excellent direction, helpful suggestions, fruitful discussions, careful effective critique and above all for their ready accessibility during the course of my study.

I am extremely thankful to **Prof. Fritz Ulrich Schade** for giving me the opportunity to do the interesting research in his group, for his valuable encouragement and parental guidance not only throughout the Ph.D. research work but also during my life in Germany. A noble man with a considerate and kind-hearted attitude for all, he has always been a source of inspiration to me all along.

I wish to thank **Prof. Helmut Esche**, head of the Ph. D. committee, a gentle, compassionate, kind-hearted and benevolent person. He was for ever and a day tremendously supportive for providing all the essential information regarding the Ph.D. procedure and throughout my stay in Germany.

I also express my sincere thanks to **Prof. Ernst Kreuzfelder** and **Mrs. Bärbel Nyadu** for providing me the flowcytometry facility. I like to give

special thanks to **Mrs. Bärbel Nyadu** for her ready help and suggestions at the times of need.

I am also very thankful to all those people who willingly and gladly helped me in a different way by providing me blood samples for my work.

I would like to express my deep gratitude to **Priv.-Doz. Dr. Gero Hilken**, Head of the animal facility, a wonderful, generous, kind-hearted and magnificent friend who helped me by providing the animal facility. He also helped in all other possible ways during the years of my stay in Germany. I am also grateful to all other members of the animal facility who helped me during my project.

I give my deep, sincere and true regards to all the mice I used and euthanized during the course of my project. Without them, this work would not have been completed. May their souls rest in peace!

I also express thanks to my colleagues who are here, **Dr. rer. nat. Daniala Plitzko**, **Mr. Joerg-Martin Bangen**, **Mrs. Marion Frisch**, **Miss Michaela Gertz**, **Mrs. Katja Bergmann**, **Dr. Adam Peszko**, as well as who have left, **Dr. Sven Lendemans**, **Priv.-Doz. Dr. Taila Mattern**, **Dr. Baher Husain** and **Dr. Daniel Schmitz** for their help, experimental expertise and helpful suggestions. Here, I specially, wish to thank **Mrs. Marion Frisch**, a kind, caring, and helping friend, who helped me in finding this laboratory to do my research. She was always there selflessly and whole-heartedly with her helping hands all the time. I thank **Miss Michaela Gertz**, a very friendly and jolly person, for her excellent technical support during my work and also **Mr. Joerg-Martin Bangen** for his cooperative and friendly nature. They all

contributed their efforts to make the lab the best place to work. Again, many thanks to Marion and Michi (Michaela).

No words will be sufficient to express my appreciation and indebtedness to **Hemant Agrawal, Manoj Kumar, Aruna Goenka Agrawal** and **Miss Claudia Brockmann**, my very good friends, who were always by my side for helpful suggestions, morale boosting and encouragement. Wonderful friends who selflessly contributed in the completion of my work.

I also express thanks to all my other Indian friends, **Kunal, Amrit, Swarna, Aparna, Savita, Satyendra, Janapriya**, and others in Germany for always giving me feel at home and their care and help at different times.

Words fall short of gratitude, I owe to my parents for their encouragement and the confidence they have in me. My younger brothers **Kunal, Rahul, Siddhatha** and his wife **Meenakshi** have been a source of moral support, joy and happiness.

It is hard to express in word my feelings and gratitude, I love to acknowledge my life partner, my Husband, **Mr. Bijaya Kumar Parida**. His love, understanding and support always encourage me to the fulfillment of my goals. Without his support this work would not have seen the light of the day.

**Meenakshi Rani**

(August 06, 2006)

# Index

## Acknowledgements

## Abbreviations

i

<b>1.</b>	<b>Introduction</b>	<b>2</b>
1.1	Pathophysiology of hemorrhagic shock and sepsis	2
1.1.1	Hemorrhagic shock and sepsis	2
1.2	Immune response and overview of cytokines	3
1.3	Antigen presenting cells	7
1.3.1	Monocytes and macrophages	7
1.3.1.1	Signaling mechanism of monocytes and macrophages	7
1.3.2	Dendritic cells	10
1.3.2.1	Dendritic cells development	10
1.3.2.2	Antigen capture, migration and maturation of dendritic cells	10
1.3.2.3	Dendritic cells induced Th cell polarization	11
1.3.2.4	Dendritic cells during polymicrobial sepsis	12
1.3.2.5	Dendritic cell loss during sepsis	12
1.3.2.6	Dendritic cells characterization during sepsis	12
1.4	Scope and restoration response	14
1.4.1	GM-CSF in general	14
1.4.2	GM-CSF as an immunomodulator	14
1.4.3	Effect of GM-CSF on mature monocytes and macrophages	15
1.4.4	Signal cascade activated by GM-CSF	15
1.4.5	GM-CSF in shock, trauma and sepsis	17
1.4.5.1	GM-CSF in hemorrhagic shock	17
1.4.5.2	GM-CSF in sepsis	18
1.4.6	GM-CSF in other clinical applications	19
1.5	Aim of study	20

<b>2.</b>	<b>Materials and methods</b>	<b>23</b>
2.1	Chemicals, Reagents and Antibodies	23
2.1.1	Chemicals	23
2.1.2	Reagents	24
2.1.3	Antibodies	25
2.2	Culture media, Buffers and Solutions	26
2.2.1	Culture media	26
2.2.2	Buffers and Solutions	26
2.2.2.1	Cell isolation and culture	26
2.2.2.2	Automated magnetic cell sorting (autoMACS)	26
2.2.2.3	SDS-PAGE, Western Blotting and EMSA	26
2.3	Cell culture methods	28
2.3.1	Human models	28
2.3.1.1	Healthy human subjects	28
2.3.2	Isolation and culture of various human cells	28
2.3.2.1	Isolation and culture of human peripheral blood mononuclear cells	28
2.3.2.2	Culture of human monocytic THP-1 cells	28
2.3.3	Mouse models	29
2.3.3.1	Mice	29
2.3.3.2	Hemorrhagic shock	29
2.3.3.3	Cecal ligation and puncture	30
2.3.3.4	Serum collection	31
2.3.4	Isolation, purification and culture of various murine cell types	31
2.3.4.1	Preparation and culture of peritoneal macrophages	31
2.3.4.1.1	Preparation of Bacteria	32
2.3.4.1.2	Macrophage viability test using MTT	32
2.3.4.2	Preparation and culture of total spleen cells	32
2.3.4.3	Preparation of lymph node cells	33
2.3.4.4	Generation and culture of mouse bone marrow cells	33

2.3.5	Isolation and purification of various cell types using automated magnetic cell sorting (auto-MACS)	34
2.3.5.1	Principle	34
2.3.5.2	Isolation of splenic dendritic cells and bone marrow derived dendritic cells	34
2.3.5.3	Isolation of splenic T cells	35
2.3.6	Labeling of cells	34
2.3.6.1	Carboxyfluorescein diacetate, succinimidyl ester labeling of T cells (Cell proliferation tracking by flow cytometry)	36
2.3.7	Analysis of cells (Flow Cytometry)	37
2.3.7.1	Principle	37
2.3.7.2	Cell surface and intracellular staining	38
2.3.7.3	Staining for <i>in vitro</i> and <i>in vivo</i> T cell proliferation assay	39
2.3.8	Cell proliferation assay	39
2.3.8.1	<i>In vitro</i> allogenic T cell assay	39
2.3.8.2	<i>In vivo</i> T cell assay	40
2.3.9	Enzyme linked immunosorbent assay	40
2.4	Protein Chemical Methods	41
2.4.1	Cytoplasmic and nuclear protein extraction	41
2.4.2	Determination of protein concentration	41
2.4.3	Sodium dodecyl sulfate polyacrylamide gel electrophoresis	41
2.4.4	Western blot analysis of MAPK and I $\kappa$ B $\alpha$	42
2.4.5	Electrophoretic mobility shift assay	43
2.4.5.1	Labelling of oligonucleotides	43
2.4.5.2	Binding reaction, gel run, transfer and detection of nuclear protein extracts	43
2.5	Statistical Analysis	44
<b>3.</b>	<b>Results</b>	<b>46</b>
3.1	Immunomodulation by GM-CSF	46
3.1.1	Immunomodulation by GM-CSF in human monocytes	46

3.1.1.1	Time and Dose kinetics for GM-CSF	46
3.1.1.2	Effect of GM-CSF on TNF- $\alpha$ and IL-8 secretion by human monocytes	47
3.1.1.3	Effect of GM-CSF priming on LPS-induced phosphorylation of I $\kappa$ B $\alpha$ and MAPKinases	48
3.1.1.4	Effect of GM-CSF on LPS-induced NF $\kappa$ B binding in the nucleus	49
3.1.2	Immunomodulation by GM-CSF in THP-1 monocytic cells	51
3.1.2.1	Time and Dose kinetics for GM-CSF	51
3.1.2.2	Effect of GM-CSF on TNF- $\alpha$ , IL-8 and IL-6 secretion by THP-1 cells	52
3.1.2.3	Effect of GM-CSF priming on LPS-induced phosphorylation of I $\kappa$ B $\alpha$ and MAPKinases by THP-1 cells	52
3.1.2.4	Effect of GM-CSF on LPS-induced NF $\kappa$ B binding in the nucleus	54
3.1.2.5	Effect of GM-CSF on translocation of NF $\kappa$ B-p50 and p65	54
3.1.3	Immunomodulation by GM-CSF after hemorrhagic shock	56
3.1.3.1	Effect of GM-CSF in normal peritoneal macrophages	56
3.1.3.1.1	Time kinetics for GM-CSF priming in normal mouse peritoneal macrophages	56
3.1.3.1.2	Effect of GM-CSF on TNF- $\alpha$ secretion in normal peritoneal macrophages	57
3.1.3.1.3	Effect of GM-CSF priming on LPS-induced phosphorylation of I $\kappa$ B $\alpha$ and MAPKinases on normal peritoneal macrophages	57
3.1.3.2	Effect of GM-CSF after hemorrhagic shock	59
3.1.3.2.1	Hemorrhagic shock model characterization	59
3.1.3.2.2	Cytokine response in peritoneal macrophages after hemorrhage	59
3.1.3.2.3	LPS-induced I $\kappa$ B $\alpha$ signaling after hemorrhage	60
3.1.3.2.4	LPS-induced ERK1/2 and p38 signaling after hemorrhage	61
3.1.3.2.5	GM-CSF preincubation enhanced the TNF- $\alpha$ production after hemorrhage	62
3.1.3.2.6	I $\kappa$ B $\alpha$ phosphorylation in GM-CSF primed macrophages after hemorrhage	63

3.1.3.2.7	P-ERK1/2 and P38 phosphorylation in GM-CSF primed macrophages after hemorrhagic shock	64
3.1.4	Immunomodulation by GM-CSF during polymicrobial sepsis	65
3.1.4.1	TNF- $\alpha$ secretion in splenic macrophages and dendritic cells	65
3.1.4.2	IL-12 secretion in splenic dendritic cells	67
3.1.4.3	Effect of GM-CSF on CD86 and CD40 on splenic DC	69
3.2	GM-CSF as a growth regulator	70
3.2.1	BMC loss during polymicrobial sepsis	70
3.2.2	Cell death during polymicrobial sepsis	71
3.2.3	Release of myeloid cells from bone marrow into the blood	73
3.2.3.1	Increased leukocyte count during polymicrobial sepsis	73
3.2.3.2	Elevated dendritic cell count during polymicrobial sepsis	73
3.2.3.3	Increased granulocyte and monocyte release during polymicrobial sepsis	74
3.2.4	Cell proliferation and DC composition during sepsis	75
3.2.4.1	Enhanced bone marrow cell proliferation during polymicrobial sepsis	75
3.2.4.2	DC population during polymicrobial sepsis	76
3.2.5	Cytokine secretion pattern during polymicrobial sepsis	78
3.2.5.1	Aberrant cytokine secretion pattern of BMDC during sepsis	78
3.2.5.1.1	Unchanged CD40, CD86 and MHC class II expression of BMDC during polymicrobial sepsis	80
3.2.5.2	Reduced cytokine secretion pattern of BMC during sepsis	81
3.2.6	T cell activation during polymicrobial sepsis	82
3.2.6.1	<i>In vitro</i> T cell-stimulatory capacity of BMDC during sepsis	82
3.2.6.1.1	Increased IFN- $\gamma$ secretion through neutralization of IL-10	85
3.2.6.2	<i>In vivo</i> T cell-stimulatory capacity of BMDC during sepsis	86
3.2.7	Different myeloid DC Progenitor during polymicrobial sepsis	88

<b>4.</b>	<b>Discussion</b>	91
<b>5.</b>	<b>Summary</b>	104
<b>6.</b>	<b>References</b>	107
<b>7.</b>	<b>Curriculum Vitae</b>	I
<b>8.</b>	<b>Publications</b>	II

## Abbreviations

APC	allophycocyanin
BCA	2,2'-bis(4-carboxyphenyl)-5,5'-bibenzimidazole
BrdU	bromodeoxyuridine
BM	bone marrow
BMDC	bone marrow derived dendritic cell
BSA	bovine serum albumin
CTL	cytotoxic T lymphocyte, CD8 <sup>+</sup> T cells
CD	cluster of differentiation
CSF	colony-stimulating factor
DMSO	dimethylsulfoxide
DNA	deoxyribonucleic acid
DTT	1,4-Dithiothreitol
EDTA	ethylenediaminetetraacetic acid
ELISA	enzyme linked immunosorbant assay
ERK	extracellular signal-regulated kinase
FACS	fluorescence activated cell sorting/scanning
FITC	fluorescein-isothiocyanate
FCS	fetal calf serum
G-CSF	granulocyte colony-stimulating factor
GM-CSF	granulocyte-macrophage-colony-stimulating factor
h	hour(s)
HEPES	<i>N</i> -(2-hydroxyethyl)-piperazine- <i>N'</i> -2-ethanesulfonic acid
HLA	human leukocyte antigen
IFN- $\gamma$	interferon gamma
Ig	immunoglobulin
i.p.	intraperitoneal
i.v.	intravenous
IL	interleukin

kD	kilodalton
LPS	lipopolysaccharide
MHC	major histocompatibility complex
MAPK	mitogen-activated protein kinase
min	minute(s)
NK cell	natural killer cell
PAGE	polyacrylamide gel electrophoresis
PBS	phosphate buffered saline
PE	phycoerythrin
PMSF	phenyl methyl sulfonyl fluoride
JNK/SAPK	c-jun kinase/stress activated protein kinase
SD	standard deviation
SDS	sodium dodecyl sulfate
SEM	standard error of mean (SD of the mean)
TBE	tris-borate-EDTA
TBS	tris buffered saline
TBST	tris buffered saline with Tween-20
T <sub>c</sub>	cytotoxic T cell
TEMED	<i>N,N,N',N'</i> -tetramethylethylenediamine
Th	helper T cell
Th1/Th2	Th cells from type 1/2
TNF	tumor necrosis factor
TRIS	tris (Hydroxymethyl)-aminomethane
VCAM	vascular cell adhesion molecule

# INTRODUCTION

---

# **1. Introduction**

## **1.1 Pathophysiology of hemorrhagic shock and sepsis**

### **1.1.1 Hemorrhagic shock and sepsis**

Hemorrhagic shock is commonly present in patients with multiple injuries in the early phase after trauma and represents one of the major pathophysiological events leading to a severe deterioration of the immune response. Hemorrhage is a condition with excessive external or internal blood loss [1, 2] and shock occurs when there is hypoperfusion of vital organs e.g. due to malfunction of the myocardium (cardiogenic shock), overwhelming infection leading to redistribution of circulating volume into the extravascular space (septic shock) or hypovolemia due to severe dehydration or hemorrhage (hypovolemic shock). Signs and symptoms of hemorrhagic shock vary depending on the volume and rate of blood loss [3]. Hemorrhagic shock leads to tissue hypoxia, acidosis, and the release of various mediators culminating the conditions to a systemic inflammatory response syndrome, SIRS [2, 4, 5]. SIRS can be due to infectious and non-infectious reasons. Along with hemorrhagic or hypovolemic shock, non-infectious conditions include trauma, burns and acute pancreatitis [6, 7]. SIRS with a documented systemic infection is termed as sepsis. Therefore, sepsis is defined as systemic inflammatory response syndrome (SIRS) along with an overt infection [8-10] which can be caused by invading bacterial, viral, fungal or parasitic microorganism itself or various products or features of the organism such as endotoxin (LPS), peptidoglycan (PGN) or lipoteichoic acid (LTA) or specific bacterial toxins [10]. This systemic inflammatory response involves immune cell dysregulation and a complex network of cytokines. A massive deterioration of the immune response during hemorrhage and sepsis occurs that may result in multi-organ failure (MOF) and even death when gets uncontrolled [7, 11].

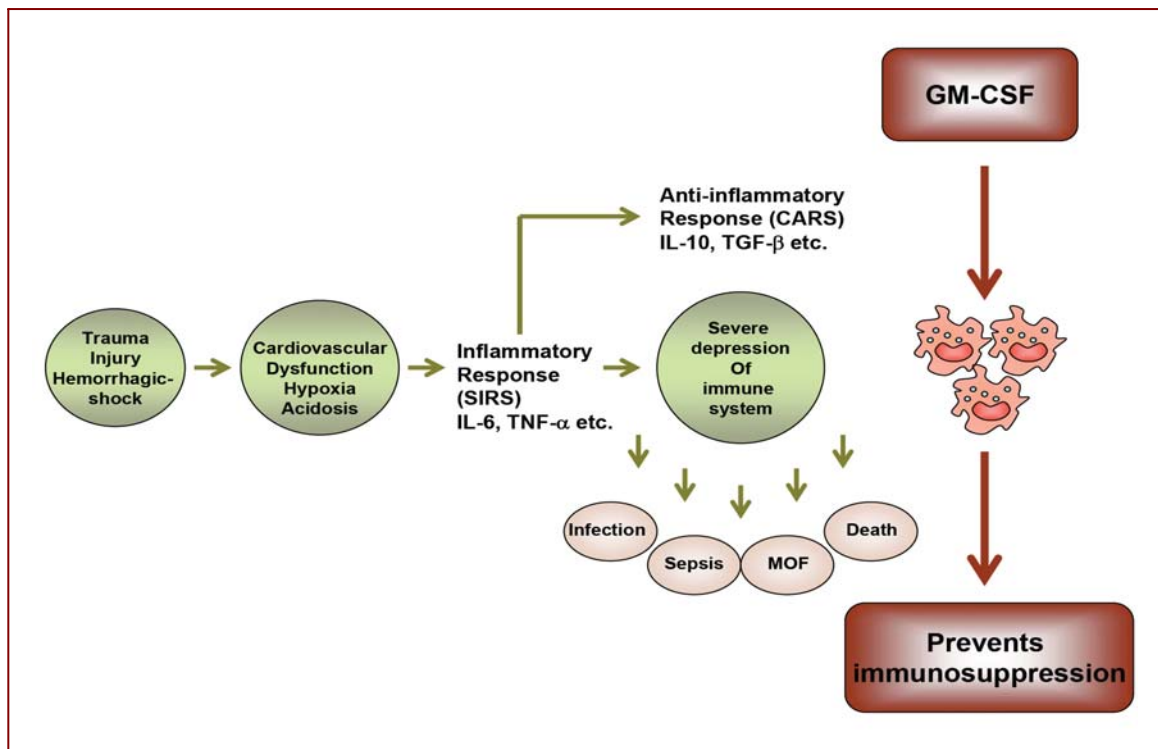


**Figure 1. Hypothesis of the cascade of events after hemorrhagic shock** that leads to the development of depressed immune responses and increased susceptibility to sepsis. GM-CSF generates new immune cells and activates circulating monocytes and resident macrophages and dendritic cells, maintaining immunocompetence following adverse circulatory conditions. The idea of the figure is from Angele MK et al [12].

## 1.2 Immune response and overview of cytokines

A normal response to an infection involves a series of complex immunologic reactions including cytokine activation of cells against infection with pathogens by production of cytokines such as TNF- $\alpha$ , interferons, interleukins and chemokines. The systemic response to infection that leads to sepsis and septic shock is mediated by a complex cytokine network. Cecal ligation and puncture (CLP) in mice causes symptoms similar to those found in septic patients and serves as a model for peritonitis and polymicrobial sepsis. The model has been a mainstay of basic science sepsis research [13, 14]. The animal models for hemorrhagic shock and sepsis undoubtedly have helped in gaining a better understanding of the immune response of the patients. In alignment with this idea similar changes in the immune system have been described in trauma and septic patients, as well as mice and rats after hemorrhagic shock and sepsis. Hemorrhagic shock leads to decreased LPS-dependent proinflammatory cytokine response of various macrophages which is associated with an increased susceptibility to bacterial infections. A dampened production of TNF- $\alpha$ , IL-6, IL-8 and IL-12 after stimulation with endotoxin has also

been shown from patients with multiple injuries [15, 16]. Hemorrhagic shock in mice and rats has been found to reduce LPS-induced TNF- $\alpha$  and IL-1 $\beta$  by splenic macrophages [17-19]. A reduction in TNF- $\alpha$  producing capacity of whole blood or peripheral white blood cells after hemorrhagic shock has been shown by many other groups [20]. Impaired induction of IL-10 expression has also been shown in the lung following hemorrhagic shock [21]. In contrast to splenic, peritoneal, and alveolar macrophages, Kupffer cells have been shown to have an enhanced capacity to produce pro-inflammatory cytokines, i.e. IL-1, IL-6, and TNF- $\alpha$  during the first 24 h after hemorrhage [22]. Similarly, an increase in cell associated TNF- $\alpha$  has been demonstrated on Kupffer cells, but not on splenic macrophages, at 2 h after hemorrhagic shock and resuscitation [23]. It should be noted that Kupffer cells and splenic and peritoneal macrophages are located in different microenvironments. Thus, the data suggest that trauma and hemorrhagic shock produce different effects on different tissue beds. Alternatively, splenic macrophages are in close contact with T cells, and mediators released by these cells after hemorrhage might depress the responsiveness of these macrophages as compared to Kupffer cells. Despite the differential cytokine release capacities of macrophages from different microenvironments, the antigen presentation capacity was depressed by macrophages in all tissue beds. Overall the suppressed cytokine production in hemorrhagic shock can be assumed as a phenomenon for immunosuppression.

Immune reactions during sepsis can be conceptualized as occurrence of an early pro-inflammatory and late compensatory anti-inflammatory response. The stringent expression of both responses seems to be decisive to determine the outcome of disease. An early pro-inflammatory response is characterized by the release of pro-inflammatory mediators, including TNF- $\alpha$ , IL-1 $\beta$ , IL-6 and chemokines (referred to as the systemic inflammatory response syndrome [SIRS]). Proinflammatory cytokine expression is counter-regulated by the release of anti-inflammatory cytokines such as IL-10 and IL-4. The latter response is generally termed as compensatory anti-inflammatory response syndrome (CARS) (**Figure 2**). The latter phase is believed to mediate the profound state of immunosuppression which occurs in association with substantial impairment in immune functions (sepsis-induced leukocyte “deactivation” or “immunoparalysis” [24]).

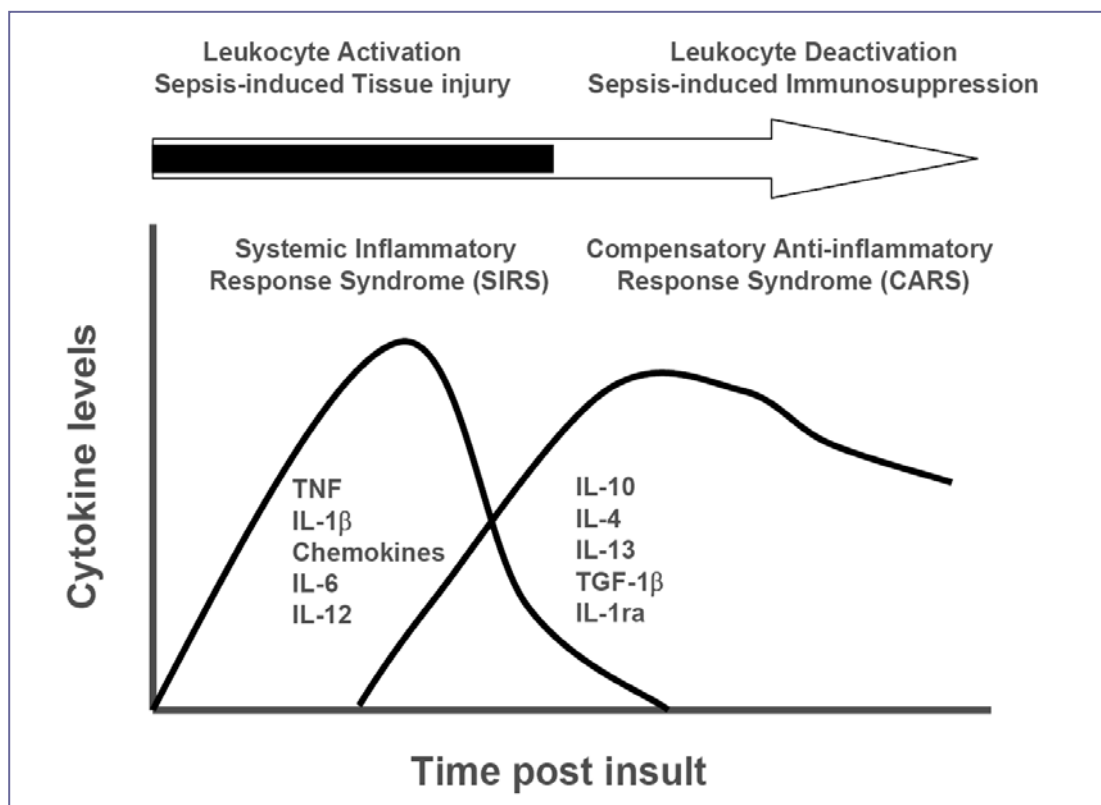


**Figure 2. Expression of cytokines during sepsis.**

As depicted in the graph, sepsis is characterized initially by an exuberant production of pro-inflammatory cytokines, leukocyte activation and tissue injury which is then followed by a release of anti-inflammatory cytokines, leukocyte deactivation and immunosuppression. The figure is adapted with required modification from van der Poll et al. [25].

The double edged role of the inflammatory response after hemorrhagic shock becomes most obvious for TNF- $\alpha$ . A primary role for TNF- $\alpha$  in sepsis or endotoxic shock is suggested by several research groups. On one hand, peak in the serum TNF- $\alpha$  levels in patients with sepsis, correlates with the mortality [26] and its neutralization helps ameliorating the survival [27]. Antibodies against TNF- $\alpha$  are shown to antagonize the lethal effects of endotoxin [28, 29] and also improve survival after lethal hemorrhagic shock [27, 30]. In aggregate, TNF- $\alpha$  neutralization yields a small but statistically significant benefit [31] for the early inflammatory phase showing high TNF- $\alpha$ . On the other hand, TNF- $\alpha$  is essential for an adequate immune response to infectious invaders. In contrast to the effect of high circulating TNF- $\alpha$  causing endothelial cell damage resulting in systemic oedema, hypotension and multiple organ failure [32], local TNF- $\alpha$  secretion is absolutely necessary to cope with infectious disease. Local effects of TNF- $\alpha$  include increased migration of macrophages, lymphocytes and polymorphonuclear leukocytes to the site of infection as well as enhanced release of antibodies, complement

and acute phase proteins [33]. Finally, TNF- $\alpha$  elimination by disruption of the gene of the TNF p55 receptor in 'knock out mice' prevented the establishment of an adequate immune response against *Mycobacterium tuberculosis* or *Listeria monocytogenes* [34, 35].

IL-10 has been most thoroughly studied out of all anti-inflammatory cytokines [36]. Synthesis of IL-10 is stimulated by pro-inflammatory cytokines like TNF- $\alpha$ , IL-1 $\beta$ , IL-6 and IL-12. IL-12 and its counterpart IL-10 play a critical role during sepsis since modulation of these cytokines influences sepsis-induced mortality. Recombinant IL-10 treatment, prior to CLP strengthens the survival [37] administration of IL-12 [38] increases sepsis-induced mortality. However, the time of intervention appears to be decisive for disease development. Absence of IL-10 during the initial inflammatory phase of sepsis is detrimental [39] whereas neutralization of IL-10 at later time points of anti-inflammatory phase is found to be beneficial [40-42].

### **1.3 Antigen presenting cells**

The antigen presentation is considered to be a key function in hemorrhage and sepsis-induced inflammatory response. Monocytes', macrophages' and dendritic cells' function as antigen presenting cells are well studied in regard to outcome of the disease [6, 43, 44].

#### **1.3.1 Monocytes and macrophages**

An intact and healthy monocyte and macrophage function is mandatory for the successful primary fight against infection. A depressed production of various cytokines has been observed in both monocytes of severely injured patients and macrophages of various origins in mice sustained to severe hemorrhage. Whole blood cultures and isolated mononuclear cells from patients with multiple injuries demonstrate a dampened production of TNF- $\alpha$ , IL-6, IL-8 and IL-12 after stimulation with endotoxin [15, 16]. Similarly, splenic macrophages from mice isolated after severe hemorrhage demonstrate a decreased synthesis of TNF- $\alpha$ , IFN- $\gamma$ , IL-2 and IL-6 [45, 46]. Severe injury and sepsis are frequently associated with a suppression of antigen presentation capacity and lack of ready response of monocytes, analyzed by the HLA-DR expression as well as a diminished capacity to produce cytokines such as TNF- $\alpha$ , IL-6 and IL-8 [45]. Low expression of HLA-DR [47] has been shown and correlated with disease state and mortality in septic patients [48-50].

##### **1.3.1.1 Signaling mechanism of monocytes and macrophages**

Activation of macrophages by LPS is commonly considered as a model for the primary response of the innate immune system to invading bacteria. Therefore, the LPS-dependent activation and intracellular signaling cascade has been analyzed extensively. Upon activation with LPS, multiple signaling pathways are activated in monocytes or macrophages (**Figure 3A and B**), such as the nuclear transcription factor NF $\kappa$ B and the mitogen-activated protein kinase (MAPK) pathway [51]. NF $\kappa$ B is under control of its inhibitor I $\kappa$ B, which is phosphorylated upon cellular stimulation with e.g. endotoxin and then liberates the active transcription factor [52-54]. MAPKs are signaling molecules, considered to be important in the regulation of various effector functions of macrophage and thereby regulate the inflammatory process [55]. These enzymes consist of proteins

that belong to three different families: extra cellular signal-regulating kinases (ERK), P38MAPK, and c-Jun N-terminal kinase/stress-activated protein kinase (JNK/SAPK). MAPK activity is involved in the early stress response caused by hemorrhage as shown for example in the lung tissue immediately after hemorrhage [56]. However, similar to the cytokine response, which is also increased early after hemorrhage followed by a downregulation, the activation of these signaling molecules parallels this pattern [57]. At least in severely injured patients the impaired cytokine response is accompanied by a reduced endotoxin-dependent activation of the nuclear transcription factor NF $\kappa$ B in human monocytes [58, 59]. Correspondingly, after hemorrhagic shock and laparotomy in female mice a lower endotoxin-induced phosphorylation of P38MAPK was observed in spleen cells in comparison to sham-operated mice [60].

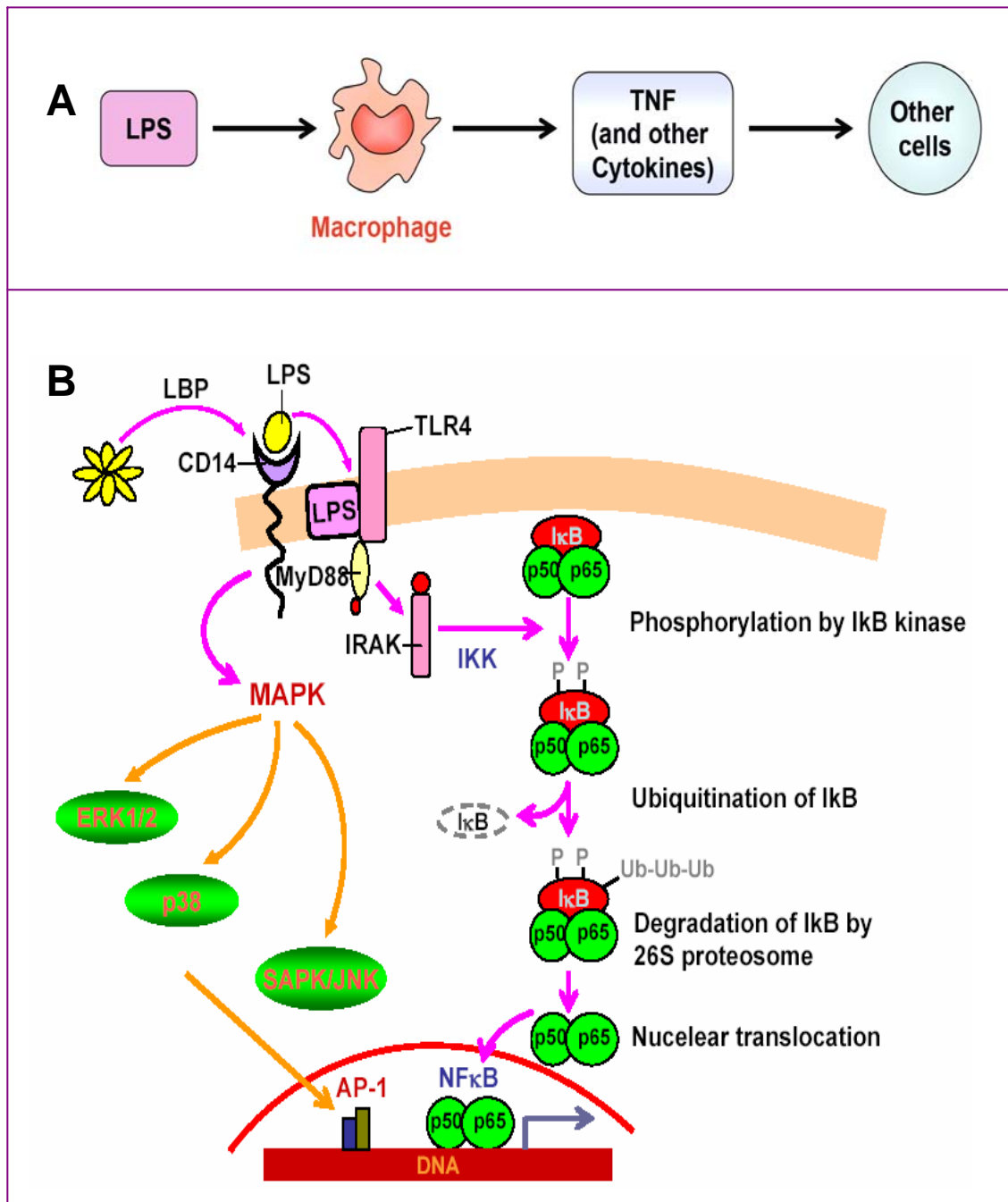


**Figure 3. Signaling pathways in macrophages upon LPS activation.**

**A)** LPS stimulation of monocytes activates different signaling pathways and consequently produces TNF. **B)** LPS binds to LPS-binding protein (LBP) in plasma and is delivered to the cell surface receptor CD14. Next, LPS is transferred to the transmembrane signaling receptor toll-like receptor 4 (TLR4). LPS stimulation of human monocytes activates several intracellular signaling pathways that include three mitogen-activated protein kinase (MAPK) pathways: extracellular signal-regulated kinases (ERK) 1 and 2, P38 and c-Jun N-terminal kinase (JNK). In addition, LPS activates the IκappaB kinase (IKK)-NF-kappaB pathway via MyD88 and IRAK which in turn phosphorylated the IκBs. Subsequent degradation by ubiquitination of IκBs permits nuclear translocation of active NFκB. These MAPK and NF-κB signaling pathways in turn activate a variety of transcription factors like NF-kappaB (p50/p65) and AP-1 (c-Fos/c-Jun) which coordinate the induction of many genes encoding inflammatory mediators. The figure is adapted with required modifications from Beutler et al [61].

## **1.3.2 Dendritic cells**

### **1.3.2.1 Dendritic cell development**

Dendritic cells (DC), first described by Steinman et al in 1972, are the most potent antigen-presenting cells and are sentinels of the immune system. Dendritic cells are derived from the CD34<sup>+</sup> bone marrow progenitors that separate into lymphoid and myeloid lineages to develop lymphoid and myeloid DC respectively [62]. These are the two distinct lineages of dendritic cell development which have been identified in mice. Lymphoid and myeloid DC differ in phenotype, localization and function. Both subsets express high levels of CD11c, MHC class II and the co-stimulatory molecules CD86 and CD40. CD8 $\alpha$  is the most reliable marker known till date to distinguish these subsets. CD8 $\alpha$  is expressed as a homodimer on the lymphoid DC but is absent from the myeloid DC subset. The common myeloid marker CD11b is expressed on myeloid CD8 $\alpha$ <sup>-</sup> DC but not on CD8 $\alpha$ <sup>+</sup> DC. Furthermore, the presence of GM-CSF expands the CD34<sup>+</sup> bone marrow progenitors to develop preferentially into myeloid DC [62, 63].

### **1.3.2.2 Antigen capture, migration and maturation of dendritic cells**

Newly generated DC migrate from the bone marrow to lymphoid and nonlymphoid tissues and become resident cells. They are located in most tissues of the body where they readily encounter invading microorganisms. Immature DC are very efficient in antigen capture and can use several pathways, such as macropinocytosis, receptor-mediated endocytosis and phagocytosis. DC in peripheral tissues process the captured microbial or viral antigens and migrate to the draining lymphoid organ where they interact with antigen-specific T cells [64]. During migration, these DC undergo major morphological, phenotypical and functional changes termed as maturation. Upon maturation, DC strongly upregulate MHC and co-stimulatory molecules like CD86, CD80, and CD40, all of which are mandatory for effective antigen presentation and T cell stimulation [65]. Due to high levels of MHC class II and co-stimulatory molecules, mature DC are very potent T cell activators and are superior in comparison to other antigen-presenting cells like macrophages or B cell, [66]. In contrast, DC that lack high levels of co-stimulatory molecules and/or do not secrete pro-inflammatory cytokines are involved in tolerance induction. In this case tolerance is mediated through activation of regulatory T (Treg) cells or through induction of T cell apoptosis [67]. Thus, depending

on the pattern of co-stimulatory molecules and secreted cytokines, DC determine the fate of the immune response [68].

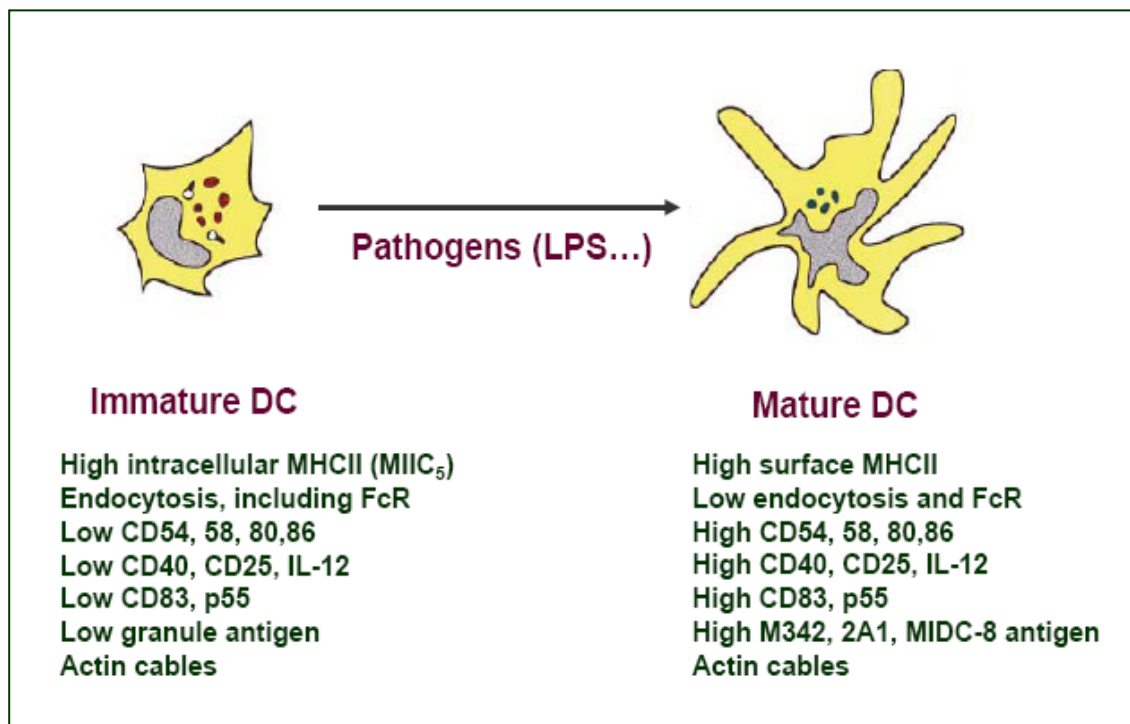


**Figure 4. Features which change during DC maturation.**

Immature DC take up and process antigen and then migrate to secondary lymphoid organs. During migration DC undergo a process of maturation. Examples of pathogenic molecules that induce maturation are lipopolysaccharide (LPS), bacterial DNA, CpG. TNF- $\alpha$  and GM-CSF are examples of cytokines, and CD40L is an example of a T-cell ligand that binds CD40 on DC and induce maturation. The figure is adapted with required modifications from Banchereau et al [64].

### 1.3.2.3 Dendritic cell-induced Th cell polarization

Dendritic cells not only induce T cells to secrete cytokines but are also themselves an important source of cytokines such as TNF- $\alpha$ , IL-1 $\alpha/\beta$ , IL-6, IL-8, IL-10, IL-12, TGF- $\beta$  and IFN- $\alpha/\beta$  [69]. During maturation, DC polarize T helper (Th) cells towards Th1 or Th2-type cells depending on the duration of the DC-T cell interaction, as well as the type of the secreted cytokines by the DC at the time of interaction (**Figure 5**) [70, 71]. DC that induce a Th1 or Th2 response are termed DC<sub>1</sub> and DC<sub>2</sub> respectively [72]. The DC<sub>1</sub>-derived cytokine IL-12 favors the differentiation of Th1 cells to secrete IFN- $\gamma$  and is important for the development of immunity against bacterial infections [73, 74]. In contrast, DC<sub>2</sub>-derived IL-10 promotes the polarization of Th cells towards Th2 to secrete IL-4, IL-5 and IL-10 that mediates immunity against extracellular parasites [64, 73, 74]. Some other cytokines like IL-3 and TNF- $\alpha$  are produced by both Th1 and Th2 cells.

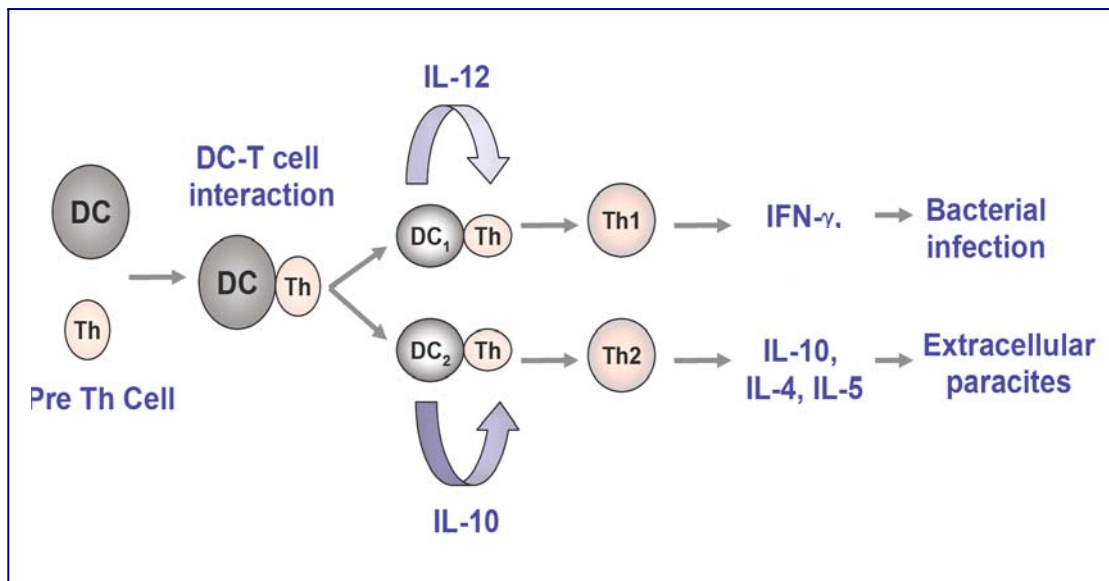


**Figure 5. Dendritic cells induced Th cell polarization.**

Subsets of DC induce T cells to differentiate towards a particular clone. If stimulated by gram negative bacteria (LPS), the DC mature into a DC<sub>1</sub> phenotype that induces naïve T cells to become Th1 cells. On the other hand, if exposed to antigens from certain helminthes, the DC mature into a DC<sub>2</sub> phenotype that induce naïve T cells to a predominantly Th2 phenotype.

#### 1.3.2.4 Dendritic cells during polymicrobial sepsis

DC are the central players in the activation of both innate and adaptive immunity and a decision maker in T cell activation [62]. A potentially deviated DC biology, function and behavior could be responsible for immunosuppression observed during shock and sepsis.

#### 1.3.2.5 Dendritic cell loss during sepsis

Indeed, apoptosis of DC in the spleen [75, 76], lymph nodes [77] and total bone marrow cells [78] during sepsis has been described, suggesting the involvement of DC during sepsis. The work from our own group provided evidence that selectively, the splenic CD4<sup>+</sup>CD8<sup>-</sup> and CD4<sup>-</sup>CD8<sup>+</sup> DC subpopulations were lost during disease development and that remaining DC from septic mice were inhibited in their capacity for T cell activation. Furthermore, depletion of the CD11c expressing cell populations results in a decreased survival rate after CLP in mice indicating that normal numbers of CD11c<sup>+</sup> DC are required for a successful outcome from severe sepsis [79].

#### 1.3.2.6 Dendritic cells characterization during sepsis

In a murine CLP model, it has been shown that there is strong maturation of splenic DC [80]. This maturation process was not only restricted to the spleen as a central lymphoid compartment but also was observed in lymph nodes distant from the site of infection.

However, maturation of DC from lymph nodes of septic mice followed a slightly delayed kinetics in comparison with splenic DC. There was a selective loss of certain DC during sepsis. Splenic DC of septic mice are shown to have an aberration in the cytokine secretion pattern toward predominant IL-10 and a failure to secrete IL-12 [81]. Therefore, DC acquired a change in the phenotype which could favor the development of Th2 cells. Consequently, all these changes might be responsible for inhibiting the effective immune response against the bacterial components through Th1 cell polarization.

## **1.4 Scope and restoration response**

### **1.4.1 GM-CSF in general**

GM-CSF, one of the first cytokines to be characterized, identified and cloned, is a 23-kDa, glycosylated, monomeric secreted protein. Murine and human GM-CSF share modest structural homology at the level of nucleotide (70%) and protein (56%) sequence [82] and do not exhibit cross-species receptor binding or biological activity. GM-CSF is produced by a variety of cell types including monocytes, endothelial cells, fibroblasts, mitogen-stimulated B-cells, T-cells and LPS-stimulated macrophages, [83, 84]. Amongst these, monocytes, macrophages and activated T cells are the primary producers of GM-CSF [84]. These cells sense invading pathogens and produce GM-CSF as part of their response. Also, they stimulate other cells, fibroblasts and endothelial cells, to produce GM-CSF secondarily. GM-CSF then works in coordination with other cytokines, IL-5 and IL-3, to maximize the granulocytic inflammatory response [85, 86].

### **1.4.2 GM-CSF as an immunomodulator**

GM-CSF is an important hematopoietic growth factor and immune stimulator. It is known to ameliorate the activation potential of monocytes which play an important role in the immune surveillance against many pathological conditions showing deactivation of monocyte functions. GM-CSF has a well recognized effect on granulocyte and macrophage maturation from hematopoietic precursors both *in vitro* and *in vivo*. In addition, GM-CSF also exerts effects on mature monocytes or macrophages and is known to potentiate the release of various cytokines such as TNF- $\alpha$ , IL-1 $\beta$  and IL-12 after LPS stimulation without inducing these mediators by its own [87, 88]. GM-CSF has also been shown to amplify the response of the mature immune system to antigen. Because of its myeloproliferative and immunostimulatory properties, GM-CSF is widely used therapeutically in a number of clinical therapies such as myelosuppressive chemotherapy [89], bone marrow transplantation [90], neonatal sepsis [91], lung injury [92], and wound healing [93]. The augmenting effects of GM-CSF have also been recognized in hemorrhagic shock [94] and sepsis [95].

### 1.4.3 Effect of GM-CSF on mature monocytes and macrophages

Beside its extensively studied role in differentiation and proliferation of monocytes and granulocytes, GM-CSF alters functions of mature monocytes and macrophages. It binds to high-affinity specific receptor found on most monocytes and has been proposed to enhance their activation potential [96]. Various *ex vivo* studies demonstrate that GM-CSF upregulates HLA-DR expression on the surface of monocytes and macrophages [97]. GM-CSF stimulates the differentiation of monocytes to macrophages and primes them to enhance the synthesis of TNF- $\alpha$ , IL-8 and IL-6 [46]. GM-CSF preferentially and selectively reactivated effectors of the innate immune response (monocytes and macrophages), without affecting the silenced adaptive immune response of T cells that are causally involved in graft rejection [98, 99]. Therefore, GM-CSF ameliorated the resistance to bacterial infection without compromising the graft.

#### **GM-CSF in monocytes and mature macrophages:**

- **Stimulation for granulocytes and monocytes**
- **Activation of mature macrophages in terms of:**
  - **Surface markers MHC Class II, ( $\uparrow\uparrow$ )**
  - **Production of various cytokines (TNF, IL-8, IL-6..) after secondary stimuli such as LPS – “priming”**
  - **Elimination of bacteria ( $\uparrow\uparrow$ )**

### 1.4.4 Signal cascade activated by GM-CSF

The effects of GM-CSF are mediated through a heteromeric receptor expressed on monocytes, macrophages and granulocytes [100]. The GM-CSF receptor is composed of GM-CSF specific  $\alpha$  and a signal transducing  $\beta$  chain that is common to receptors for GM-CSF, IL-3 and IL-5 [101, 102]. Although the GM-CSF receptor itself is devoid of tyrosine kinase activity the phosphorylation of a large number of intracellular signaling molecules occurs upon GM-CSF binding to the receptor [103]. GM-CSF binds with low affinity to the  $\alpha$ -chain, which then associates with the  $\beta$ -chain, thus increasing a chain

binding affinity, and initiates JAK2 autophosphorylation [104] and post receptor signaling. Signal transmission occurs through multiple pathways, each requiring distinct regions of the  $\alpha$  [105] and  $\beta$  [106, 107] receptor chains (**Figure 6**). GM-CSF mediated intracellular signaling molecules include members of the signal transducer and activator of transcription (STAT) family, the Ras/Raf-1 system and several mitogen-activated protein kinases (MAPK) [101, 102, 108-110]. GM-CSF was found to activate STAT 3 and 5 in human neutrophils via phosphorylation mediated by a receptor-associated Janus family tyrosine kinase 2 (JAK2) [111]. GM-CSF also activates Ras [112] and Raf-1 [113], P38 MAPK [114, 115] and the extracellular signal-related kinase 1 and 2 (ERK1/2) [116]. In the activation of ERK1/2 the cytoplasmic part of the  $\beta$  receptor, the adapter protein Shc, Ras and Raf-1 and consecutive activation of the ERK kinase MEK1/2 appears to be involved. ERK1 and ERK2 are not the only MAPK that are activated by GM-CSF. Phosphorylation of P38, a kinase involved in cellular responses to stress, by GM-CSF stimulation has been reported to occur in human neutrophils [117]. Activation of the third group of MAPK, the JNK/SAPK kinases, by GM-CSF in different types of cells was also observed [118-121]. The mechanism through which this pathway is activated is not completely understood but JAK2 are likely to take part [118, 119]. GM-CSF also activates PI3K in the cells, an event dependent on tyrosine phosphorylation [113, 122-126]. Kinases that are downstream of PI3K are also activated by GM-CSF. PKB is shown to be rapidly activated by GM-CSF in human granulocytes, a process dependent on PI3K [123, 127]. However, there is no direct evidence for GM-CSF-mediated direct activation of NF $\kappa$ B in monocytes or macrophages.

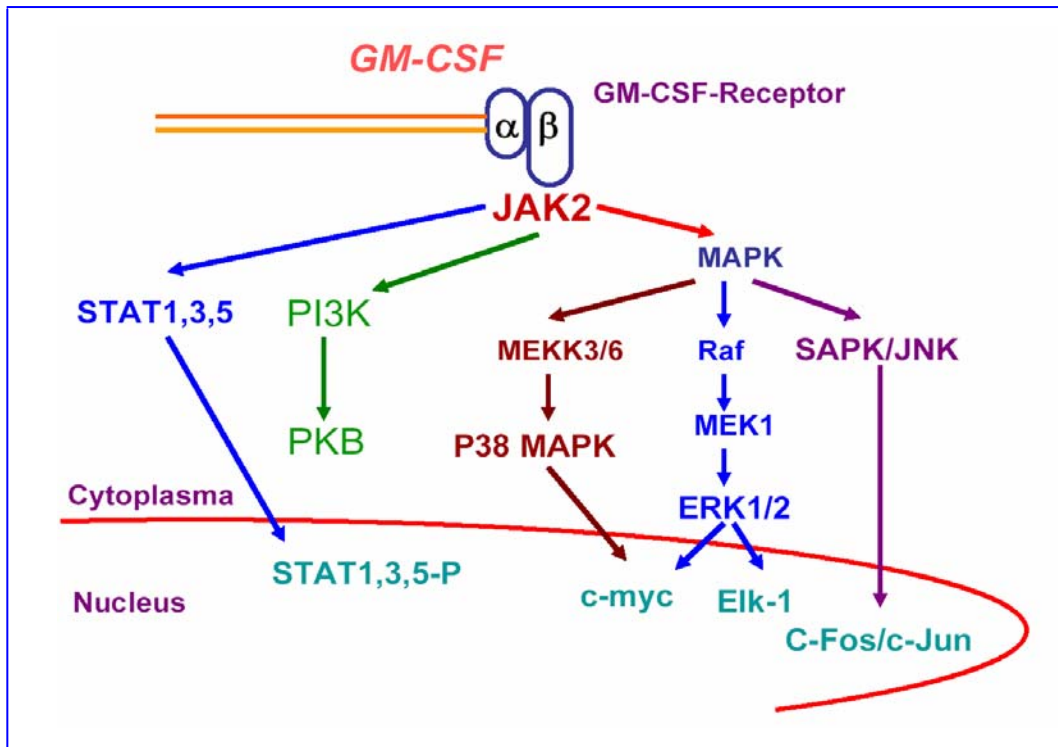


**Figure 6. GM-CSF signaling pathway.**

GM-CSF binds to high affinity GM-CSF receptor and initiates JAK2 autophosphorylation bound to the  $\beta$  subunit. Phosphorylation of JAK2 results to multiple signaling pathway including STAT1,3,5, PI3K and various MAPK culminating into different transcription factors.

## 1.4.5 GM-CSF in shock, trauma and sepsis

### 1.4.5.1 GM-CSF in hemorrhagic shock

The immune functions after hemorrhagic shock in experimental settings or after severe injury in patients, however, is not irreversible, but can be counteracted by immunostimulating compounds. GM-CSF, which stimulates proliferation and differentiation of myeloid bone marrow progenitor cells, can also enhance effector functions of mature monocytes and macrophages. On the basis of this function, GM-CSF has been shown to counteract the depressed TNF- $\alpha$ -producing capacity after severe trauma as well as the reduced expression of antigen-presenting Human Leukocyte Antigen (HLA)-DR on the surface of human monocytes after septic shock [96, 97]. GM-CSF has been reported to restore the reduced TNF- $\alpha$  production by splenic and peritoneal macrophages after hemorrhagic shock in rats [94]. On the other hand, GM-CSF contributes to relevant cytokine production of TNF- $\alpha$ , IL-1 and IL-6 in LPS-mediated septic shock [128, 129].

#### 1.4.5.2 GM-CSF in sepsis

During sepsis, early systemic hyper-inflammation induces systemic anti or hypo-inflammation which can lead to “immunoparalysis”. Sepsis being a biphasic syndrome may require an immunomodulating therapeutic approach targeting the patient’s immunocompetence. A patient with sepsis in a stage of hyper-inflammation may need anti-inflammatory therapy and on the other hand a patient in “immunoparalysis” needs immunoreconstitution or immunostimulatory therapy [130]. It has been proposed that the later anti-inflammatory response causes monocytes to downregulate HLA-DR expression and become deactivated or dysfunctional indicating an enhanced susceptibility to infection [131, 132]. Also, a deficit in circulatory GM-CSF was observed in the patients with the systemic inflammatory response syndrome (SIRS) suggesting that these patients may have a decreased ability to activate their monocytes [133, 134]. GM-CSF may restore the activation potential of monocytes. Reversal of immunoparalysis has been reported by rhGM-CSF in patients with severe sepsis where GM-CSF administration upregulated HLA-DR expression on monocytes. Furthermore, with the elevated TNF- $\alpha$  response, this upregulation of a monocytic activation marker is paralleled by a functional recovery [95]. GM-CSF restored the response of monocytes by abrogating their spontaneous and activation-induced (LPS) apoptosis from septic patients [96]. GM-CSF is proposed to restore immunologic functions from septic patients [96] and can prevent immune paralysis in endotoxin-desensitized mice [135].

#### **GM-CSF in shock and sepsis:**

- **Restores the activation potential of monocytes**
- **Restores depressed *ex vivo* TNF- $\alpha$  synthesis and HLA-DR expression after trauma, and during sepsis *in vitro***
- **Counteracts downregulation of TNF- $\alpha$  response during *in vitro* and *in vivo* endotoxin tolerance**
- **Normalizes depressed TNF- $\alpha$  response of peritoneal macrophages after hemorrhage in mice and rats *in vivo***

#### 1.4.6 GM-CSF in other clinical applications

GM-CSF, being a myeloproliferative and immunostimulatory cytokine, has a wide range of applications in other pathological conditions. Because GM-CSF stimulates the production and speeds up the differentiation of myeloid progenitors, it has been widely used as an adjuvant to shorten the duration of neutropenia, time to complete therapy and mean total days of intravenous antibiotic use after myelosuppressive cancer chemotherapy [89, 136]. GM-CSF has been shown to promote myeloid engraftment in bone marrow transplantation [137, 138] or hematopoietic stem cell transplantation [139]. GM-CSF enhanced neutrophil proliferation and also upregulated bactericidal function of both neutrophils and monocytes and decreased mortality in critically ill septic neutropenic neonates [91, 140, 141]. The positive response of GM-CSF treatment in neutropenic patients with infection raised the hope that stimulation by GM-CSF may aid critically ill non-neutropenic, sepsis patients to clear infection and ameliorate survival [142, 143]. Effect of GM-CSF could be of great clinical value to the patients with pre-existing alveolar epithelial dysfunction and are markedly susceptible to acute lung injury. GM-CSF overexpression in the murine lung resulted in resistance to lethal acute lung injury because of hyperoxia [92]. GM-CSF has been reported in animal studies to promote healing of infected wounds [144] and has been shown to be effective, when given subcutaneously, in the management of chronic refractory wounds [93].

#### **GM-CSF in Clinics:**

- **Established indication:**
  - Bone marrow stimulation after myelosuppressive chemotherapy
  - promote myeloid engraftment in bone marrow transplantation

## 1.5 Aim of the Research

Hemorrhagic shock and sepsis has been shown to induce immunosuppression by monocyte and macrophage deactivation, reducing antigen presentation, altering cytokine expression, modulating acquired immune response from a Th1 to Th2 type response and increased lymphocyte apoptosis. Progress in the realm of GM-CSF as an immunomodulator has enabled its potential to counteract the hemorrhage and sepsis-induced immune dysfunctions partly or completely in both clinical and experimental approaches. Through the ongoing knowledge of GM-CSF in therapeutic applications in the field of trauma and sepsis, GM-CSF treated monocytes or macrophages may be confronted with bacterial components such as LPS. Although, the effect of GM-CSF on cytokine production by monocytes and macrophages after LPS-stimulation has been documented in the literature, the underlying intracellular mechanisms remain to be elucidated. The signaling events activated in monocytes or macrophages after stimulation with LPS or GM-CSF alone have been copiously described. However, the intracellular cascades activated in a combined stimulation with GM-CSF and LPS have not yet been investigated.

The aim of the study was to analyze the effect of GM-CSF as an immunostimulatory substance after hemorrhage and cecal ligation and puncture (CLP), a model for severe polymicrobial sepsis. In particular, it was intended 1) to determine the effect of an *in vitro* treatment with GM-CSF of peritoneal macrophages for LPS-induced TNF- $\alpha$  production in a hemorrhagic shock model. 2) To determine the effect of an *in vitro* treatment with GM-CSF of splenic macrophages for LPS-induced TNF- $\alpha$  production and dendritic cells for CpG-treated IL-12 production during polymicrobial sepsis. 3) To explain the underlying mechanisms of GM-CSF activation of the TNF- $\alpha$  response in terms of I $\kappa$ B $\alpha$  (also NF $\kappa$ B) and MAPKinase (ERK1/2 and P38) signaling pathways. It is to be investigated first in normal human circulating monocytes, human monocytic cell line, THP-1 and then to be extended to the mouse model of hemorrhagic shock. It is well established especially for neutropenic septic patients suggesting a predominant effect of GM-CSF on the bone marrow. Therefore, the next aim of the study was to study the role

of GM-CSF as a growth regulator during polymicrobial sepsis especially for bone marrow derived dendritic cells. With the emphasis 4) to explain the GM-CSF effect on the bone marrow level during sepsis. To investigate whether sepsis additionally modulates bone marrow cells especially the progenitor cells of dendritic cells in terms of their differentiation, expression of co-stimulatory molecules, cytokine pattern and *in vivo* and *in vitro* antigen presentation capacity.

# MATERIALS AND METHODS

---

## 2. Materials and methods

### 2.1 Chemicals, Reagents and Antibodies

#### 2.1.1 Chemicals

All the chemicals and reagents used throughout this work were of analytical grade and purchased from different companies as stated in **Table 1**.

**Table 1: List of chemicals**

Name	Source (Supplier/Company)
$\beta$ -Mercaptoethanol	Sigma, Deisenhofen Germany
Acrylamide	Fluka, Neu-Ulm, Germany
Ammonium chloride	Fluka
Ammoniumpersulfate (APS)	Promega, Mannheim, Germany
Bicine	Sigma
Boric acid	Sigma
Bovine serum albumin (BSA)	Sigma
Bromophenol blue	BioRad, Munich, Germany
Calcium chloride	Merck, Darmstadt, Germany
Diethylether	Merck
di-Sodiumhydrogen phosphate	Merck
Dimethyl sulphoxide (DMSO)	Sigma
Dithiothreitol (DTT)	Serva, Heidelberg, Germany
EDTA	Promega/Sigma
Ethanol	Backer, Griesheim, Germany
Geneticin (G418)	Invitrogen, Karlsruhe, Germany
Glycerol	Serva/Sigma
Glycine	Sigma/Merck
HCl (32%)	Merck
HEPES	Sigma/Serva
Kanamycin	Sigma

Leupeptin	Sigma
Magnesium chloride	Sigma
Methanol	Backer
Nonidet-P 40	Fluka
Penicillin G	Seromed, Munich, Germany
PMA	Sigma
PMSF	Roche, Mannheim, Germany
Potassium chloride	Merck
Potassium hydrogen carbonate	Fluka
Sodium azide	Merck
Sodium chloride	Merck/Fluka
Sodium dihydrogen phosphate	Merck
Sodium dodecyl sulfate (SDS)/Lauryl sulfate	Sigma
Sodium hydroxide pellets	Merck
Streptomycin	Seromed
TBST	Sigma
TEMED	Sigma
Tris (hydroxymethyl)-aminomethane	Sigma/Merck
Tween-20	Sigma
Urea	Fluka

### 2.1.2 Reagents

Recombinant human GM-CSF derived from *E. coli* K12 (Molgramostin, Leucomax) was purchased from Novartis Pharma, Nürnberg, Germany. Murine recombinant GM-CSF and CD40 ligand (CD40L), IL-10 and IFN- $\gamma$  were purchased from R&D systems, Wiesbaden, Germany. Synthetic phosphorothioated CpG 1668 oligonucleotides (Sequence: TCCATGACGTTCCCTGATGCT) [145] were purchased from Qiagen, Köln, Germany. Concanavalin A (ConA), Dimethyl sulphoxide (DMSO), Ionomycin, Lipopolysaccharide (LPS, *E. coli* 026:B6), and Phorbol 12-Myristate 13-Acetate (PMA) were purchased from Sigma (Deisenhofen, Germany). Ova-peptide (OVA 323-339; peptide sequence: ISQAVHAAHAEINEAGR) was purchased from MoBiTec, Göttingen and PGN was purchased from InvivoGen, Hamburg, Germany. All reagents were free of detectable LPS contaminations as tested using Limulus amoebocyte assay.

### 2.1.3 Antibodies

Antibodies were purchased from Acris (Hiddenhausen); Becton Dickinson (BD) Biosciences (Heidelberg), eBiosciences (Frankfurt); Caltag (Hamburg); R&D Systems (Wiesbaden-Nordenstadt), Immunotools (Friesoythe) Germany (**Table 2**).

**Table 2: Antibodies**

Antibody	Clone	Conjugation	Amount (in 50 µl)	Isotype	Source
CD16/CD32	2.4G2	No Conjugation	5 µl	Rat IgG <sub>2b</sub> , κ	BD PharMingen
IL-10	JES5-16E3	No Conjugation	---	Rat IgG <sub>2b</sub> , κ	BD PharMingen
IL-10	JES052A5	No Conjugation	---	Rat IgG <sub>1</sub>	R&D Systems
CD4	RM4-5	FITC	0.25 µg	Rat IgG <sub>2a</sub> , κ	BD PharMingen
CD4 (L3T4)	YTS 191.1.2	FITC	2 µl	Rat IgG <sub>2b</sub>	ImmunoTools
CD8α (Ly-2)	53-6.7	FITC	0.125 µg	Rat IgG <sub>2a</sub> , κ	BD PharMingen
CD11b	M1/70	PerCP-Cy5.5	0.2 µg	Rat IgG <sub>2b</sub> , κ	BD PharMingen
CD11c	HL3	APC	0.1 µg	IgG <sub>1</sub> , λ	BD PharMingen
CD40	HM40-3	FITC	0.1 µg	IgM, κ	eBiosciences
CD40	23-Mar	FITC	0.25 µg	Rat IgG <sub>2a</sub> , κ	BD PharMingen
CD45/CD14	2D1/MfP9	FITC/PE	20 µl	Mouse IgG1	BD PharMingen
CD86 (B7-2)	GL1	PE	0.02 µg	Rat IgG <sub>2a</sub> , κ	BD PharMingen
D011.10 TCR	KJ1-26	APC	10 µg	Rat IgG <sub>2a</sub>	Caltag
F4/80	Cl:A3-1(F4/80)	APC	5 µl	Rat IgG <sub>2b</sub>	Acris
Gr-1	RB6-8C5	FITC	0.5 µl	Rat IgG <sub>2b</sub>	ImmunoTools
I-A/I-E	2G9	biotin	0.5 µg	Rat IgG <sub>2a</sub> , κ	BD PharMingen
I-A/I-E	2G9	FITC	0.03 µg	Rat IgG <sub>2a</sub> , κ	BD PharMingen
IFN-γ	XMG1.2	PE	0.4 µg	Rat IgG <sub>1</sub>	BD PharMingen
IL-2	JES6-5H4	PE	0.2 µg	Rat IgG <sub>2b</sub>	BD PharMingen
IL-4	11B11	PE	0.8 µg	Rat IgG <sub>1</sub>	BD PharMingen
IL-12	C15.6	PE	0.4 µg	Rat IgG <sub>1</sub>	BD PharMingen
TLR4/MD-2	MTS510	PE	0.4 µg	Rat IgG <sub>2a</sub> , κ	eBiosciences
TNF-α	MP6-XT22	PE	0.1 µg	Rat IgG <sub>1</sub>	BD PharMingen

## 2.2 Culture media, Buffers and Solutions

### 2.2.1 Culture media

Very low endotoxin medium, VLE RPMI 1640 (Biochrom, Berlin, Germany) containing 10% heat-inactivated fetal calf serum (FCS, Biochrom, Berlin, Germany) was used for all types of cultures. The FCS was heat inactivated for 30 min at 56°C. Medium was supplemented with 10 mM HEPES, 2 mM L-Glutamine, 0.06 mg/ml Penicillin, 0.02 mg/ml Gentamicin and 0.05 mM  $\beta$ -Mercaptoethanol.

### 2.2.2 Buffers and Solutions

All the buffers were prepared in sterile conditions and filtered if necessary, through 0.22  $\mu$ m filter, to sterilize heat labile components. Millipore distilled three-fold deionised water was used for preparing the buffers.

#### 2.2.2.1 Cell isolation and culture

<i>Blendzyme Buffer (10 x, 50 ml)</i>	CaCl <sub>2</sub> (133 mg); HEPES (1 M, 5 ml); KCl (186.4 mg); MgCl <sub>2</sub> (47.6 g); NaCl (4.383 g)
<i>RBC lysis buffer (0.15 M, 200 ml)</i>	KHCO <sub>3</sub> (0.2 g); Na <sub>2</sub> EDTA.2H <sub>2</sub> O (7.44 g); NH <sub>4</sub> Cl (1.658 g)
<i>Cluster dissociation buffer</i>	7.5 mM EDTA; 2.5% FCS in deionised water

#### 2.2.2.2 Automated magnetic cell sorting (autoMACS)

<i>Binding Buffer</i>	0.5% FCS in PBS
<i>Running Buffer</i>	2 mM EDTA; 0.5% FCS in Phosphate-buffered saline (PBS, Gibco, Germany)
<i>Rinsing Solution</i>	2 mM EDTA in PBS
<i>Cleaning Solution</i>	70% v/v ethanol

#### 2.2.2.3 SDS-PAGE, Western Blotting and EMSA

<i>Sample Buffer</i>	Bromo Phenol Blue (0.05% w/v); Glycerol (1 ml); Solution B (see <b>Table 3</b> ; 1:5 dilutions)
<i>Sample Buffer Mix</i>	$\beta$ -Mercaptoethanol (200 $\mu$ l); Sample Buffer (200 $\mu$ l); 10% SDS (400 $\mu$ l); 10 M Urea (500 $\mu$ l)
<i>Running buffer</i>	Solution B (see <b>Table 3</b> ; 1:5 dilution)

<b><i>Western Blot Tank Buffer</i></b>	39 mM Glycine; 20% Methanol; 0.0375% SDS; 48 mM Tris;
<b><i>TBS (pH 8.0)</i></b>	0.0027 M KCl; 0.138 M NaCl; 0.05 M Tris
<b><i>TBST (pH 8.0)</i></b>	TBS with 0.05% Tween-20
<b><i>TBE (0.5x, pH 8.2)</i></b>	45 mM Boric Acid; 20 mM EDTA (pH 8.0); 45 mM Tris-HCl

## **2.3 Cell culture methods**

### **2.3.1 Human models**

#### **2.3.1.1 Healthy human subjects**

Fifteen healthy human volunteers with an age range from 27-40 years were included in the study. All the volunteers gave their informed consent to donate blood for the experiments.

### **2.3.2 Isolation and culture of various human cells**

#### **2.3.2.1 Isolation and culture of human peripheral blood mononuclear cells**

Blood was drawn from healthy individuals and peripheral blood mononuclear cells (PBMC) were isolated by Ficoll (Biochrom, Berlin, Germany) density gradient centrifugation (550 x g, 30 min at room temperature) and washed twice (300 x g, 10 min at room temperature) with PBS. To enrich the monocytes, PBMC were resuspended and allowed to adhere, in tissue culture flasks for 3 h before nonadherent cells were removed by washing with PBS. Adherent cells were cultured overnight in RPMI 1640 medium supplemented with 2% human AB<sup>+</sup> serum before stimulation was started. This procedure resulted in >80% monocytic cell purity as confirmed by FACS analysis using CD14 staining.

PBMC were seeded at a density of  $1 \times 10^7$  in tissue culture flasks or  $4 \times 10^5$  cells/200  $\mu$ l/well in 96-well flat bottom microtiter plates for signaling and cytokine analysis respectively. The isolated monocytes were incubated with or without 10 ng/ml recombinant human GM-CSF. After 6 h, GM-CSF was removed by medium exchange. For the control incubations, the medium was exchanged at the corresponding time point. The cells were further incubated in the presence or absence of 10 ng/ml LPS from *Salmonella friedenau* (phenol-extracted protein- and DNA-free LPS, kindly provided by H. Brade, Forschungsinstitut Borstel, Germany). The LPS stimulation was given for 45 min to the cells in tissue culture flasks for the analysis of signaling molecules and in 96-well plate for 4 h for cytokine analysis.

#### **2.3.2.2 Culture of human monocytic THP-1 cells**

THP-1 is a human monocytic cell line, derived from a human acute monocytic leukemia patient and was obtained from DSMZ, Braunschweig, Germany. Cells were cultured in

RPMI 1640 medium containing 10% of FCS (Sigma) in 60 mm Petri-dishes and used for the experiments.

To analyze the various cytokine production, THP-1 monocytes ( $2 \times 10^5$  cells/200  $\mu$ l/well) were seeded in 96-well flat bottom microtiter plate for overnight and next day, the cells were stimulated with or without 10 ng/ml (also with different doses to determine the dose concentration) recombinant human GM-CSF (Molgramostin, Leucomax) for different time periods as indicated in the figure legends. After 6 h, GM-CSF was removed by medium exchange and the cells were stimulated with different doses of LPS (1-100  $\mu$ g/ml) from *Salmonella abortus equi* (Sigma) for additional 4 h. Afterwards supernatants were collected, stored at  $-20^{\circ}\text{C}$  until cytokine detection. For analysis of different signaling molecules, corresponding incubations with or without GM-CSF were set up in 60 mm Petri-dishes and the cells were stimulated with or without 10  $\mu$ g/ml LPS for 45 min and used for further analysis.

### **2.3.3 Mouse models**

#### **2.3.3.1 Mice**

Both male and female BALB/c mice and male C57BL/6 mice were purchased from Harlan Winkelmann, Borchon, Germany. Male and female D011.10 TCR<sup>tg</sup> transgenic mice were bred in our own animal facility. All mice weighed up to 20-30 g, 6- 8 weeks old, were housed in sound-proof holding room at an ambient temperature of  $24.0 \pm 0.5^{\circ}\text{C}$  under 12 h light/dark cycle. The mice had free access to standard lab chow and tap water ad libitum. All mice were allowed to habituate to the animal laboratory conditions for one week before starting the experiments. All animal experiments were carried out according to the German animal protection law and were approved by the “Bezirksregierung” Duesseldorf, Germany.

#### **2.3.3.2 Hemorrhagic shock**

For the induction of hemorrhagic shock, mice were anaesthetized by an intramuscular (i.m.) injection of 100 mg/kg body weight of Ketamine Hydrochloride (CEVA, Sante Animale, Duesseldorf, Germany) and 10 mg/kg Xylazin (CEVA, Sante Animale) after inhalation of Isoflurane. Mice were placed in supine position, a groin incision was performed, the femoral artery was aseptically cannulated with a 24-Gauge polyethylene tubing (Introcan, Braun-Melsungen, Germany) using minimal dissection technique. The

catheter was connected to a blood pressure analyzer (Combitrans Monitoring-Set, Modell II, Art. Nr. 05201675; Braun Melsungen, AG) and hemorrhage was started by blood withdrawal over the same catheter until the mean arterial pressure (MAP) of  $50 \pm 5$  mm Hg was reached. The hemorrhagic shock was maintained for 35-40 min before resuscitation was started with the shed blood 1:2 diluted (anticoagulated with heparin) with warm (37°C) Ringer-solution. After reperfusion the catheter was removed, the femoral artery was ligated and the groin incision was closed. The animals were allowed to awake and were returned to their cages. Control animals were anaesthetized and operated correspondingly; the femoral artery surgically prepared and the vessel was ligated (sham operation).

### **2.3.3.3 Cecal ligation and puncture**

For induction of polymicrobial sepsis, the cecal ligation and puncture (CLP) model (**Figure 7**) developed by Chaudry *et al.* [146] was used, with some modifications. Mice were anaesthetized by an intramuscular (i.m.) injection of 100 mg/kg body weight of animal Ketamine (CEVA, Sante Animale) and 10 mg/kg Xylazin (CEVA, Sante Animale) after inhalation of Isoflurane. Mice were placed in supine position and 1 cm incision was made for mid-line laparotomy (**Figure 7, Panel 1**). The cecum was exposed (**Figure 7, Panel 2**) and ligated (**Figure 7, Panel 3**) at half of the cecum length with 5-0 silk suture (Ethicon, Norderstedt, Germany) and was punctured (**Figure 7, Panel 4**) once with a 17-Gauge needle (Klinika, Usingen, Germany). A small amount of cecum contents was extruded (**Figure 7, Panel 5**) through the puncture and the cecum was replaced into the peritoneal cavity. One ml of 0.9% sodium chloride (Delta Select, Dreieich, Germany) was given intraperitoneally (i.p.) for resuscitation. The peritoneal wall and the skin were closed (**Figure 7, Panel 6**) in a double layer technique with 5-0 silk sutures. Control animals were anaesthetized and operated correspondingly with laparotomy alone (sham operation). The CLP model led to severe polymicrobial sepsis with a mortality rate of 60-70% within 36 h of operation.

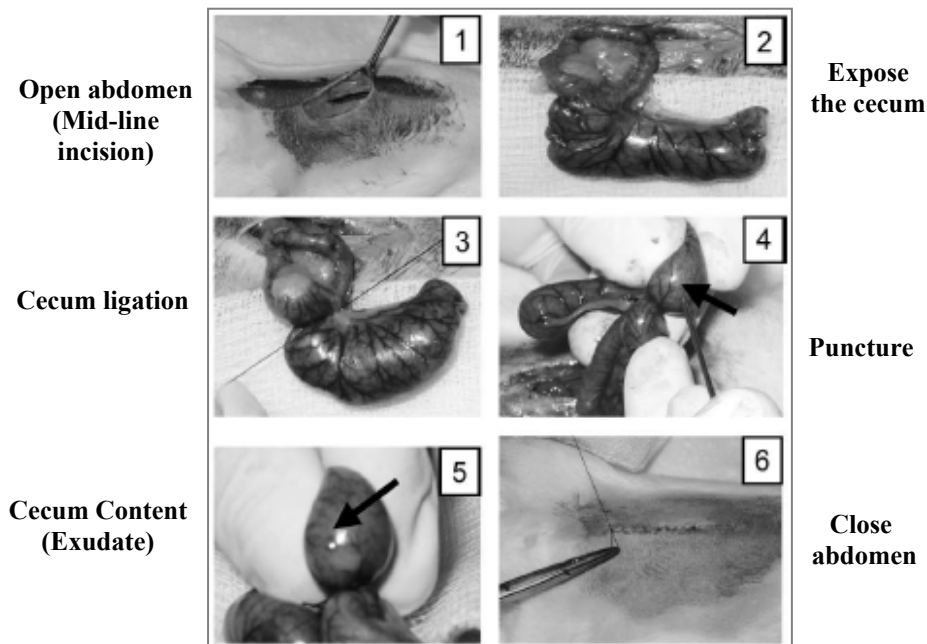


**Figure 7. Cecal ligation and puncture model**  
Figure adapted from Hubbard *et al.* [147]

#### 2.3.3.4 Serum collection

Blood was drawn from healthy BALB/c mice. The mice were dissected and opened from the upper part of the diaphragm, the heart was punctured with scissor and the blood was collected. The blood was kept at room temperature for 15 min for clotting, centrifuged at 1100 x g for 10 min at 4°C and the serum was collected and stored at -20°C until further use.

### 2.3.4 Isolation, purification and culture of various murine cell types

#### 2.3.4.1 Preparation and culture of peritoneal macrophages

For the isolation of peritoneal macrophages, 5 ml ice cold RPMI 1640 medium was injected into the peritoneal cavity and was aspirated after 2 min under sterile conditions. The cells were then centrifuged (300 x g, 10 min, 4°C), resuspended in ice cold RPMI 1640 medium until further use.

To analyze the cytokine production, peritoneal macrophages ( $1 \times 10^5$  cells/200  $\mu$ l/well) were seeded in 96-well flat bottom microtiter plate for 3 h and non-adherent and non-viable cells were removed thereafter in order to enrich peritoneal macrophages. The macrophages were incubated overnight and the next day, cells were stimulated with or without 10 ng/ml recombinant murine GM-CSF (Sigma). After 6 h, GM-CSF was

removed by medium exchange and the cells were stimulated in the presence or absence of 1 ng/ml LPS from *Salmonella friedenau* for 4 h. Afterwards supernatants were collected, stored at -20°C and later on used for cytokine detection. For analysis of different signaling molecules the peritoneal cells were washed once (818 x g, 5 min, and 4°C) and the cultures (1 x 10<sup>6</sup> cells/ml) were set up in RPMI 1640 medium with 10% of FCS (Sigma) in 60 mm Petri-dishes. After 3 h, the non-adherent and non-viable cells were removed by vigorously pipetting in order to enrich peritoneal macrophages. These macrophage cultures were incubated with and without 10 ng/ml GM-CSF for 6 h before cells were stimulated in the presence or absence of 1 ng/ml LPS (*Salmonella friedenau*) for 45 min and used for further analysis.

#### **2.3.4.1.1 Preparation of Bacteria**

Peritoneal lavage containing the bacterial flora was collected from both sham and septic mice using 1 ml PBS. The bacterial flora was cultured in 25 ml BacTec medium (BD, Biosciences) and optical density (OD) was measured at different time points until a plateau phase was reached. The bacterial cells were harvested, centrifuged (6500 x g, 15 min, and 4°C) and resuspended in 100 µl of PBS. Thereafter, the bacteria were heat inactivated at 80°C for 15 min and stored at -80°C until further use.

#### **2.3.4.1.2 Macrophage viability test using MTT**

To check viability of the enriched macrophages and to rule out changes in the total amount of adherent macrophages caused by the experimental design, a viability test was performed after stimulation and removal of the supernatants. Therefore, cells were incubated with 100 µl RPMI 1640 with 1 mg/ml of the tetrazolium salt MTT (Sigma) which is reduced to formazan by the activity of mitochondrial dehydrogenases. After 3 h of incubation and cell lyses with isopropanol formazon formation was measured at 550 nm with a reference wavelength of 690 nm.

#### **2.3.4.2 Preparation and culture of total spleen cells**

Total spleen cells (TSC) were prepared by collagenase digestion using 0.02 U/ml Blendzyme 2 (Section 2.2.2, Roche, Grenzach-Wyhlen, Germany) at 37°C for 18 min. Spleens were meshed through a cell strainer (70 µm, BD Biosciences) into a Petri-dish and were transferred into a falcon tube by passing through a different cell strainer (40 µm, BD Biosciences) and incubated in culture medium containing 5 mM EDTA for 5

min for dissociation of cell clusters. The cells were collected and resuspended in 500  $\mu$ l of ammonium chloride lysis buffer (**Section 2.2.2**) per spleen, to lyse the red blood cells (RBC). The cells were mixed gently, 5 ml of culture medium was added and the cells were underlain thereafter with 2 ml of FCS and centrifuged (300 x g, 10 min, and 4°C). After washing, total spleen cells (TSC) were counted and used for further experiments. TSC ( $0.5 \times 10^6$  cells/500  $\mu$ l/well) were cultured in culture medium in 48-well plates with or without GM-CSF (10 ng/ml), CpG (5  $\mu$ g/ml) and IFN- $\gamma$  (10 ng/ml) for 18 h. Non-adherent cells were harvested and used for IL-12 intracellular staining.

#### **2.3.4.3 Preparation of lymph node cells**

Popliteal lymph nodes were isolated and flushed with culture medium using a 27-Gauge needle. Remaining tissue was minced through a cell strainer (40  $\mu$ m, BD Biosciences). After pooling, lymph node cells (LNC) were incubated in culture medium containing 2 mM EDTA in order to dissociate cell clusters and were used for the cultures. Isolated LNC were used for FACS staining.

#### **2.3.4.4 Generation and culture of mouse bone marrow cells**

Bone marrow-derived dendritic cells were generated using the procedures of Lutz *et al.* [148]. Mice from healthy, sham and septic groups were euthanized by cervical dislocation; femurs and tibiae were removed and cleaned of tissue, and sterilized in 70% ethanol for 1 min and washed with PBS twice. Both ends of each bone were cut, and the marrow was flushed with culture medium (using a 27-Gauge needle). The bone marrow cells (BMC) were mixed to disrupt the cell aggregates and RBC were lysed with an ammonium chloride lysis buffer (**Section 2.2.2**). The cells were centrifuged (300 x g, 10 min, and 4°C), washed and counted. BMC were seeded at a density of  $2 \times 10^6$  in 100 mm Petri-dish (Falcon, BD Biosciences) in 10 ml of culture medium containing 20 ng/ml murine recombinant GM-CSF. Ten ml of culture medium containing 20 ng/ml murine recombinant GM-CSF was added to the plates after 3 d of culture. On d 7, nonadherent and loosely adherent cells were harvested, washed in PBS, counted and used for further experiments. The non-adherent cells on d 7 were termed as bone marrow derived dendritic cells (BMDC) and were 70-80% positive for the DC marker CD11c as confirmed by FACS analysis.

BMC on d 0 and BMDC on d 7 were counted and cultured ( $0.5 \times 10^6$  cells/500  $\mu$ l/well) in 48-well plates with Bacterial lysate (different dilutions), CpG (5  $\mu$ g/ml), LPS (10, 100 and 1000 ng/ml), LPS (100 ng/ml) + CD40L (2.5  $\mu$ g/ml) or PGN (3  $\mu$ g/ml). The supernatants were collected after 18 h and stored at -20°C until analysis for different cytokine ELISA.

## 2.3.5 Isolation and purification of various cell types using automated magnetic cell sorting (auto-MACS)

### 2.3.5.1 Principle

MACS Technology is based on MACS MicroBeads and automated MACS separator (Figure 8), and MACS columns. MACS MicroBeads are super-paramagnetic particles coupled to highly specific monoclonal antibodies and are used to magnetically label the target cell population. When MACS columns are placed in a MACS separator, the MACS column matrix provides a magnetic field strong enough to retain the labeled cells. Cells of interest (positive selection) or to be depleted (negative selection) are labeled with the specific magnetic beads and retained on the column. Unlabeled cells pass through and can be collected as the unlabeled fraction. The retained cells are eluted from the MACS column after removal of the magnetic field. The purity of the separated cells is generally 90-99%.



**Figure 8. autoMACS Separator.**  
View at a glance (left) and an open view (right)

### 2.3.5.2 Isolation of splenic dendritic cells and bone marrow derived dendritic cells

Isolated TSC or BMDC were centrifuged (300 x g, 10 min, 4°C) and the cells were resuspended in 500  $\mu$ l of binding buffer (Section 2.2.2) per  $10^8$  cells (same volume of buffers and reagents for fewer cells also but scaled up accordingly if the cells exceeded more than  $10^8$ ). Then 50  $\mu$ l of MACS Basic MicroBeads (pre diluted as 1:10 in binding

buffer) were added to the cell suspension and mixed gently and thoroughly for few sec. The cells were washed by adding 12-15-fold volume of binding buffer, centrifuged and resuspended in 500  $\mu$ l of binding buffer and proceeded for negative depletion (to remove unwanted materials and cells e.g. RBC) using auto MACS depletion program (possel). The negative unlabeled fraction was collected, counted and used for the isolation of CD11c<sup>+</sup> cells.

The negative cells were adjusted to 10<sup>8</sup> cells/400  $\mu$ l in binding buffer. 100  $\mu$ l of CD11c<sup>+</sup> MACS MicroBeads per 400  $\mu$ l of cell suspension were added, mixed gently and thoroughly and incubated for 15 min in the dark at 4°C with intermittent shaking of the cells every 5 min. The cells were washed by adding 12 to 15-fold volume of binding buffer, centrifuged and resuspended in 500  $\mu$ l of binding buffer and proceeded for positive selection (to select the cells of interest) using the autoMACS positive selection program (posseld). The positive fraction (containing purified DC) was collected, centrifuged and resuspended in culture medium. The purified DC (generally 85-90% purity as confirmed by CD11c staining by FACS analysis) were counted and used for further experiments.

Purified splenic DC were cultured in culture medium containing 0.3 ng/ml GM-CSF in the absence or presence of additional 10 ng/ml GM-CSF and 5  $\mu$ g/ml CpG in 96-well flat bottom plates (1 x 10<sup>5</sup> cells/well). After 18 h, supernatants were collected and stored at -20°C until analysis for different cytokine ELISA. Purified BMDC harvested on d 7 (BMDC) were used in titrated amounts for *in vitro* T cell assay (described later, **Section 2.3.8.1**).

### **2.3.5.3 Isolation of splenic T cells**

Splenic T cells were isolated using Pan T cell isolation kit (Miltenyi), according to the manufacturer's instructions. Non-T cells, i.e. B cells, NK cells, dendritic cells, macrophages, granulocytes and erythroid cells were indirectly magnetically labeled by using a cocktail of biotin conjugated cell specific antibodies and anti-biotin MicroBeads. Isolation of highly pure T cells was achieved by depletion of magnetically labeled cells. Therefore, isolated TSC including RBC (as described above) were centrifuged (300 x g for 10 min at 4°C) and resuspended in 400  $\mu$ l of binding buffer per 10<sup>8</sup> cells (same volume of buffers and reagents for fewer cells also but scaled up accordingly if the cells exceeded more than 10<sup>8</sup>). First, 100  $\mu$ l of the biotin-antibody cocktail against CD45R (B220), DX5, CD11b (Mac-1) and Ter-119 was added to the cells, mixed and incubated

for 10 min in dark at 4°C and then 300 µl of binding buffer followed by 200 µl of anti-biotin MicroBeads were added, mixed and incubated for additional 15 min in the dark at 4°C. The cells were washed by adding 12-15-fold volume of binding buffer, centrifuged and resuspended in 500 µl of binding buffer and proceeded for depletion (to remove unwanted non-T cells) using autoMACS depletion program (deplete). The negative unlabeled fraction (containing purified T cells) was collected, centrifuged and resuspended in culture medium. The purified T cells (>90% purity as confirmed by FACS analysis) were counted and used for further experiments.

## 2.3.6 Labeling of cells

### 2.3.6.1 Carboxyfluorescein diacetate, succinimidyl ester labeling of T cells

#### (Cell proliferation tracking by flow cytometry)

Carboxyfluorescein diacetate, succinimidyl ester (CFDA SE, also called CFSE) staining is a simple and sensitive method that permits the study of specific populations of proliferating cells and the identification of 7-10 successive cell generations. CFDA SE is a fluorescein molecule containing a succinimidyl ester functional group and two acetate moieties. CFDA SE is a non-fluorescent dye that diffuses into the cytoplasm of cells. There the dye is cleaved by intracellular esterases and becomes highly fluorescent amine-reactive product and forms dye-protein adducts that are not transferred to adjacent cells (**Figure 9**). The dye is retained by the cells throughout their development and is inherited equally by daughter cells after division, resulting in the sequential halving of mean fluorescence with each generation. When analyzed by flow cytometry, this sequential halving of fluorescence is visualized as distinct peaks and can be used to track division progression. Application includes analysis of cell division by flow cytometry for *in vitro* and *in vivo* studies.

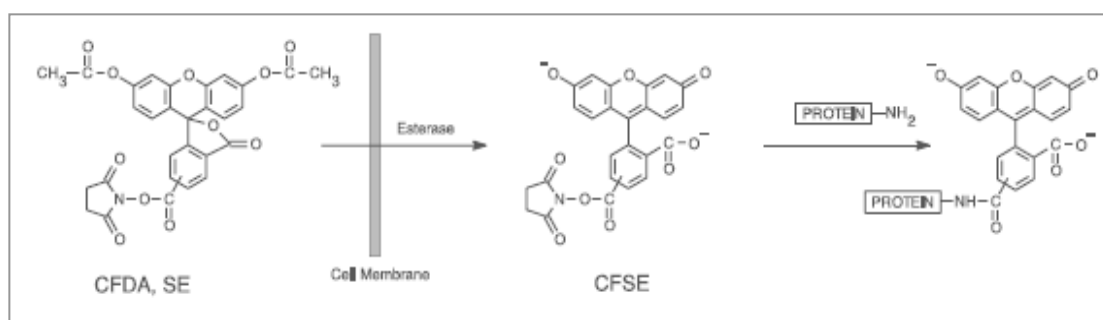


**Figure 9. Mechanism of cellular labeling by CFDA SE.**

CFDA SE is a non fluorescent molecule that spontaneously penetrates cell membranes and is converted to a fluorescent CFSE by intracellular esterases. Amine-reactive coupling of CFSE to proteins results in stable long-term intracellular retention.

The Vybrant CFDA SE Cell Tracer Kit (Molecular Probes, Göttingen, Germany) was used for the analysis of non-specific and antigen-specific T cell proliferation, both *in vitro* and *in vivo*. Isolated T cells ( $4-8 \times 10^6$  in 500  $\mu$ l) were centrifuged (300 x g, 10 min, and 4°C) and resuspended in prewarmed PBS. CFDA SE stock solution (10 mM) was prepared by dissolving it in DMSO and the appropriate amount of CFDA SE (0.5 and 1.5  $\mu$ M for *in vitro* and *in vivo* T cell assay respectively) was added to the T cells. The cells were mixed well and incubated for 12 min at 37°C in a water bath, centrifuged (300 g, 6 min, room temperature), resuspended in 1 ml of fresh prewarmed medium and again incubated for 30 min at 37°C. The cells were then centrifuged again and resuspended in prewarmed medium (1 ml). The T cell number was determined and used for *in vitro* and/or *in vivo* study as described later.

### **2.3.7 Analysis of cells (Flow Cytometry)**

Flow cytometry was used for the analysis of various cells e.g. BMC, BMDC, splenic DC and TSC. Single cells were prepared and stained for surface markers and intracellular cytokines and was analyzed using flow cytometry.

#### **2.3.7.1 Principle**

Flow cytometry is a tool for the measurement (meter) of characteristics of single cells (cyto) as they flow through a series of detectors. A pressurized hydrodynamic focusing, laser beam(s), flow cell/laser intercept, a series of light detectors (PMTs) and a data analysis station are the main components of a flow cytometer. Cell samples in suspension pass through the sheath fluid under hydrodynamic pressure that makes the cells to flow in a defined stream of single file. The moving cell hits the focused beam of laser lights and the light is scattered in the forward direction (FSC, indicates size of the cell) and in the side direction (SSC, indicates contents and the granularity of the cell) with respect to the laser beam. This information is picked up by one of a series of photomultiplier tubes (PMTs) detectors and converted into a form suitable for computer storage and subsequent analysis (**Figure 10**)

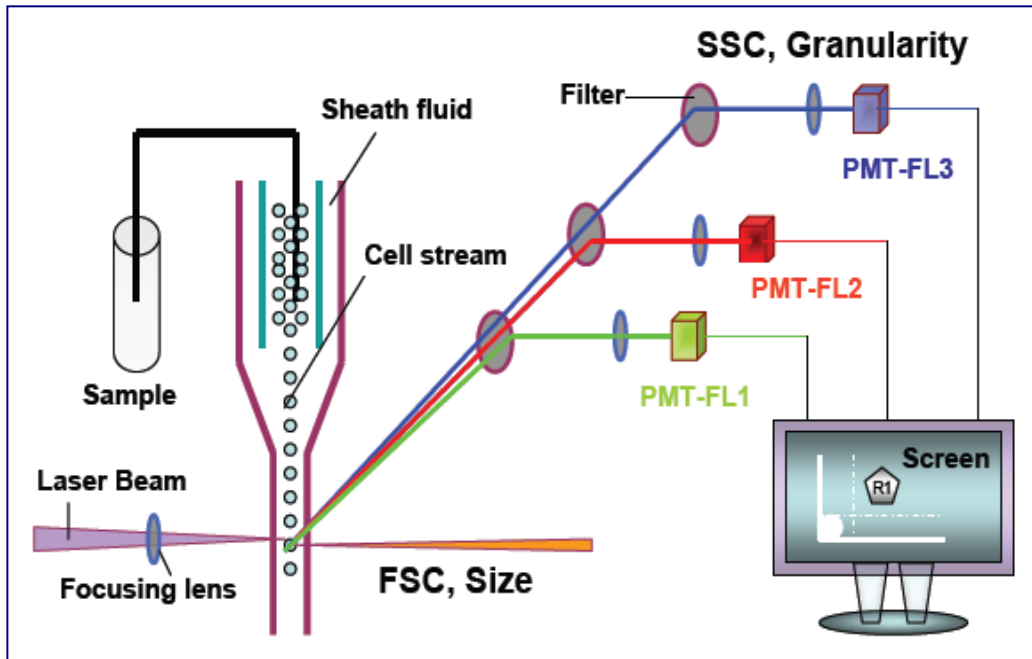


Figure 10. Schematic diagram of Flow Cytometry

### 2.3.7.2 Cell surface and intracellular staining

For the staining of cell surface markers, single cells ( $1 \times 10^6$ ) were prepared and transferred to 96-well-round bottom plate. The cells were washed (400 x g, 6 min, and 4°C) in Cell Wash (BD Biosciences). The cells were resuspended in 50  $\mu$ l of Cell Wash containing Fc block (1  $\mu$ g, BD Biosciences) for blocking unspecific binding and incubated on ice for 6 min. Then, 50  $\mu$ l antibody mixture (**Table 2**) containing anti-CD11c (APC) in combination with anti-IAd (FITC, Biotin), anti-CD8 (FITC), anti-CD4 (PE), anti-TLR4 (PE), anti-Gr1 (FITC), anti-CD11b (PerCPCy5.5), anti-CD40 (FITC), anti-CD86 (PE) was added. Anti-CD45 (FITC) was used in combination with anti-CD14 (PE). For the staining of blood cells, antibodies were added directly to the blood and incubated for 15 min either in normal FACS tubes or TruCount tubes (BD Biosciences), for the determination of absolute counts of leukocytes in blood. After 15 min on ice, cells were washed and resuspended in Cell Wash. For intracellular staining, cells were stimulated and incubated for the last 4-6 h in the presence of monensin (GolgiStop 0.66  $\mu$ l/ml, BD Biosciences). After surface staining using anti-CD11c (APC) or anti-CD4 (FITC) antibodies, cells were fixed and permeabilized using Cytofix/Cytoperm (BD Biosciences) for 20 min at room temperature in the dark and centrifuged. After washing twice with permeabilization buffer (BD Biosciences), intracellular cytokines were stained using anti-IL-12p40 (PE) or anti-TNF- $\alpha$  (PE) antibodies and washed again for

two times. The cells were resuspended in Cell Wash at the last step. Appropriate isotype controls were used for all staining. All data were acquired using a FACScalibur (BD Biosciences) and analyzed using Cell Quest Pro software (BD Biosciences). If possible, the FL-3 channel was used to exclude autofluorescent cells. Living cells were selected according to forward- and side-scatter properties. Total BMC, BMDC number per mouse was calculated as % CD11c cells x total number of cells per bone marrow/100.

### **2.3.7.3 Staining for *in vitro* and *in vivo* T cell proliferation assay**

**For *in vitro* T cell proliferation**, the adherent cells were harvested and transferred to 96-well-round bottom plate. The cell clusters were dissociated through addition of cluster dissociation buffer (**Section 2.2.2**) for 20 min at room temperature. After washing (400 x g, 5 min, and 4°C) with Cell Wash, the proliferated T cells (CFSE-labeled) were stained using anti-CD4 (PE) antibody (BD Biosciences). A constant number of CaliBRITE APC beads (BD Biosciences) were added to allow the acquisition of equal parts per culture. In order to exclude the dead cells, 7-Amino-actinomycin D (7-AAD; 4 µg/ml, Molecular Probes) was used. For data acquisition, a constant number of 10,000 CaliBRITE APC beads were counted. Living CD4<sup>+</sup> T cells (CD4<sup>+</sup> 7-AAD<sup>-</sup>) were gated, and the T cell proliferation was determined.

**For *in vivo* T cell proliferation**, the LNC were stained for proliferated T cells (CFSE-labeled) using anti-CD4 (PE) antibody and anti-D011.10 TCR (APC). Proliferating T cells (CD4<sup>+</sup>D011.10<sup>+</sup>) were gated, and the number of divided cells, showing less than the maximal CFSE fluorescence intensity, was determined.

## **2.3.8 Cell proliferation assay**

### **2.3.8.1 *In vitro* allogenic T cell assay**

The titrated amounts of purified BMDC ( $2 \times 10^4$  -  $0.065 \times 10^4$  cells) from BALB/c mice, in 200 µl/well were seeded in 96-well-flat bottom plates in triplicates. Purified splenic T cells from C57BL/6 mice were labeled with CFSE, counted and added ( $2 \times 10^5$  T cells/well) to the plated BMDC. After d 3, the supernatants were collected and stored at -20°C for the analysis of cytokines by ELISA. The adherent cells were harvested and stained using fluorescent antibodies and the proliferation was determined by FACS (**Section 2.3.7.3**).

### **2.3.8.2 *In vivo* T cell assay**

DO11.10 TCR transgenic mice that encode a T cell receptor that is specific for a chicken ovalbumin (OVA) peptide, amino acids 323-339, presented by the MHC class II molecule, were used to determine *in vivo* T cell activation. Splenic T cells were purified from the transgenic mice and were labeled with CFSE (1.5  $\mu$ M). T cells ( $5 \times 10^6/100 \mu$ l PBS) were injected intravenously (i.v.) into the tail vein of a healthy, female BALB/c mouse. After 24 h, BMDC ( $2 \times 10^6/2$  ml/well) were stimulated in 6 well plates with 100  $\mu$ g/ml ovalbumin (OVA, Sigma) in the presence or absence of CpG (5  $\mu$ g/ml) for 7 h. After washing twice,  $0.5 \times 10^6$  BMDC, in a volume of 30  $\mu$ l PBS, were then injected into the foot pad of BALB/c mice which had received the T cells, from the transgenic mice, the day before. Three days later, the mice were sacrificed, draining (popliteal) lymph nodes (LN) were harvested and the lymph node cells (LNC) were prepared as described earlier (**Section 2.3.4.3**). The LNC were used for the determination of T cell proliferation by using FACS (**Section 2.3.7.3**). Further, the isolated LNC were cultured ( $4 \times 10^5$  cells/200  $\mu$ l/well) in 96-well, flat bottom plate and restimulated with 10 and 50  $\mu$ g/ml ovalbumin and 0.1 and 1  $\mu$ g/ml ova peptide (OVA 323-339, MoBiTec) in triplicates. After 3 d, the supernatants were collected and used for cytokine ELISA.

### **2.3.9 Enzyme linked immunosorbent assay**

Sandwich enzyme linked immunosorbent assay (ELISA) was used for the detection and quantification of cytokines secreted into different human and mouse cell culture supernatants. Capture antibodies were coated onto plastic 96-well microtiter plates, which were noncovalently adsorbed primarily as a result of hydrophobic interactions. The plates were blocked to avoid non-specific bindings and unbound materials were washed away. The captured cytokine proteins were detected using biotin-conjugated detection antibodies followed by an enzyme-labeled streptavidin step. The chromogenic substrate tetramethylbenzidine (TMB) was added and the level of colored product generated by the bound, enzyme-linked detection reagents was measured spectrophotometrically using an ELISA-plate reader at an OD of 450 nm with the reference OD at 570 nm. The concentration of different cytokines was measured using serial dilution of specific cytokine standards of known concentrations. Different ELISA kits were purchased from Beckman Coulter Company (Human IL-6, IL-8 and TNF- $\alpha$ ),

Krefeld; Biosource (TNF- $\alpha$ ), Solingen; and R & D Systems (Mouse IFN- $\gamma$ , IL-2, IL-10, IL-12p40, IL-12p70 and TGF- $\beta$ 1), Weisbaden, Germany.

## **2.4 Protein Chemical Methods**

### **2.4.1 Cytoplasmic and nuclear protein extraction**

Cytoplasmic and nuclear proteins were extracted by using 'NE-PER Nuclear and Cytoplasmic Extraction Reagent' Kit (Pierce, Perbio, Bonn, Germany). After LPS stimulation, the cell layer was washed with ice cold PBS containing 0.5% NaVO<sub>3</sub>. Cells were scraped off from the culture flasks or the Petri-dishes using a rubber policeman cell scraper (Nunc, Wiesbaden, Germany) and centrifuged (200 x g, 10 min, 4°C). The cell pellet was resuspended in Cytoplasmic Extraction Reagent (CER) with a set of protease inhibitors (Pierce) for 10 min on ice. The cells were centrifuged (12000 x g, 5 min, and 4°C) and the supernatants containing cytoplasmic proteins were collected. The cell pellet containing the nuclear proteins was resuspended in Nuclear Extraction Reagent (NER) for 15 min on ice and centrifuged (12000 x g, 10 min, and 4°C). The supernatants containing nuclear proteins were collected. Both cytoplasmic and nuclear extracts were stored at -80°C until further use.

### **2.4.2 Determination of protein concentration**

The BioRad *DC* Protein Assay kit was used to determine the protein concentration of cytoplasmic and nuclear protein extracts following the manufacturer's instructions. Protein concentration was measured with a spectrophotometer at an optical density (OD) of 700 nm. BSA was used as a standard with a detection limit of 16 pg/ml.

### **2.4.3 Sodium dodecyl sulfate polyacrylamide gel electrophoresis**

Sodium dodecyl sulfate polyacrylamide gel electrophoresis (SDS-PAGE) was used to separate out the proteins on the basis of size from the cytoplasmic protein extracts. Protein samples were prepared using the sample buffer mix (**Section 2.2.2**) in 1:1 ratio with sample by boiling for 5 min at 95°C. Ten to fifty micrograms of proteins were subjected to 10% SDS-polyacrylamide gel (composition as described in **Table 3**) and run at 120 V (constant voltage) until the dye front reached the bottom. Pre-stained SDS-PAGE standard (BioRad Laboratories) was used to know the molecular weight of different proteins.

**Table 3. Composition for the preparation of 10% polyacrylamide gel**

<b>Solution</b>	<b>10%</b>
<b>A.</b> 22.2% (w/v) Acrylamide; 0.6%(w/v) N,N-Methylene-Bis-Acrylamide	6.3 ml
<b>B.</b> 0.5 M Tris; 0.5 M N,N- Bis-(Hydroxyethyl)-Glycine (Bicine, C <sub>6</sub> H <sub>13</sub> NO <sub>4</sub> )	4 ml
<b>C.</b> 10 M Urea	6 ml
Distilled H <sub>2</sub> O	2.7 ml
<b>D.</b> TEMED	15 µl
<b>E.</b> APS, 15 mg/ml	1 ml

#### **2.4.4 Western blot analysis of MAPK and I $\kappa$ B $\alpha$**

The proteins, separated by SDS-PAGE, were transferred from the gel onto nitro-cellulose membranes (BioRad Laboratories) using Hoefer wet electro-transfer system. Membranes were blocked with blocking solution (Roche Diagnostics, Mannheim, Germany) for 1 h at room temperature, washed 5 times for 5 min each using Tris Buffered Saline with Tween-20 (TBST) and incubated with the respective primary antibodies (Cell Signalling Technology, Frankfurt, Germany) for various MAPK and I $\kappa$ B $\alpha$  for overnight at 4°C. I $\kappa$ B $\alpha$  and phosphorylated I $\kappa$ B $\alpha$  were detected using a 1:1500 dilution. P-ERK1/2 (1:1500), ERK1/2 (1:1500), P-P38 (1:800), P38 (1:800) were detected using antibodies reacting specifically with the phosphorylated or the unphosphorylated forms of the proteins. The primary antibody against the phosphorylated I $\kappa$ B $\alpha$  was specific for the detection of the phosphorylated serine 32 residue, while the phosphorylated-specific MAPK antibody detected the phosphorylated threonine 202 and tyrosine 204 residues of ERK1/2 and threonine 180 and tyrosine 182 of P38MAPK. The membranes were incubated with a secondary antibody (peroxidase-conjugated goat anti-rabbit IgG) for 1 h at room temperature (Roche Diagnostics). After 5 washes with TBST, the blots were developed using chemiluminescence horseradish peroxidase substrate (Roche Diagnostics) for 5 min and were exposed to x-ray films (Kodak, Stuttgart, Germany). Loading controls for each signaling molecule were carried out on the same membranes after analyzing the phosphorylated proteins and stripping using a restore western blot stripping buffer (Pierce) for 30 min at 37°C and secondary western blot with antibodies detecting the total amount of the respective kinase.

#### **2.4.5 Electrophoretic mobility shift assay**

Electrophoretic mobility shift assay (EMSA) is a technique for studying gene regulation and determining protein-DNA interactions. The assay is based on the observation that complexes of protein and DNA migrate through a non-denaturing polyacrylamide gel more slowly than free DNA fragments or double-stranded oligonucleotides, resulting in a “shift” in migration of the labeled DNA band. Double-stranded oligonucleotides (Santa Cruz Biotechnology, Heidelberg, Germany) containing the wild-type consensus DNA binding sequences for NF $\kappa$ B (5'-AGTTGAGGGGACTTTCCCAGGC-3') were used. Labeling of oligonucleotides and EMSA was done according to the instructions of the biotin 3'-end DNA Labeling Kit and 'LightShift Chemiluminescent EMSA' Kit, respectively (Perbio Science).

##### **2.4.5.1 Labeling of oligonucleotides**

A concentration of 1 nmol/ml sense and anti-sense oligonucleotides was prepared using Tris-HCl Buffer (10 mM, pH8). On ice, 10  $\mu$ l 5x reaction buffer, 5  $\mu$ l of sense or anti-sense oligonucleotide, 5  $\mu$ l Biotin-N4-CTP, 5  $\mu$ l of Terminal Deoxynucleotidyl Transferase (TdT, 2U/ $\mu$ l prepared in 1x reaction buffer) and 25  $\mu$ l H<sub>2</sub>O was mixed to have 50  $\mu$ l reaction volume. The reaction mix was incubated for 30 min at 37°C. Then 2.5  $\mu$ l EDTA (0.2 M) was added to the reaction mix to stop the labeling reaction. Labeled sense and anti-sense oligonucleotides were mixed in 1:1 ratio (50  $\mu$ l each), incubated for 1 h at room temperature and then stored at -20°C until further use.

##### **2.4.5.2 Binding reaction, gel run, transfer and detection of nuclear protein extracts**

Twenty micro liter of binding reaction per test sample, positive control and the competition reactions containing 3  $\mu$ g of nuclear proteins was prepared (**Table 4**), and incubated for 20 min at room temperature. Loading buffer (5  $\mu$ l of 5 x stock) was added to each binding reaction and was used for the electrophoresis. The DNA-protein samples were separated on 6% native polyacrylamide gels at 100 V (constant voltage) in 0.5 x TBE (**Section 2.2.2**). After electrophoresis, gels were transferred to nylon membranes in an electroblotting unit (Transphor, LKB, Munich, Germany) in 0.5 x TBE, cooled to 10°C for 30 min with 380 mA. After transfer, the membranes were cross-linked at 120 mJ/cm<sup>2</sup> using a UV cross-linker (Biometra, Göttingen, Germany), blocked with 'LightShift' (Perbio Science) for 15 min and then treated with streptavidin-horseradish

peroxidase conjugate for 15 min. After washing, the membranes were incubated for 5 min in substrate equilibration buffer and for 5 min in an enhanced luminol substrate for horseradish peroxidase (HRP) and were exposed to Hyperfilm ECL films.

**Table 4. Preparation of Binding reactions**

Component	Final Amount	Reactions		
		+ ve Control	Test	Competition
Ultrapure Water	---	12 ml	---	---
10 x Binding Buffer	1X	2 $\mu$ l	2 $\mu$ l	2 $\mu$ l
50% Glycerol	2.50%	1 $\mu$ l	1 $\mu$ l	1 $\mu$ l
100 mM MgCl <sub>2</sub>	5 mM	1 $\mu$ l	1 $\mu$ l	1 $\mu$ l
1 $\mu$ g/ $\mu$ l Poly (dI•dC)	50 ng/ $\mu$ l	1 $\mu$ l	1 $\mu$ l	1 $\mu$ l
1% NP-40	0.05%	1 $\mu$ l	1 $\mu$ l	1 $\mu$ l
Unlabeled NF-kB (competition)	200 nmol/ml	---	---	2 $\mu$ l
Control DNA (Biotin-EBNA)	20 fmol	1 $\mu$ l	---	---
EBNA Extract	1 Unit	1 $\mu$ l	---	---
Protein Extract	3 $\mu$ g	---	3 $\mu$ g	3 $\mu$ g
Biotin End-Labeled NF-kB DNA	1 nmol/ml	---	2 $\mu$ l	2 $\mu$ l
<b>Total Volume</b>	---	<b>20 <math>\mu</math>l</b>	<b>20 <math>\mu</math>l</b>	<b>20 <math>\mu</math>l</b>

## 2.5 Statistical Analysis

For analysis of independent parameters between each individual group the Mann-Whitney-U-test was used. For comparison of cultures with and without GM-CSF incubation a paired Wilcoxon test was applied. The paired Student's *t*-test was used to compare differences between sham and CLP groups. The unpaired Student's *t*-test was used to compare differences between replicates of cell cultures within one experiment. Values are expressed either as mean and standard deviation (Mean  $\pm$  SD) or mean and standard error of mean (Mean  $\pm$  SEM) as indicated. A p-value  $\leq$  0.05 was considered to be significant.

# RESULTS

---

## 3. Results

### 3.1 Immunomodulation by GM-CSF

#### 3.1.1 Immunomodulation by GM-CSF in human monocytes

Granulocyte-Macrophage Colony Stimulating Factor (GM-CSF) is a haematopoietic growth factor with immunomodulating activity. Besides its extensively studied role in differentiation and proliferation of monocytes and granulocytes, GM-CSF alters functions of mature monocytes and macrophages. So, GM-CSF potentiates the release of various cytokines such as TNF- $\alpha$ , IL-1 $\alpha$  and IL-1 $\beta$  after LPS stimulation without inducing these mediators by its own [87, 88, 149]. Based on the growing interests in its immunostimulatory properties, the underlying mechanisms of GM-CSF on LPS-induced TNF- $\alpha$  secretion of human monocytes was examined. First, the optimal dose and time of GM-CSF in terms of priming of LPS-induced cytokine synthesis was analyzed in human monocytes.

##### 3.1.1.1 Time and Dose kinetics for GM-CSF

In order to determine the optimal time and dose of GM-CSF for priming of TNF- $\alpha$  production by human monocytes, peripheral blood monocytes (PBMC) were incubated with different doses of GM-CSF for different time periods. Monocytes were stimulated for 4 h with LPS from *S. friedenaui*, since former experiments had revealed a significant TNF- $\alpha$  secretion in the supernatant at this time point. The increased LPS-induced TNF- $\alpha$  synthesis caused by GM-CSF reached its maximum after a preincubation period of 6 h and remained stable up to 24 h (**Figure 11A**). Furthermore, the GM-CSF effect on TNF- $\alpha$  synthesis revealed a dose dependency. The maximal response was observed at a dose of 100 ng/ml GM-CSF (**Figure 11B**). Based on these data, the further experiments to characterize and modulate GM-CSF priming for TNF- $\alpha$  and also IL-8 production by isolated monocytes were performed with a dose of 10 ng/ml and 6 h preincubation. The

dose of 10 ng/ml GM-CSF was chosen, since this was the peak level observed in pharmacokinetic studies in the clinical application of GM-CSF.

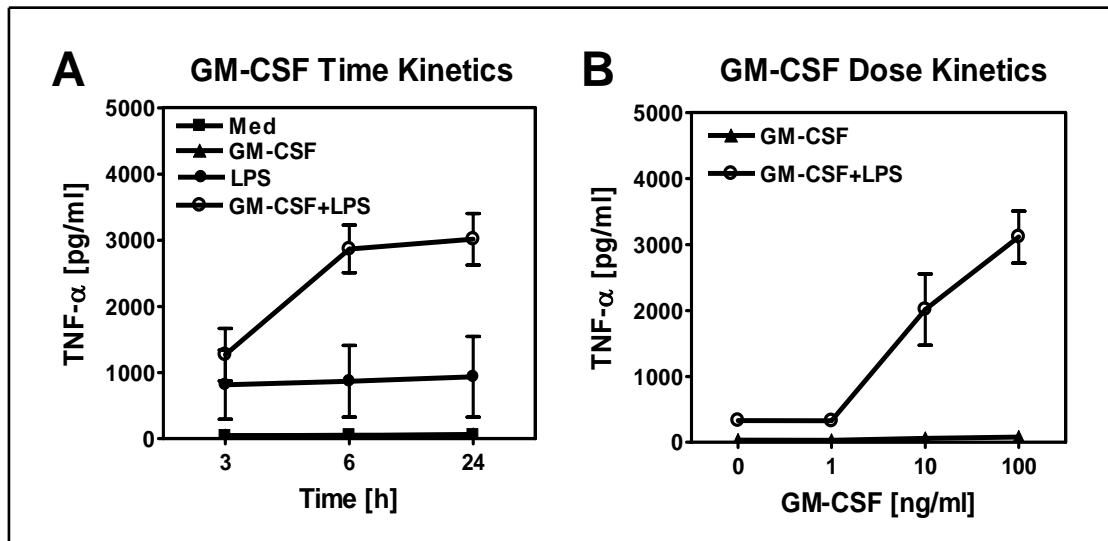


**Figure 11. Time- and dose-dependent effect of GM-CSF on LPS-induced TNF- $\alpha$  production.**

(A) TNF- $\alpha$  production of monocytes expressed as mean  $\pm$  SD of three independent experiments. The cells were preincubated with rhGM-CSF over different periods of time as shown and thereafter stimulated with 10 ng/ml LPS for 4 h. Unstimulated samples served as controls (Med). (B) TNF- $\alpha$  production by monocytes expressed as mean  $\pm$  SD of triplicate experiments. The cells were preincubated with different doses of rhGM-CSF and thereafter 10 ng/ml LPS stimulation for 4 h.

### 3.1.1.2 Effect of GM-CSF on LPS-induced TNF- $\alpha$ and IL-8 secretion of human monocytes

With the above standardized time and dose conditions, GM-CSF increased the LPS-induced TNF- $\alpha$  synthesis (**Figure 12A**) by a factor of 4.8 (range 2.3-5.9,  $n=14$ ,  $p < 0.0005$  in Student's T-test) and IL-8 synthesis (**Figure 12B**) by a factor of 2.6 (range 1.2-5.6,  $n=14$ ,  $p < 0.0005$  in Student's T-test). In none of these experiments, an increase of TNF- $\alpha$  secretion was observed after the preincubation with GM-CSF in the absence of LPS (**Figure 12A**). However, IL-8 synthesis was slightly increased upon GM-CSF preincubation alone (**Figure 12B**).

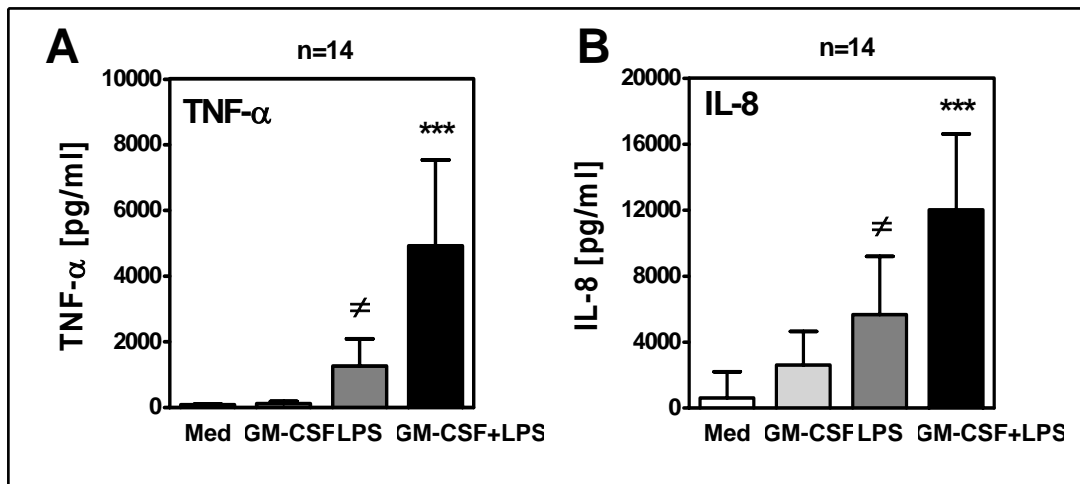


**Figure 12. Increased TNF- $\alpha$  and IL-8 production after GM-CSF preincubation in human monocytes.** (A) TNF- $\alpha$  and (B) IL-8 production by monocyte cultures carried out in triplicates. Data shown is mean  $\pm$  SD of indicated numbers of pooled experiments. The cells were preincubated with 10 ng/ml of rhGM-CSF for 6 h and thereafter stimulated with 10 ng/ml LPS for 4 h. Unstimulated samples served as controls (Med).  $\neq$  indicates statistical significant difference to LPS vs. GM-CSF and \* indicates statistical significant difference to GM-CSF+LPS vs. LPS for both TNF- $\alpha$  and IL-8 synthesis in Student's T-test. n: number of independent experiments.  $\neq$  and \*\*\*,  $P < 0.0005$ .

### 3.1.1.3 Effect of GM-CSF priming on LPS-induced phosphorylation of I $\kappa$ B $\alpha$ and MAPKinases

In order to analyze the signaling cascades involved in the GM-CSF-mediated priming of LPS-induced TNF- $\alpha$  synthesis, different MAPKinases and the phosphorylation of I $\kappa$ B $\alpha$  were detected by Western blotting. GM-CSF is known to activate various MAPKinases [114]. It has been shown that GM-CSF induces phosphorylation of MEK1/2 and ERK1/2 in human neutrophils [114, 150]. In the present study, we observed the induction of ERK1/2 phosphorylation by LPS, however, to a much lesser degree than by GM-CSF alone. LPS stimulation after GM-CSF preincubation did not further increase the phosphorylation of these signaling molecules (**Figure 13**). The P38 MAPK was marginally induced by GM-CSF alone in monocytes. A clear induction was observed after LPS alone, but the most pronounced signal was shown in GM-CSF primed monocytes (**Figure 13**). The amount of unphosphorylated MAPkinases was affected neither by LPS nor by GM-CSF. Human monocytes preincubated with GM-CSF (10 ng/ml) for 6 h and stimulated thereafter with LPS (10 ng/ml) for 45 min showed an enhanced phosphorylation of I $\kappa$ B $\alpha$  compared to LPS alone while GM-CSF on its own had no effect (**Figure 13**).

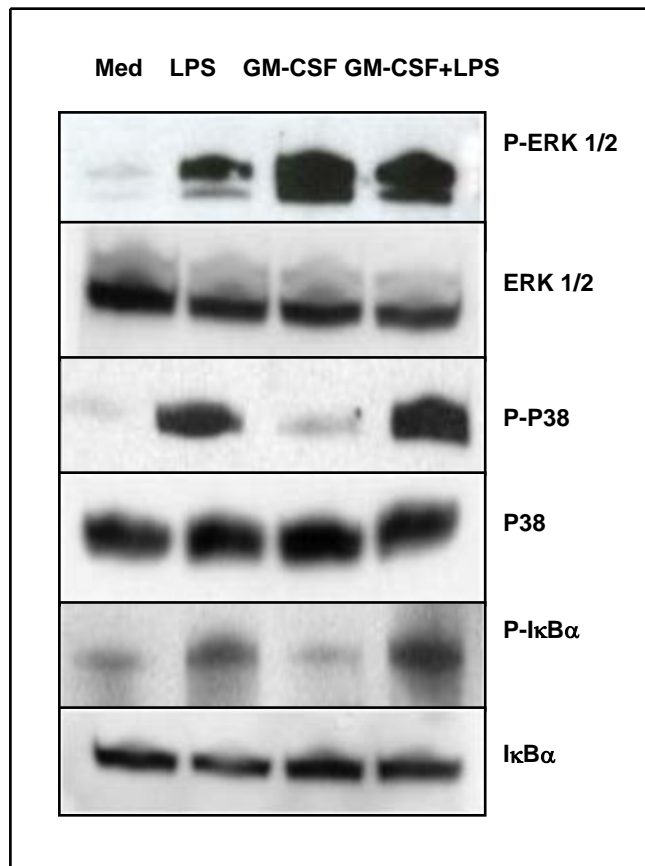


**Figure 13. Effect of GM-CSF on phosphorylation of IκBα and MAPK.**

Western blot of 20 μg cytoplasmic protein extracts from isolated human monocytes after 6 h preincubation with or without GM-CSF. After preincubation, GM-CSF was removed, cells were washed twice with PBS and afterwards stimulated with LPS (10 ng/ml) for 45 min and compared to untreated (no GM-CSF, shown as Med) and unstimulated (no LPS, only preincubation with GM-CSF). The phosphorylated forms of ERK1/2, P38 kinase and IκBα are shown from the top to bottom of the figure as indicated. The total amount of each kinase as loading control is shown in the panel below the phosphorylated forms. A representative blot of three independent experiments is shown.

#### 3.1.1.4 Effect of GM-CSF on LPS-induced NFκB binding in the nucleus

TNF-α gene activation depends on the binding of the NFκB transcription factor to its promoter in the nucleus. The binding of the transcription factor was analyzed by EMSA. Analysis was performed after preincubation with GM-CSF (10 ng/ml for 6 h) and subsequent LPS-stimulation (10 ng/ml) for 45 min. Former experiments revealed a maximal NFκB binding after 45 min of LPS stimulation. Electromobility shift assay showed that LPS alone caused binding of the transcription factor as expected (**Figure 14, Lane 2**). While GM-CSF in the absence of LPS did not increase NFκB binding compared to unstimulated controls (**Figure 14, Lanes 1 vs. 3**). However, corresponding to the enhanced TNF-α protein production after GM-CSF preincubation, an increased

NF $\kappa$ B binding was observed after GM-CSF preincubation and subsequent LPS stimulation (**Figure 14, Lane 4**).

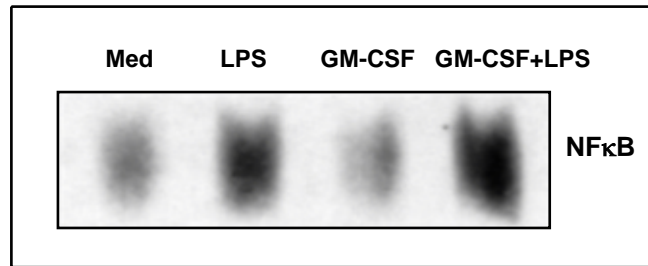


**Figure 14. Effect of GM-CSF priming on LPS-induced NF $\kappa$ B binding.**

EMSA with 3  $\mu$ g nuclear protein extracts of human monocytes for NF $\kappa$ B oligonucleotides. The cells were preincubated with or without GM-CSF (10 ng/ml) for 6 h, washed twice with PBS and subsequently, stimulated with LPS (10 ng/ml) for 45 min. A representative blot of three independent experiments is shown.

### 3.1.2 Immunomodulation by GM-CSF in THP-1 cells

After we observed the GM-CSF priming in LPS-induced human monocytes, we continued the same approach for THP-1 human monocytic cell line as a model for human peripheral blood monocytes (PBMC). We did the standardization experiment to know whether the dose and the time for THP-1 cells are same as observed in human PBMC. Afterwards, we continued to see the effect of GM-CSF on LPS-induced THP-1 monocytes with regard to TNF- $\alpha$  synthesis and the involved signaling pathway.

#### 3.1.2.1 Time and Dose kinetics for GM-CSF

The time and the dose standardization of GM-CSF and LPS for priming of TNF- $\alpha$  production by human THP-1 cells were performed to determine their optimal dose and time. The cells were preincubated with different doses of GM-CSF and then were stimulated with LPS from *S. friedenaui*. The optimal time for the maximum priming effect in LPS-induced TNF- $\alpha$  synthesis by GM-CSF was observed as early as after 90 min and was stable up to 24 h (Figure 15A, shown only up to 6 h). The priming effect of GM-CSF was also dose dependent and the maximal response was observed at a dose of 10 ng/ml GM-CSF (Figure 15B). Based on these data, all the further experiments were performed with a dose of 10 ng/ml GM-CSF for 90 min preincubation and subsequent LPS stimulation for 4 h.

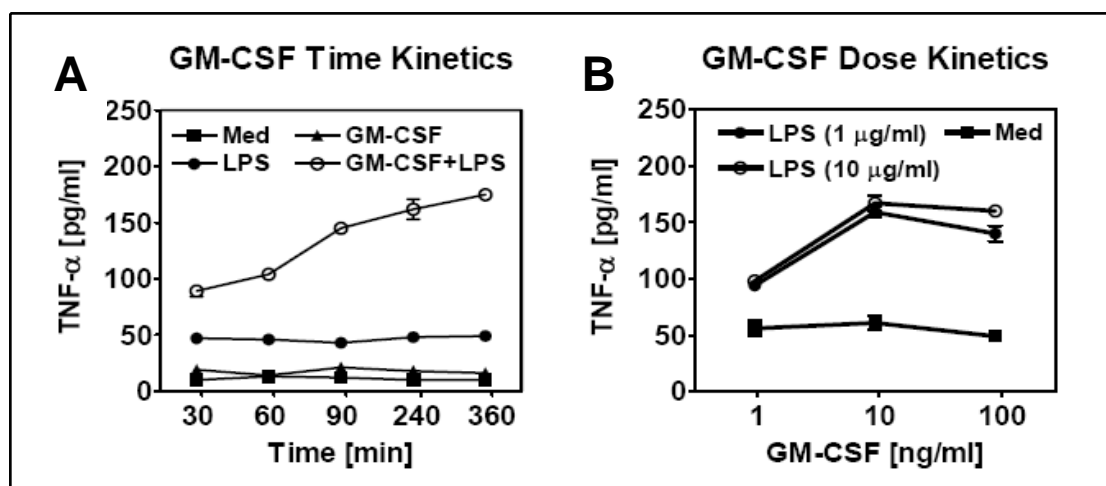


**Figure 15. Time- and dose-dependent effect of GM-CSF on LPS-induced TNF- $\alpha$  production.**

(A) TNF- $\alpha$  production by THP-1 cell cultures carried out in triplicates. Data shown is mean  $\pm$  SD of indicated numbers of pooled experiments. The cells were preincubated with rhGM-CSF (10 ng/ml) at different time points as shown. After preincubation with GM-CSF, the cells were stimulated with 1  $\mu$ g/ml LPS for 4 h. (B) TNF- $\alpha$  production by THP-1 cells expressed as mean  $\pm$  SD of cell cultures carried out in triplicates after preincubation with different doses of rhGM-CSF for 90 min. After preincubation with GM-CSF the cells were stimulated with 1 and 10  $\mu$ g/ml LPS for 4 h. Unstimulated samples served as controls (Med). Data shown is representative of three independent experiments.

### 3.1.2.2 Effect of GM-CSF on LPS-induced TNF- $\alpha$ , IL-8 and IL-6 secretion by THP-1 cells

Following the above shown standardized time and dose conditions, GM-CSF at a dose of 10 ng/ml for 90 min preincubation increased LPS-induced (1  $\mu$ g/ml for 4 h) TNF- $\alpha$  synthesis (**Figure 16A**) by a factor of 2.5 (range 1.9-3.4, n=7,  $p < 0.005$  in Student's T-test) and IL-8 synthesis (**Figure 16B**) by a factor of 2.4 (range 1.9-3.6, n=8,  $p < 0.0005$  in Student's T-test). In none of these experiments, an increase of TNF- $\alpha$  was observed after the preincubation with GM-CSF in the absence of LPS. We did not observe a significant IL-6 secretion in THP-1 cells neither after LPS alone nor with GM-CSF and subsequent LPS stimulations (**Figure 16C**).

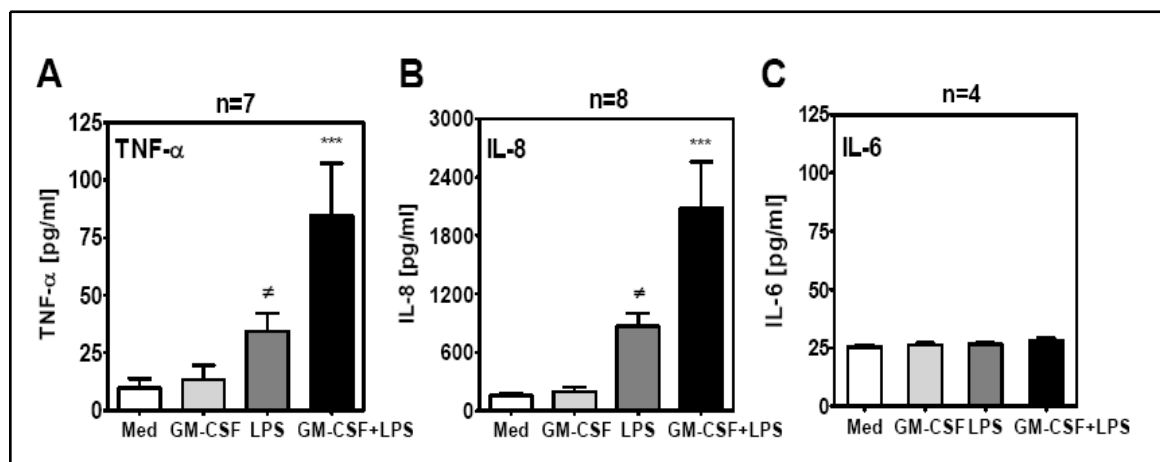


**Figure 16. Increased TNF- $\alpha$  and IL-8 but unchanged IL-6 production by THP-1 cells after GM-CSF preincubation.**

(A) TNF- $\alpha$  (B) IL-8 and (C) IL-6 production by THP-1 cell cultures carried out in triplicates. Data shown is mean  $\pm$  SD of indicated numbers of pooled experiments. The cells were preincubated with 10 ng/ml of rhGM-CSF. After 90 min, the cells were stimulated with 1  $\mu$ g/ml LPS for 4 h. Unstimulated samples served as controls (Med). # indicates statistical significant difference to LPS vs. GM-CSF and \* indicates statistical significant difference to GM-CSF+LPS vs. LPS for both TNF- $\alpha$  and IL-8 synthesis in Student's T-test. n: number of independent experiments. # and \*\*\*,  $P < 0.0005$ .

### 3.1.2.3 Effect of GM-CSF priming on LPS-induced phosphorylation of I $\kappa$ B $\alpha$ and MAPKinases

In order to analyze the signaling cascade involved in the GM-CSF-mediated priming of LPS-induced TNF- $\alpha$  synthesis in THP-1 cells, we examined different MAPKinases and the phosphorylation of I $\kappa$ B $\alpha$  by Western blotting. Similar to human monocytes, phosphorylation of ERK1/2 in THP-1 cells was also induced by LPS, however, to a lesser degree than by GM-CSF alone. Unlike human monocytes, LPS stimulation after GM-CSF preincubation further increased the phosphorylation of these signaling molecules (**Figure 17**). The P38 MAPK was marginally induced by GM-CSF alone in

THP-1 cells. A clear induction was found after LPS treatment alone, but the most pronounced signal was observed in LPS-treated THP-1 cells preincubated with GM-CSF (**Figure 17**). JNK, another member of the MAP kinase family, also showed more pronounced phosphorylation after GM-CSF preincubation and LPS stimulation in comparison to LPS or GM-CSF alone (**Figure 17**). The amount of unphosphorylated MAPkinases was affected neither by LPS nor by GM-CSF (**Figure 17**). THP-1 cells, preincubated with GM-CSF (10 ng/ml) for 30 min and stimulated thereafter with LPS (1  $\mu\text{g/ml}$ ) for 45 min showed an enhanced phosphorylation of I $\kappa$ B $\alpha$  compared to LPS alone, while GM-CSF on its own had no effect and was the same as the control signal (**Figure 17**) which was accompanied by a corresponding opposite pattern of the total I $\kappa$ B protein as a step for protease-dependent degradation subsequent to phosphorylation.

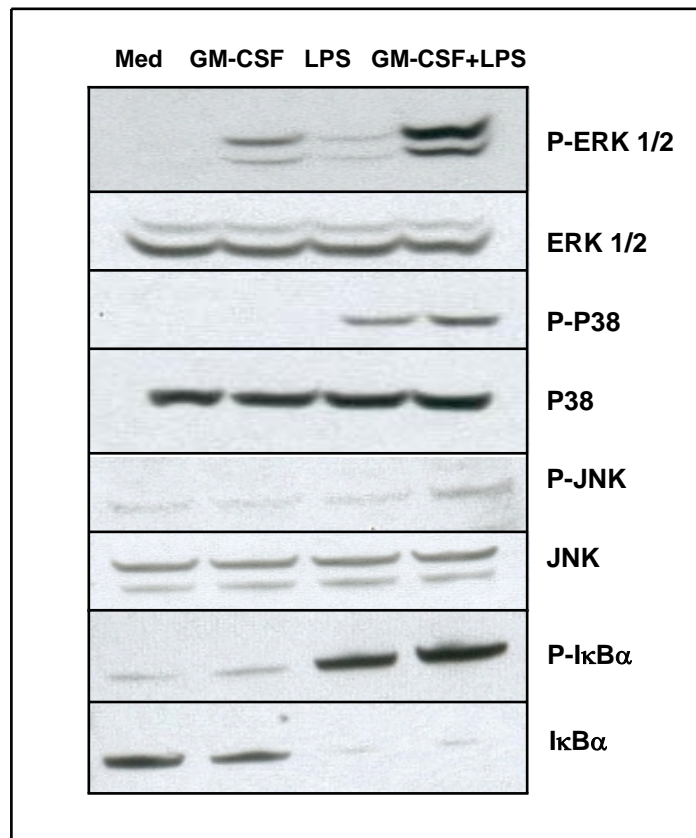


**Figure 17. Effect of GM-CSF on phosphorylation of I $\kappa$ B $\alpha$  and MAPK.**

Western blot of 25  $\mu\text{g}$  cytoplasmic protein extracts from THP-1 cells after 90 min preincubation with or without GM-CSF. After preincubation, GM-CSF was removed, cells were washed twice with PBS and afterwards stimulated with LPS (1  $\mu\text{g/ml}$ ) for 45 min. The phosphorylated forms of ERK1/2, P38 MAPKinase, JNK and I $\kappa$ B $\alpha$  are shown from the top to bottom of the figure as indicated. The total amount of each kinase as loading control is shown in the panel below the phosphorylated forms. The blot shown is representative of a minimum of three independent experiments.

#### 3.1.2.4 Effect of GM-CSF on LPS-induced NFκB binding in the nucleus

The binding of the transcription factor NFκB to its promoter was also analyzed in THP-1 cells using EMSA. Analysis was performed after preincubation with GM-CSF (10 ng/ml for 90 min) and subsequent LPS-stimulation (1 μg/ml) for 45 min. EMSA results showed that LPS alone caused binding of the transcription factor as expected (**Figure 18, Lane 3**), while GM-CSF alone did not induce any NFκB binding when compared to unstimulated controls (**Figure 18, Lanes 1 vs. 2**). However, corresponding to the enhanced TNF-α protein production after GM-CSF activation, an increased NFκB binding was observed after GM-CSF preincubation and subsequent LPS stimulation (**Figure 18, Lane 4**). Wild type (WT) unlabeled NFκB oligonucleotides were included for the competition reaction as negative control (**Figure 18, Lane 5**)

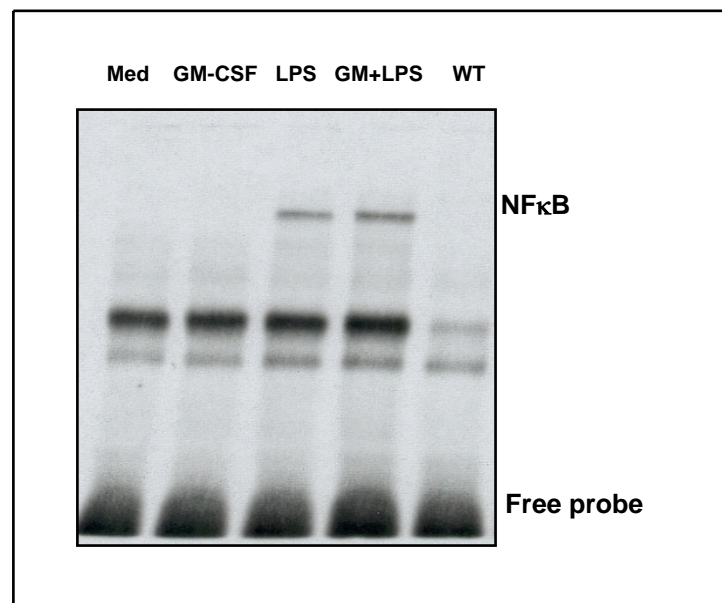


**Figure 18. Effect of GM-CSF priming on LPS-induced NFκB binding.**

EMSA with 3 μg nuclear protein extracts of THP-1 cells for NFκB oligonucleotides. The cells were preincubated with 10 ng/ml GM-CSF (Lane 2) for 90 min. After preincubation, GM-CSF was removed, cells were washed twice with PBS and stimulated with LPS (1 μg/ml) for 45 min (Lane 4). Unstimulated samples served as controls (Lane 1). Wild type (WT) NFκB oligonucleotides were taken as the EMSA control (Lane 5). The blot shown is representative of a minimum of three independent experiments.

#### 3.1.2.5 Effect of GM-CSF on translocation of NFκB- p50 and p65

NFκB consists of hetero (p50/p65) - or homodimers (p50/p50). Therefore, not only binding of the transcription factors but also the levels of the total protein amount of corresponding transcription factor NFκB subunits p50 and 65 were analyzed by Western blotting (**Figure 19**). The experiments were performed with a dose of 10 ng/ml GM-CSF for 90 min preincubation and with subsequent LPS-stimulation (1 μg/ml, 45 min). These

experiments revealed that GM-CSF preincubation plus LPS-stimulation leads to elevated nuclear levels of the NF $\kappa$ B component p65 and to a lesser degree of p50.

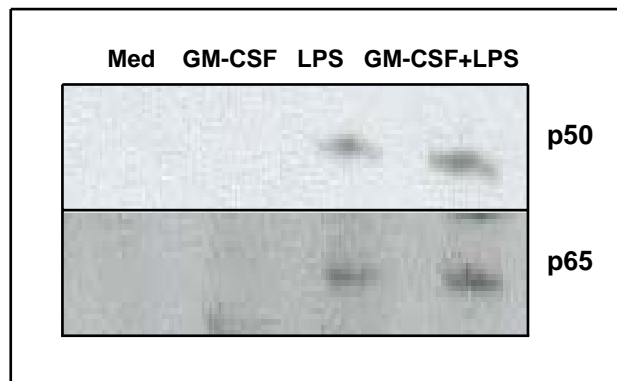


**Figure 19. Effect of GM-CSF priming on LPS-induced translocation of p50 and p65.**

Immunoblots carried out with 25  $\mu$ g nuclear protein extracts for the NF $\kappa$ B components p50 and p65 of human THP-1 cells after 90 min preincubation with or without GM-CSF. After preincubation GM-CSF was removed, cells were washed twice with PBS and afterwards stimulated with LPS (1  $\mu$ g/ml) for 45 min. The blot shown is representative of a minimum of three independent experiments.

### 3.1.3 Immunomodulation by GM-CSF after hemorrhagic shock

GM-CSF could successfully prime both the human monocytes as well as THP-1 cells up to a significant level for TNF- $\alpha$  synthesis after LPS stimulation. The cytokine synthesis was paralleled by a correspondingly enhanced MAPkinase and I $\kappa$ B $\alpha$  signaling. This immunostimulatory capacity of GM-CSF was then harnessed for an immunosuppressed system after hemorrhagic shock. Before proceeding for hemorrhagic shock model directly, the effect of GM-CSF was studied in peritoneal macrophages of normal untreated mice. Afterwards, we continued to investigate the effect of GM-CSF on LPS-induced peritoneal macrophages with regard to TNF- $\alpha$  synthesis and the involved MAPKinase and NF $\kappa$ B regulating I $\kappa$ B $\alpha$  signaling after hemorrhagic shock.

#### 3.1.3.1 Effect of GM-CSF in normal peritoneal macrophages

##### 3.1.3.1.1 Time kinetics for GM-CSF priming in normal peritoneal macrophages

Characterization of GM-CSF effect was determined in normal peritoneal macrophages from untreated mice in terms of dose and time dependency. GM-CSF priming for LPS-stimulated TNF- $\alpha$  response was a time-dependent phenomenon. The effect started as early as after 1 h preincubation and further increased until a preincubation period of 6 h and stayed stable for at least 10 h (data not shown). Therefore, all further experiments were performed with a preincubation period of 6 h. The enhanced TNF- $\alpha$  response after 6 h preincubation with GM-CSF and subsequent LPS stimulation showed a dose-dependency also, both sensitizing macrophages for lower LPS doses and increasing the maximal response (**Figure 20**).

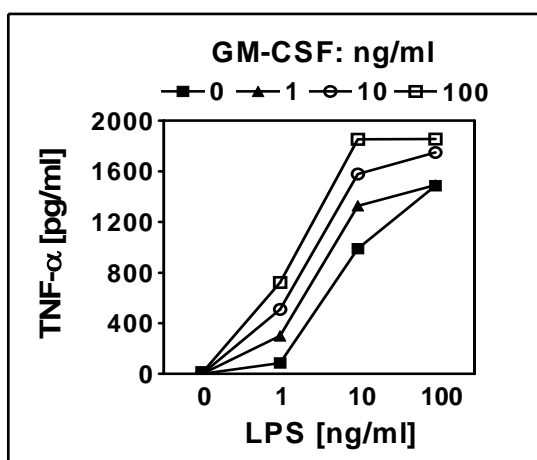


**Figure 20. Priming of TNF- $\alpha$  response after GM-CSF incubation.**

Peritoneal macrophages were pooled (2-3 mice) from normal mice and incubated in triplicates for 6 h with different doses of GM-CSF as indicated in the figure and subsequently stimulated with the different LPS-doses shown on the x-axis for 4 h before TNF- $\alpha$  was detected in the supernatant. Data shown is representative of 3 independent experiments.

### 3.1.3.1.2 Effect of GM-CSF on TNF- $\alpha$ secretion in normal peritoneal macrophages

With the standardized time and dose conditions of 10 ng/ml GM-CSF preincubation for 6 h and subsequent 1 ng/ml LPS-stimulation for 4 h for mouse peritoneal macrophages, increased TNF- $\alpha$  synthesis (**Figure 21**) by a factor of 4.07 (range 1.6-10.7, n=10, p< 0.0007 in Student's T-test). However, increase of TNF- $\alpha$  production was observed in none of these experiments after the preincubation with GM-CSF in the absence of LPS.

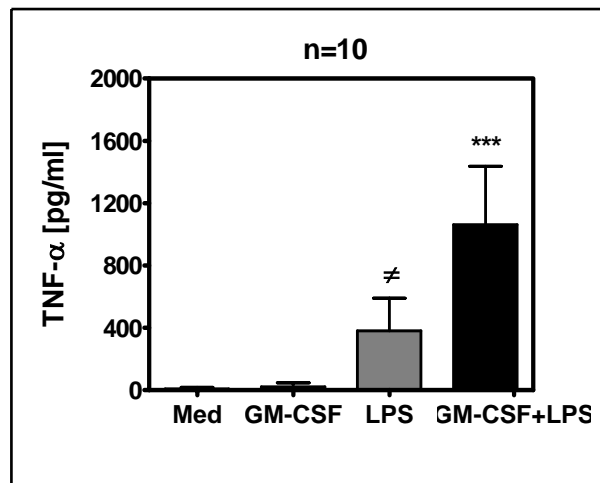


**Figure 21. Priming of TNF- $\alpha$  response after GM-CSF incubation**

Peritoneal macrophages were pooled (2-3 mice) and incubated in triplicates. The cells were preincubated with or without 10 ng/ml GM-CSF. After 6 h, the macrophages were stimulated with 1 ng/ml LPS for 4 h and the supernatants were collected for TNF- $\alpha$  ELISA. Untreated samples served as the control (Med). Values are expressed as mean  $\pm$  SEM of pooled experiments.  $\neq$  indicates statistical significant difference to LPS vs. GM-CSF and \* indicates statistical significant difference to GM-CSF+LPS vs. LPS for TNF- $\alpha$  synthesis. n: number of independent experiments.  $\neq$  and \*\*\*,  $P < 0.0005$ .

### 3.1.3.1.3 Effect of GM-CSF priming on LPS-induced phosphorylation of I $\kappa$ B $\alpha$ and MAPKinases in normal peritoneal macrophages

Before analyzing the signaling involved in the GM-CSF-mediated priming of LPS-induced TNF- $\alpha$  synthesis after hemorrhagic shock, we analyzed untreated mice for different MAPKinase signaling cascade and the phosphorylation of I $\kappa$ B $\alpha$  by Western blotting. The increase in cytokine synthesis after GM-CSF preincubation led to a more intense activation of the signaling molecules ERK1/2, P38MAPK and I $\kappa$ B $\alpha$  at 45 min after LPS stimulation (**Figure 22B**). The priming effect of GM-CSF on I $\kappa$ B $\alpha$  phosphorylation and ERK1/2 activation was also visible at earlier time points of LPS stimulation (15 and 30 min, **Figure 22A**).

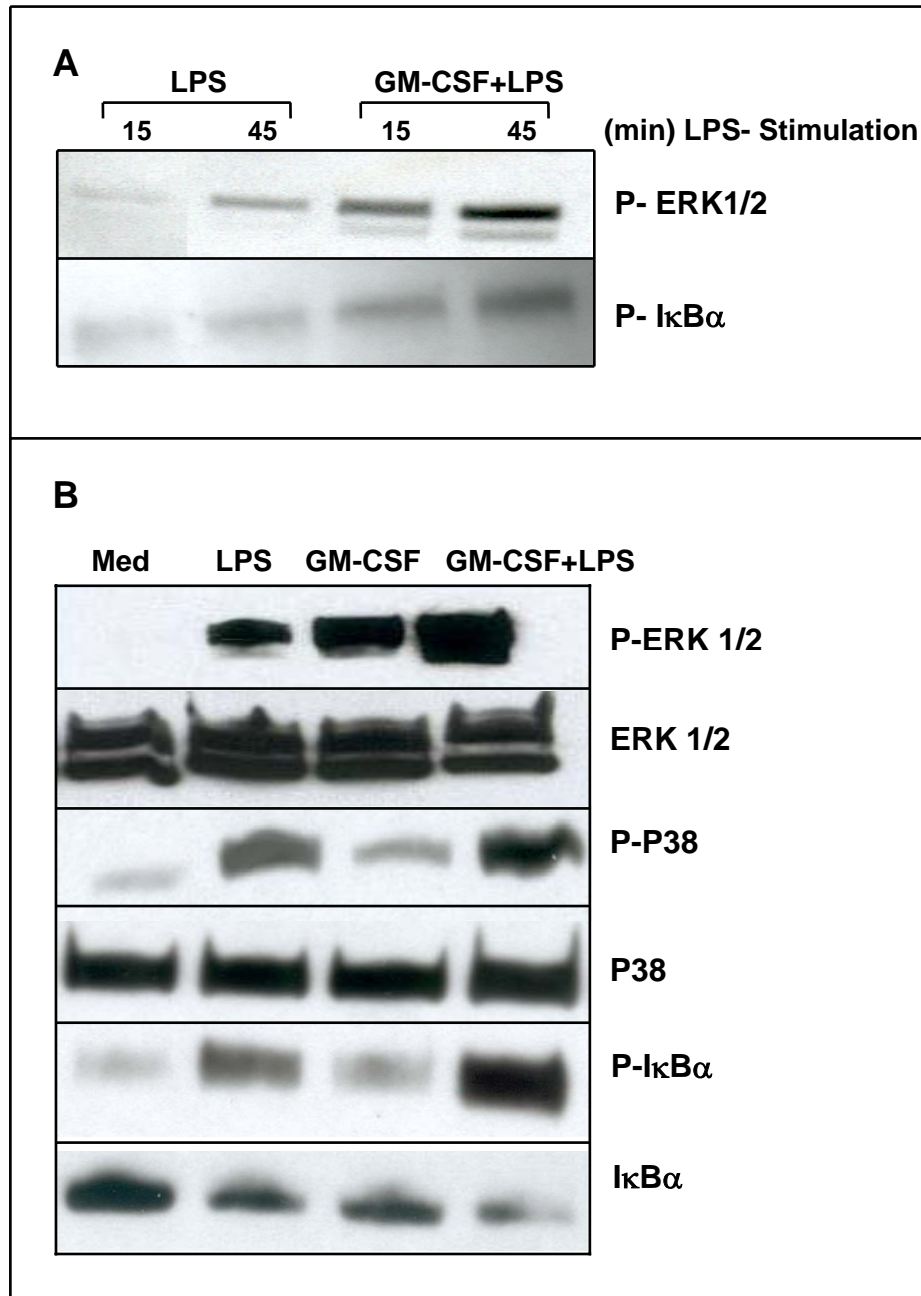


**Figure 22. Elevated MAPKinase and IκBα phosphorylation after GM-CSF preincubation and subsequent LPS stimulation.**

(A) Peritoneal macrophages (pooled cells from 3 mice) were harvested from the normal healthy mice and preincubated with or without GM-CSF for 6 h and then stimulated for different time periods (15 and 45 min) with LPS. Cytoplasmic proteins were extracted and P-ERK1/2 and P-IκBα were analyzed by Western blotting. Both P-ERK1/2 and P-IκBα were enhanced more after 45 min of LPS stimulation than that of 15 min. (B) Peritoneal macrophages (pooled cells from 3 mice) were harvested from the normal healthy mice and incubated for 6 h with GM-CSF (10 ng/ml) and 45 min with LPS (1 ng/ml) along with their respective controls. Cytoplasmic proteins were extracted and IκBα, ERK1/2 and P38MAPK were analyzed by Western blotting using specific antibodies for phosphorylated IκBα, ERK1/2 and P38MAPK. The respective control antibody was used to detect the total amount of each kinase. GM-CSF enhanced LPS-stimulated IκBα, P38 and ERK1/2 phosphorylation, while only ERK1/2 and to a lesser degree P38 were activated by GM-CSF on its own. The blot shown is representative for a minimum of three independent experiments.

### 3.1.3.2 Effect of GM-CSF after hemorrhagic shock

It has been shown that GM-CSF renders the capacity to enhance monocytes' and macrophages' effector functions after shock as well as during sepsis [95-97]. GM-CSF is also reported to restore the reduced TNF- $\alpha$  production of splenic and peritoneal macrophages after hemorrhagic shock in rats [94]. On the basis of these immunostimulatory properties of GM-CSF, we also analyzed the effect of GM-CSF applied *in vitro* on peritoneal macrophages after hemorrhagic shock in mouse model.

#### 3.1.3.2.1 Hemorrhagic shock model characterization

In the first set of experiments the blood pressure-dependent mortality of the hemorrhagic shock model was established. While a shock with a mean arterial pressure (MAP) of 35 mm Hg for 45 min resulted in 100% mortality within 48 h, a MAP of 45 mm Hg for 45 min caused 40% mortality. A MAP of 50 mm Hg caused only 20% mortality and after 55 mm Hg no deaths were observed. The survival rate (%) and the corresponding withdrawn blood volumes are shown in **Table 5**. Since the primary scope of the study was to analyze the deterioration of the immune response after hemorrhagic shock, all further experiments were performed with 50 mm Hg shock.

**Table 5. Survival rate after hemorrhagic shock**

MAP [mm Hg]	sham	55	50	45	35
Survival [%]	100	100	80	60	0
Bleeding volume [ $\mu$ l]	0	270 $\pm$ 82	740 $\pm$ 117	1320 $\pm$ 103	2000 $\pm$ 150

Survival rate is shown as percentage, 72 h after hemorrhagic shock with different mean arterial pressure. The corresponding withdrawn blood volume is indicated in the second row (mean  $\pm$  standard deviation). Survival rate was calculated out of 10 animals per group. Survival after 72 h equals long term survival, since no animal died in the subsequent 4 weeks.

#### 3.1.3.2.2 Cytokine response in peritoneal macrophages after hemorrhage

Hemorrhagic shock of 50 mm Hg MAP for 45 min leads to an impairment of the animals' immune response after 20 h. Peritoneal macrophages isolated 20 h after hemorrhagic shock showed a significantly decreased production of TNF- $\alpha$  after *in vitro* stimulation with LPS in comparison to macrophages from sham-operated animals (**Figure 23**).

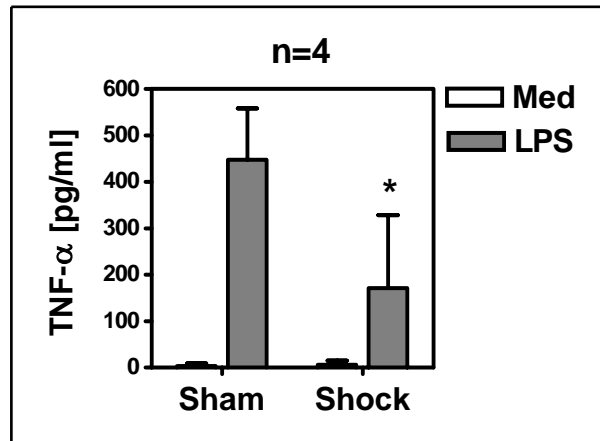


**Figure 23. Decreased TNF- $\alpha$  production in LPS-stimulated cells.**

Peritoneal macrophages were harvested 20 h after hemorrhage (Shock) or sham-operation (Sham) and incubated for 4 h with (grey bars) or without LPS (white bars). Cellular supernatants were collected and TNF- $\alpha$  was detected by ELISA. Hemorrhage caused a significant reduction of LPS-induced TNF- $\alpha$  synthesis. Data represent mean  $\pm$  SD of 4 independent experiments with pooled macrophages of 2 mice /group. \* Means statistical significant difference to shock vs. sham LPS for TNF- $\alpha$  synthesis in Mann-Whitney-U-Test. \*,  $p < 0.05$ .

### 3.1.3.2.3 LPS-induced I $\kappa$ B $\alpha$ signaling after hemorrhage

The Nuclear Factor (NF) $\kappa$ B is considered to be the predominant transcription factor that regulates TNF- $\alpha$  response in most cells. NF $\kappa$ B is under control of its inhibitor I $\kappa$ B and is only transferred to the nucleus upon phosphorylation and ubiquitin-dependent degradation of I $\kappa$ B (**Figure 3**). Therefore, the activation of the NF $\kappa$ B pathway was indirectly analyzed by determination of the phosphorylated form of the cytoplasmic inhibitor of NF $\kappa$ B, the I $\kappa$ B $\alpha$  protein. P-I $\kappa$ B $\alpha$  was enhanced upon LPS stimulation in both sham and shock mice, however, the phosphorylation were less intense in macrophages from mice after hemorrhagic shock than after sham operation. Nonphosphorylated I $\kappa$ B $\alpha$  signal was found to be more intense after hemorrhage as expected. Thus, in peritoneal macrophages harvested 20 h after hemorrhage the reduced TNF- $\alpha$  production after LPS stimulation was accompanied by a decreased I $\kappa$ B $\alpha$  phosphorylation while the unphosphorylated form of I $\kappa$ B $\alpha$  was enhanced after hemorrhagic shock (**Figure 24**).

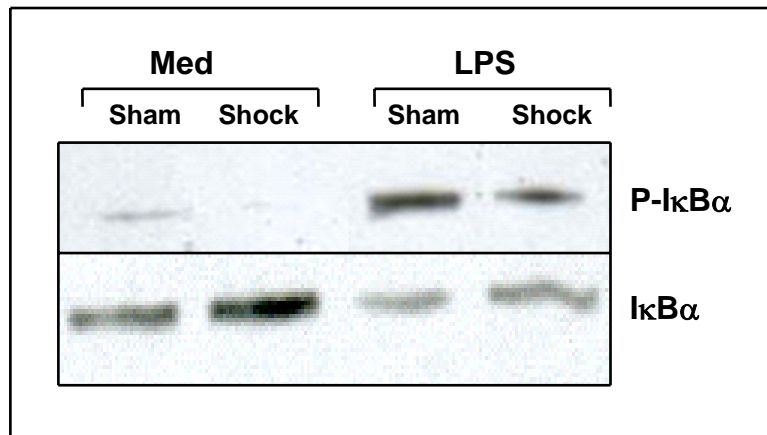


**Figure 24. LPS-induced IκBα phosphorylation in peritoneal macrophages after hemorrhage.** Peritoneal macrophages (pooled cells from 2-3 mice/group) were harvested 20 h after hemorrhage (Shock) or sham-operation (Sham) and incubated for 45 min with or without LPS (Med). Cytoplasmic proteins were extracted and both phosphorylated as well as nonphosphorylated IκBα was analyzed by Western blotting. The blot shown is representative of a minimum of three independent experiments.

#### 3.1.3.2.4 LPS-induced ERK1/2 and P38 signaling after hemorrhage

Various cytokines including TNF- $\alpha$  are regulated by cytoplasmic kinases belonging to the MAPK family. Both the P38MAPK and ERK1/2 were analyzed in peritoneal macrophages isolated 20 h post hemorrhagic shock with and without LPS-stimulation. In accordance with the response of IκBα phosphorylation, ERK1/2 activation was also found to be less in peritoneal macrophages isolated 20 h after hemorrhagic shock when compared with the response in peritoneal cells harvested from sham-operated animals. In contrast, the P38MAPK was found to be obviously induced after shock in peritoneal macrophages even without additional LPS-stimulation. After LPS-application *in vitro* the phosphorylation of P38MAPK was much more intense than in correspondingly treated cells from sham-operated mice (**Figure 25**).

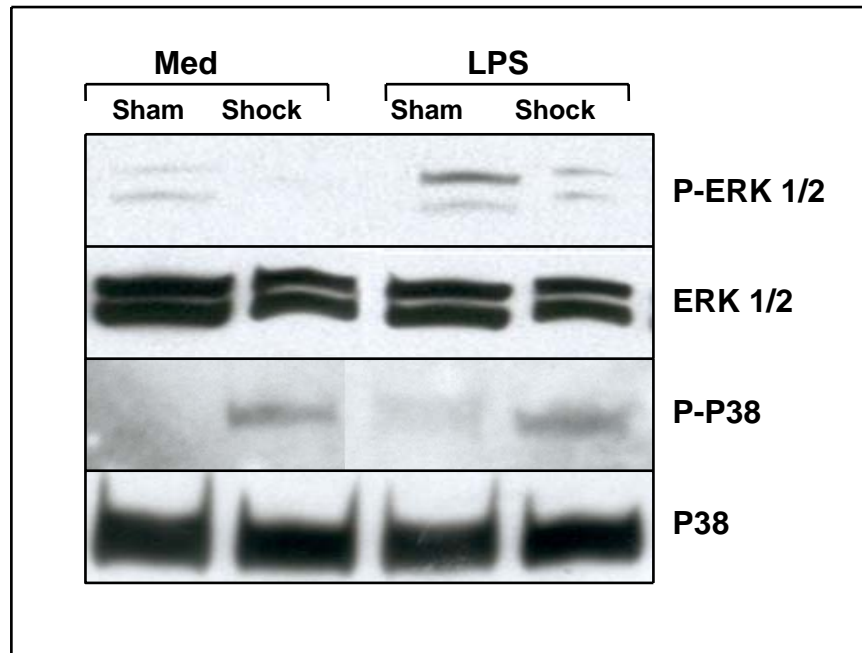


**Figure 25. LPS-induced P38 and ERK1/2 signaling in peritoneal macrophages after hemorrhage.**

Peritoneal macrophages (pooled cells from 2-3 mice/group) were harvested 20 h after hemorrhage (Shock) or sham-operation (Sham) and incubated for 45 min with or without LPS. Cytoplasmic proteins were extracted; P-P38 and P-ERK1/2 were analyzed by Western blotting. Blots were probed sequentially with anti-P38 and anti-ERK1/2 antibodies to determine the total amount of the respective kinase loaded. The blot shown is representative of a minimum of three independent experiments.

### 3.1.3.2.5 GM-CSF preincubation enhanced the TNF- $\alpha$ production after hemorrhage

When GM-CSF is applied *in vitro* on peritoneal macrophages harvested from mice 20 h after hemorrhagic shock, GM-CSF slightly, but significantly enhances the LPS-induced TNF- $\alpha$  synthesis (**Figure 26**). The stimulatory effect of GM-CSF in macrophages from shocked animals was less obvious and only 1.6 fold in comparison to a 2.3 fold increase in macrophages from sham-operated animals. However, the treatment with GM-CSF *in vitro* was sufficient to activate TNF- $\alpha$  production to the level of peritoneal cells from sham-operated mice without GM-CSF incubation, which can be assumed as normal TNF- $\alpha$ -producing capacity (Shock+LPS+GM-CSF vs. Sham+LPS;  $p=0.234$ ).

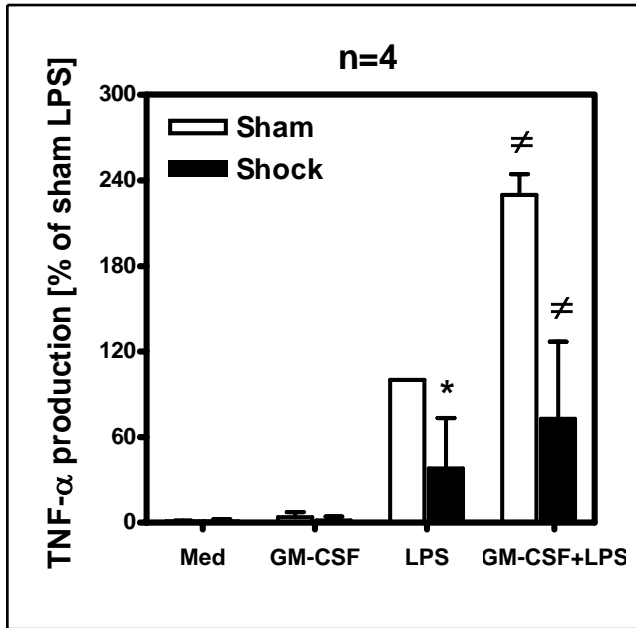


**Figure 26. Elevated TNF- $\alpha$  production after GM-CSF preincubation after hemorrhage.**

Peritoneal macrophages were harvested 20 h after hemorrhage (Shock) or sham-operation (Sham) and incubated first for 6 h with GM-CSF (10 ng/ml) and then 4 h with LPS (1 ng/ml) along with their respective controls. TNF- $\alpha$  production is expressed as percentage of LPS-induced TNF- $\alpha$ -production of the sham-operated animals of each set of experiments. Data represent mean  $\pm$  SEM of 4 independent experiments with pooled macrophages of 2 mice /group. \* means statistical significant different to sham-operated mice after LPS-stimulation with a p-value < 0.05 in Mann-Whitney-U-Test;  $\neq$  indicates statistical difference to incubation without GM-CSF (Wilcoxon-Test for unpaired samples).

### 3.1.3.2.6 I $\kappa$ B $\alpha$ phosphorylation in GM-CSF primed macrophages after hemorrhage

The modest increase of TNF- $\alpha$  production of peritoneal macrophages from hemorrhagic animals after GM-CSF incubation was accompanied by comparable changes of phosphorylated I $\kappa$ B $\alpha$ . However, similar as the TNF- $\alpha$  production, I $\kappa$ B $\alpha$  activation was also much more primed by GM-CSF in peritoneal cells from sham-operated mice while the unphosphorylated form of I $\kappa$ B $\alpha$  was decreased after hemorrhagic shock as expected (Figure 27).

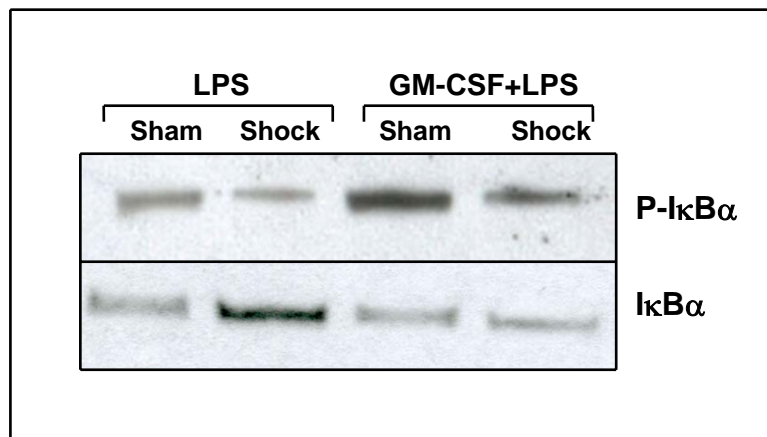


**Figure 27. I $\kappa$ B $\alpha$  phosphorylation in GM-CSF primed macrophages after hemorrhage**

Peritoneal macrophages (pooled cells from 2-3 mice/group) were harvested 20 h after hemorrhage (Shock) or sham-operation (Sham) and incubated first for 6 h with GM-CSF (10 ng/ml) and then 45 min with LPS (1 ng/ml) along with their respective controls. Cytoplasmic proteins were extracted and P-I $\kappa$ B $\alpha$  was analyzed by Western blotting. The blot shown is representative of a minimum of three independent experiments.

### 3.1.3.2.7 P-ERK1/2 and P38 phosphorylation in GM-CSF primed macrophages after hemorrhagic shock

In contrast to the modest effect of GM-CSF treatment in terms of TNF- $\alpha$  production, the signaling molecules ERK1/2 and P38 were obviously enhanced by GM-CSF preincubation in both macrophages from sham-operated and shocked mice. GM-CSF given *in vitro* activated both the P38MAPK and ERK1/2 phosphorylation in peritoneal macrophages after hemorrhage. The stimulation of ERK1/2 by GM-CSF in cells from hemorrhagic animals was similar to the level of ERK1/2 from sham-operated mice, which may be assumed as the “normal” level. The upregulation of P38MAPK after hemorrhagic shock was found to be even more elevated after GM-CSF treatment (Figure 28).

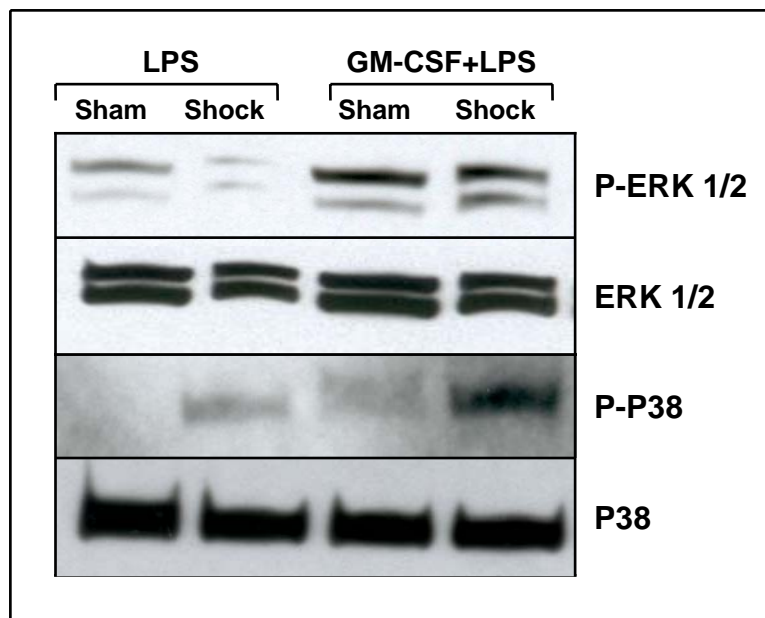


**Figure 28. ERK1/2 and P38 phosphorylation after hemorrhage and GM-CSF incubation**

Peritoneal macrophages (pooled cells from 2-3 mice/group) were harvested 20 h after hemorrhage (Shock) or sham-operation (Sham) and incubated first for 6 h with GM-CSF (10 ng/ml) and then 45 min with LPS (1 ng/ml) along with their respective controls. Cytoplasmic proteins were extracted and P-ERK1/2 and P-P38 were analyzed by Western blotting using specific antibodies for phosphorylated ERK1/2 and P38MAPK and the respective control antibody detecting the total amount of each kinase. The blot shown is representative of a minimum of three independent experiments.

### 3.1.4 Immunomodulation by GM-CSF during polymicrobial sepsis

GM-CSF is known to enhance monocytes' and macrophages' effector functions after shock as well as during sepsis [87, 88, 94, 95]. GM-CSF restores the capacity of splenic and peritoneal macrophages for TNF- $\alpha$  secretion in response to LPS. With the results shown above, GM-CSF partly but not completely, could restore the suppressed immune functions of murine peritoneal macrophages after hemorrhagic shock. Like hemorrhagic shock, sepsis leads to the development of immunosuppression that is associated with the impaired capacity of antigen presenting cells (APC) in the spleen to respond to bacterial stimuli. To test whether GM-CSF might reverse the suppressive state of APC in the spleen during sepsis, the secretion of pro-inflammatory cytokines by splenic macrophages and dendritic cells was analyzed in the presence of GM-CSF.

#### 3.1.4.1 TNF- $\alpha$ secretion by splenic macrophages and dendritic cells

The capacity of GM-CSF to modulate the TNF- $\alpha$  production by LPS-induced antigen presenting cells such as splenic macrophages and dendritic cells was investigated during polymicrobial sepsis. Total spleen cells (TSC) were prepared after 24 h sham or CLP operation since former experiments had revealed a significant TNF- $\alpha$  secretion in the supernatant at this time point. TSC were cultured with or without 10 ng/ml LPS each in the presence or absence of 20 ng/ml GM-CSF. Unstimulated cells served as the control (Med). The cells were stained for macrophages and dendritic cells using F4/80<sup>+</sup> and CD11c<sup>+</sup> surface markers, respectively. Intracellular expression of TNF- $\alpha$  was determined in F4/80<sup>+</sup> macrophages and CD11c<sup>hi</sup> dendritic cells by means of FACS.

Concerning macrophages, the production of TNF- $\alpha$  was low in the absence of any stimulation (Med) from both control and septic mice (**Figure 29A**). Stimulation with GM-CSF alone did not enhance the level of TNF- $\alpha$  and was found to be similar to the level of unstimulated cells after sham and CLP operation. Upon LPS stimulation, 25% of splenic macrophages after sham operation produced TNF- $\alpha$ . Splenic macrophages after CLP also produced TNF- $\alpha$  but to a lesser extent (1.6-fold; **Figure 29A, CLP vs. sham, LPS**) than macrophages from control animals upon LPS-stimulation. The treatment with GM-CSF enhanced the capacity of LPS-induced macrophages to synthesize TNF- $\alpha$ , both after CLP and sham operation (1.6-fold and 1.3-fold, respectively; **Figure 29A**). The presence of GM-CSF during LPS stimulation increased the percentage of TNF- $\alpha$ -

producing macrophages from septic mice up to levels observed for LPS-stimulated macrophages from healthy controls.

Dendritic cells from both control and septic mice, like macrophages, produced low levels of TNF- $\alpha$  in the absence of any stimulation (Med, **Figure 29B**). GM-CSF stimulation alone did not enhance the level of TNF- $\alpha$  and was found to be similar to the level of unstimulated cells after sham and CLP operation. Twenty-four hours post CLP; dendritic cells did not show any response to LPS stimulation and showed a strong reduction in TNF- $\alpha$  producing capacity (70%; **Figure 29B, CLP vs. sham, LPS**). GM-CSF treatment of LPS-induced dendritic cells from mice of both the groups increased the TNF- $\alpha$  secretion (**Figure 29B**) to a similar degree as for the macrophages (1.5-fold of DC vs. 1.6-fold of macrophages, **Figure 29A vs. B, GM-CSF + LPS**). In spite of an increase in TNF- $\alpha$  production after GM-CSF treatment by dendritic cells, the percentage of TNF- $\alpha$  producing DC from septic mice did not reach the levels found for LPS-stimulated DC from sham mice (71% suppression, **Figure 29B, CLP vs. sham, GM-CSF + LPS**).

Thus, sepsis-associated reduction in LPS-induced TNF- $\alpha$  production is more pronounced in dendritic cells than in macrophages. GM-CSF enhanced the LPS-induced TNF- $\alpha$  synthesis of macrophages up to the levels from LPS-treated macrophages from sham mice. However, GM-CSF did not compensate the strong suppression of dendritic cells from septic mice.

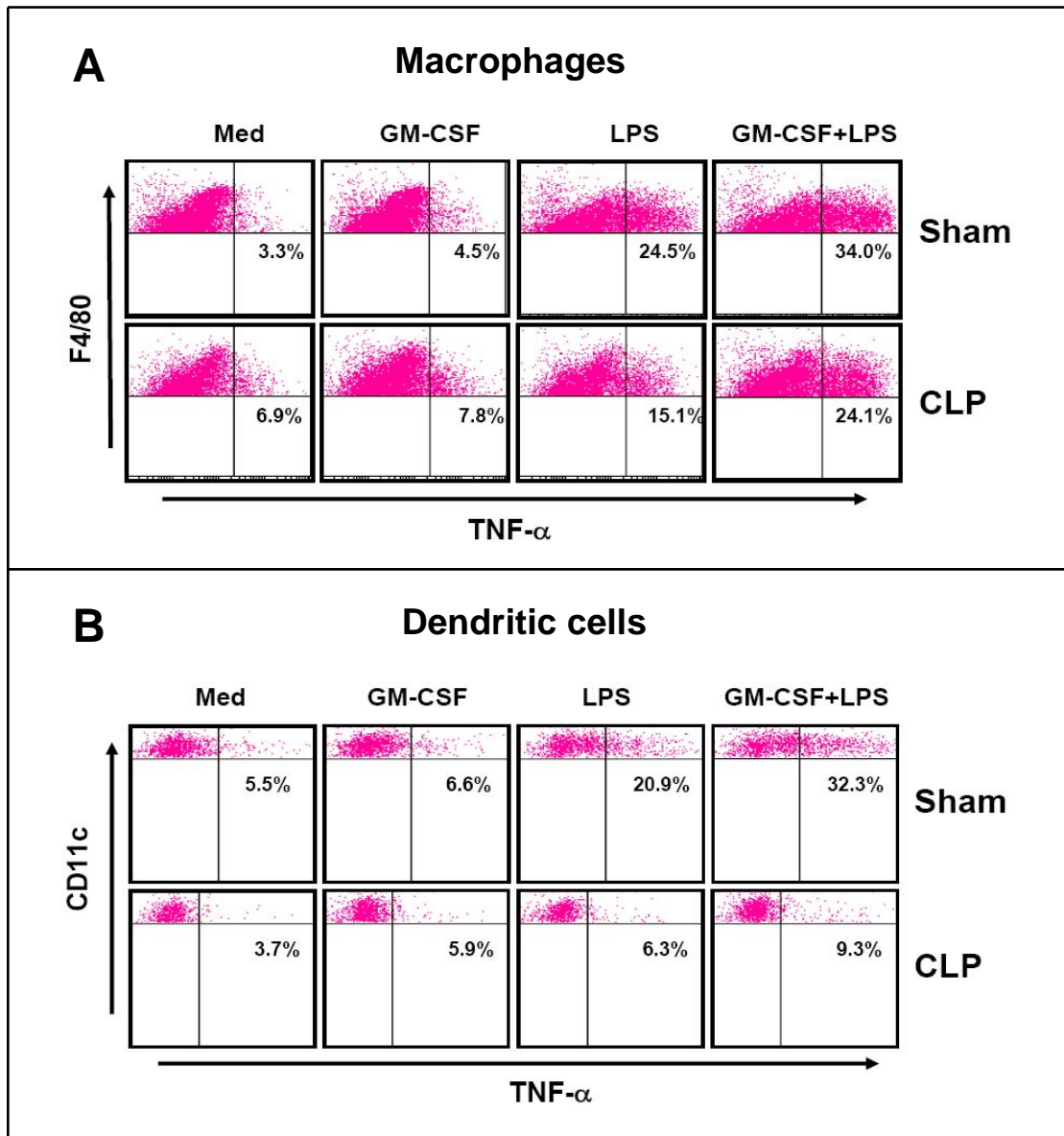


**Figure 29. Enhanced TNF- $\alpha$  production after GM-CSF treatment.**

Total spleen cells were pooled (n=3-4 per group) 24 h post sham or CLP operation and stimulated with or without 10 ng/ml LPS each in the presence or absence of 20 ng/ml GM-CSF for 1 h. Unstimulated cells served as the control (Med). After 4 h further incubation with monensin, spleen cells were stained for F4/80 (A) and CD11c (B) surface markers and intracellular TNF- $\alpha$  (common for Figure A and B). F4/80 and CD11c<sup>hi</sup> cells were gated. Quadrant lines were set according to the isotype control antibody, staining less than 1-2% of the cells. Numbers indicate percentage of TNF- $\alpha$ -positive cells. The FACS data are representative of 3 independent experiments.

### 3.1.4.2 IL-12 secretion by splenic dendritic cells

Reduction of IL-12 production by dendritic cells has been documented after polymicrobial sepsis [80]. In this study, we investigated the role of GM-CSF for the modulation of LPS-induced DC to enhance IL-12p40 production during sepsis. Twenty-four hours after CLP or sham operation, total spleen cells were prepared and cultured with or without 5  $\mu$ g/ml CpG each in the presence or absence of 20 ng/ml GM-CSF.

Unstimulated cells served as the control (Med). Intracellular expression of IL-12p40 was determined in CD11c<sup>hi</sup> dendritic cells by means of FACS. A low percentage of DC from sham and CLP mice produced IL-12p40 in the absence of any stimulation (**Figure 30**). GM-CSF stimulation alone showed a similar percentage of IL-12p40 producing dendritic cells. More than 50% of DC from sham mice but only 12% of DC from septic produced IL-12p40 upon stimulation with CpG (**Figure 30, CLP vs. sham, CpG**). GM-CSF treatment slightly enhanced the IL-12p40 production from CpG-stimulated cells in case of sham operated animals (1.3-fold; **Figure 30, Sham, GM-CSF + CpG vs. CpG only**) while the effect of GM-CSF was much more pronounced in DC from septic mice (1.9-fold, **Figure 30, CLP, GM-CSF + CpG vs. CpG only**). However, the presence of GM-CSF during CpG stimulation did not restore the capacity of DC to produce IL-12p40 similar to DC from sham mice and thus did not compensate the strong suppression of dendritic cells in septic animals.

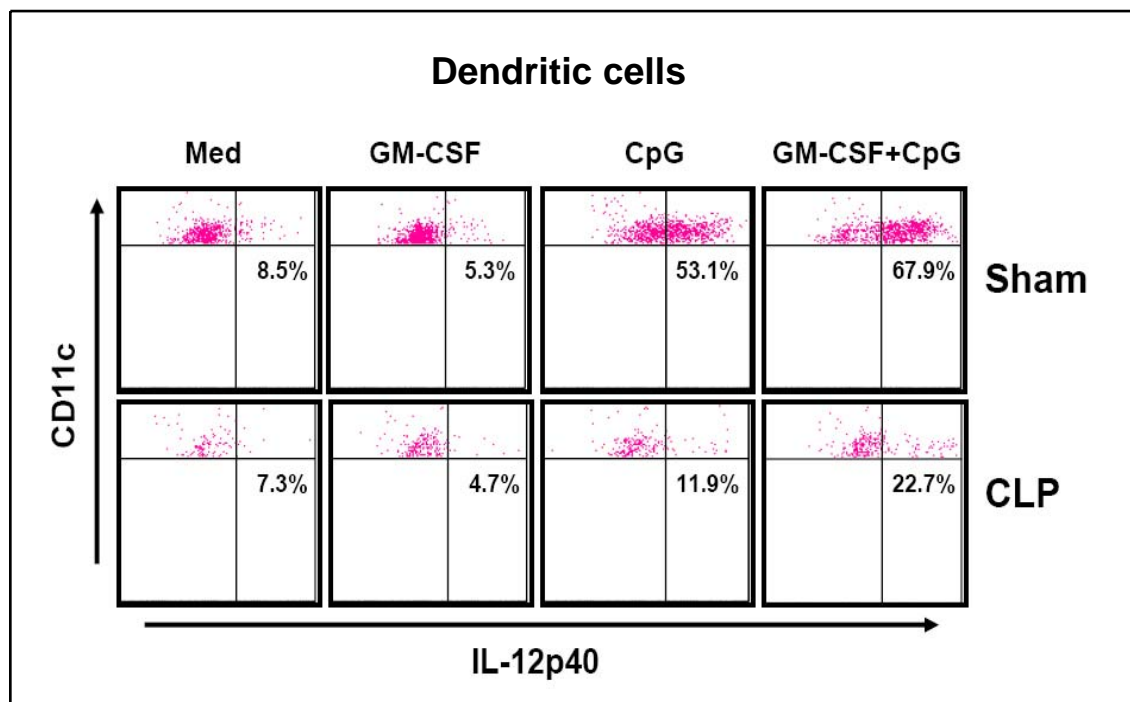


**Figure 30. Enhanced IL-12p40 production after GM-CSF treatment.**

Total spleen cells were pooled (n=3-4 per group) 24 h post sham or CLP operation and stimulated with or without 5 µg/ml CpG each in the presence or absence of 20 ng/ml GM-CSF for 18 h. Unstimulated cells served as the control (Med). After 4 h further incubation with monensin, spleen cells were stained for CD11c surface marker and intracellular IL-12p40. CD11c<sup>hi</sup> cells were gated. Quadrant lines were set according to the isotype control antibody, staining less than 1-2% of the cells. Numbers indicate percentage of TNF-α-positive cells. The FACS data are representative of 3 independent experiments.

### 3.1.4.3 Effect of GM-CSF on CD86 and CD40 on splenic DC

To test whether GM-CSF affects the expression of co-stimulatory molecules on splenic dendritic cells, the expression of CD86 (**Figure 31A**) and CD40 (**Figure 31B**) on splenic CD11c<sup>hi</sup> DC was determined 24 h post CLP and sham operation. GM-CSF alone after sham operation enhanced the expression of CD86 but not of CD40 on dendritic cells. Upon LPS stimulation, the expression of both CD86 (5-fold) and CD40 (4-fold), on DC from sham mice was increased. DC from septic mice only weakly increased the expression of these co-stimulatory molecules upon stimulations with LPS. GM-CSF alone increased the expression of CD86 but not of CD40 on DC from septic animals. The presence of GM-CSF during LPS-stimulation significantly increased the expression of CD86 on DC from septic mice (in comparison to stimulation with LPS alone). GM-CSF did not change the LPS-mediated expression of CD86 on DC from sham mice or of CD40 on DC from both the groups. Thus, GM-CSF could restore at least in part the decreased upregulation of CD86 on DC from septic mice upon stimulation with LPS.

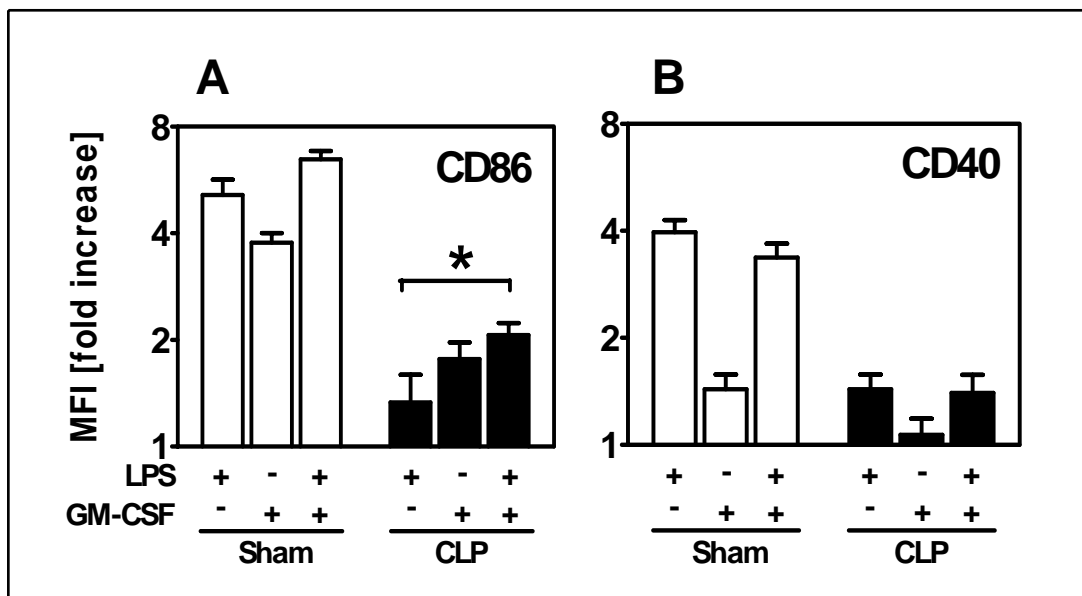


**Figure 31. Maturation of splenic DC during sepsis.**

Total spleen cells were pooled (n=3-4 per group) 24 h post CLP and sham operation and stimulated with or without 10 ng/ml LPS each in the presence or absence of 20 ng/ml GM-CSF for 18 h. The cells were stained for CD11c, CD86, CD40 and isotype controls. CD11c<sup>hi</sup> cells (DC) were used for gating. The ratio of MFI values of CD86 (A) and CD40 (B) upon stimulation versus medium control (set as 1) was calculated from DC from septic (black bars) and sham (open bars) mice. Data show mean  $\pm$  SD of three to four independent experiments. \* indicates significant difference ( $p < 0.05$ ) between LPS and GM-CSF+LPS groups.

## 3.2 GM-CSF as a growth regulator

GM-CSF is one of the members of colony stimulating factors that are required for the survival, proliferation, and differentiation of hematopoietic progenitor cells of myeloid and erythroid origin. In developing bone marrow, GM-CSF stimulates immature myelomonocytic progenitor cells to proliferate and differentiate. In addition to its function as a growth factor, GM-CSF primes the mature cells from these lineages, so when they encounter an invading pathogen, they are capable of initiating a full defense reaction [151]. Therefore, the effect of GM-CSF on the development of bone marrow progenitors of dendritic cells was further explained. It has been shown by our research group that DC from the spleen undergo strong modulation in terms of their phenotype and cytokine production patterns. There was a DC loss during polymicrobial sepsis and the remaining DC showed an aberration in the cytokine secretion that favored the development of Th2 cells [80]. In order to understand, whether sepsis additionally modulates the progenitor cells of DC, the effect of GM-CSF on the development of bone marrow progenitors, especially for the dendritic cells was studied. The effect during polymicrobial sepsis in terms of modulation of progenitor cells of DC and DC differentiation, expression of co-stimulatory molecules, cytokine secretion and *in vitro* and *in vivo* T cell activation was investigated.

### 3.2.1 BMC loss during polymicrobial sepsis

To understand the effects of sepsis on total bone marrow cell count, these cells were analyzed 24 h after CLP or sham operation. The BMC were prepared and enumerated. A reduced number of BMC was found in septic mice in comparison to sham mice, indicating a clear and significant loss of 40% of BMC (**Figure 32**).

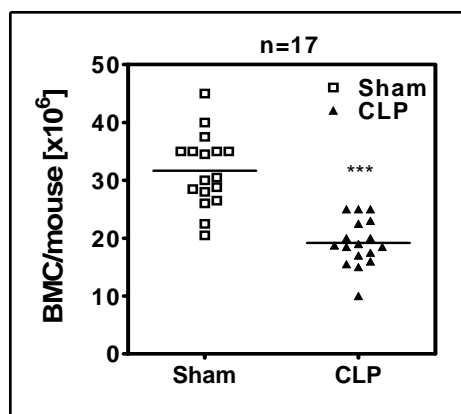


**Figure 32. BMC count during sepsis.**

Twenty-four hours post CLP or sham operation, total BMC were pooled (n=2-3 per group) from sham (open squares) and CLP (filled triangles) mice and counted. Data show absolute counts  $\pm$  mean of BMC of all the individual experiments. n: Number of total experiments as indicated. Asterisks indicate statistically significant difference between CLP and sham group. \*\*\*,  $P < 0.0005$ .

### 3.2.2 Cell death during polymicrobial sepsis

Increased cell death could be one of the possible explanations of cell loss in the bone marrow after CLP operation. To address this parameter, apoptosis was checked in order to know whether there is enhanced cell death in the bone marrow during sepsis. Sham and septic BMC were stained for Annexin-V in combination with 7-AAD, a vital dye, to simultaneously distinguish live, early apoptotic and late apoptotic/dead cells. In early apoptotic cells, the membrane phospholipids phosphatidylserine (PS) is translocated and thereby exposed to the external cellular environment. Annexin V has a high affinity for PS and binds to cells with exposed PS. Annexin V staining precedes the loss of membrane integrity, which accompanies the latest stages of cell death resulting from either apoptotic or necrotic processes. Therefore, staining with Annexin V was used in conjunction with a vital dye, such as 7-Amino-actinomycin D (7-AAD) to allow the discrimination of early apoptotic cells. Viable cells were Annexin V and 7-AAD negative. Cells that were in early apoptosis were Annexin V positive and 7-AAD negative (**Figure 33A, R1 and B**). Early induction of apoptosis was 3.6-fold more in septic BMC as compared to BMC from sham mice. Cells that are in late apoptosis/cell death were positive for both Annexin V and 7-AAD (**Figure 33A, R2 and B**) and were 2.2-fold more after cecal ligation and puncture. Total apoptotic and dead cells were the combination of R1+R2 region cells and showed overall 2.5 fold more dead cells after 24 h sepsis (**Figure 33A, R1+R2 and B**).

Additionally, Caspase-3, another apoptotic cells marker, was checked to determine the percentage of dead cells. Caspases are the main effectors of apoptosis or programmed cell death (PCD) and their activation leads to characteristic morphological changes of the cell consequently leading to its death. Initiator caspases are the first to be activated which cleave and activate the effector caspases e.g. caspase-3, that gives the signal for cell death. Caspase-3 staining of BMC further strengthened the data from Annexin-V and 7-AAD staining and also showed an increase of 2.5-fold in apoptotic cells 24 h post CLP as compared to BMC of sham mice (**Figure 33C, R1 and D**).

However, the percentage of dead cells as such was low in both sham and septic BMC not reaching more than 6%, albeit the number of dead cells was higher in BMC isolated from septic mice as compared to BMC from sham mice, shown by both Annexin-7-AAD (**Figure 33A and B**) and caspase-3 staining (**Figure 33C and D**).

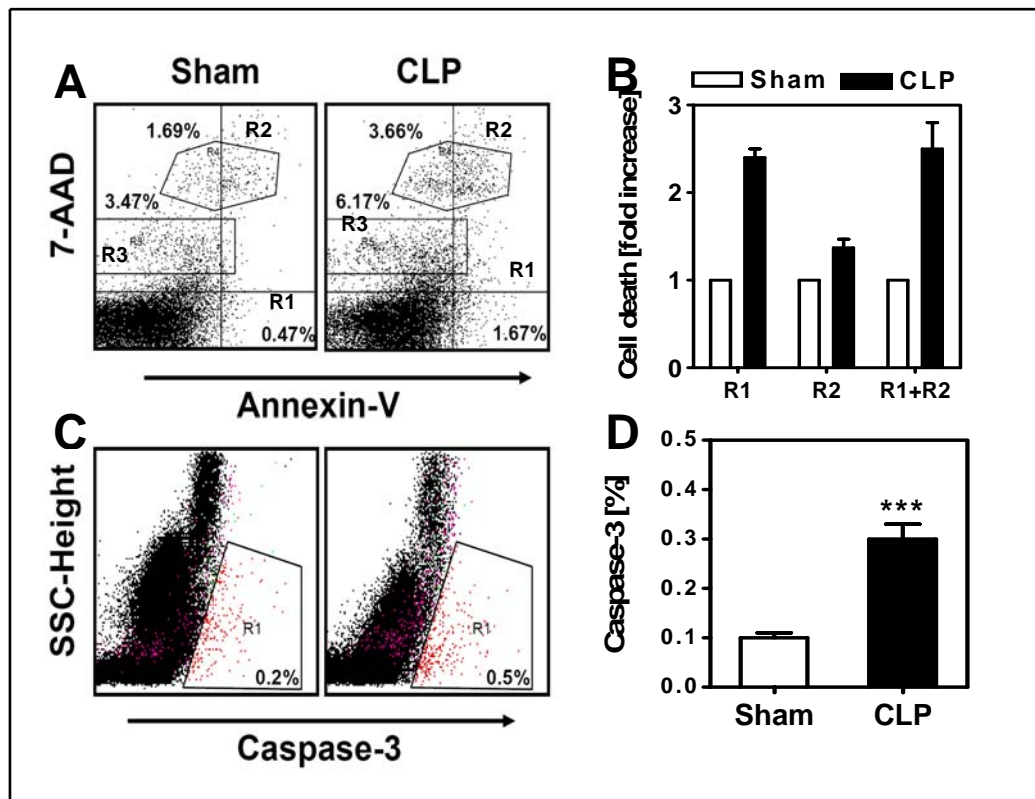


**Figure 33. Cell death in the bone marrow during polymicrobial sepsis.**

Twenty-four hours post CLP or sham operation, total BMC were pooled (n=2-3 per group) and stained for Annexin-V in combination with 7-AAD or for Caspase-3. (A) Representative dot plot showing Annexin-V and 7-AAD staining with individual gating for Annexin-V<sup>+</sup> cells (R1), Annexin-V<sup>+</sup> and 7-AAD<sup>+</sup> cells (R2) and 7-AAD<sup>+</sup> cells (R3). (B) Data showing mean  $\pm$  SD of three independent experiments showing 3 different populations from region R1, R2 and R1 + R2 as gated in part-A from sham and septic BMC. The ratios were calculated as fold increase of percentage values of BMC from septic (black bars) versus sham (open bars) mice to compensate for variations between different experiments. (C) Representative dot plot for Caspase-3 staining against SSC-Height with Caspase-3 gated as R1. (D) Caspase-3 staining from 3-4 individual mice per group. Values are shown as percentage of Caspase-3<sup>+</sup> cells from sham (open bars) and septic (black bars) BMC. Asterisks indicate statistically significant difference between CLP and sham group. \*\*\*,  $P < 0.0005$ .

### 3.2.3 Release of myeloid cells from bone marrow into the blood

Enhanced release of myeloid cells from the bone marrow could be another explanation for the reduced numbers of BMC during sepsis. To investigate this possibility, cell number and cellular composition of whole blood were analyzed.

#### 3.2.3.1 Increased leukocyte count during polymicrobial sepsis

First, the total leukocyte count in the blood was analyzed. Blood was collected and stained for the leukocyte marker, CD45. Blood isolated from septic mice clearly showed a significant increase in total leukocyte count (5.3-fold) as compared to sham mice (**Figure 34A**), indicating the enhanced release of these cells from bone marrow into the blood.

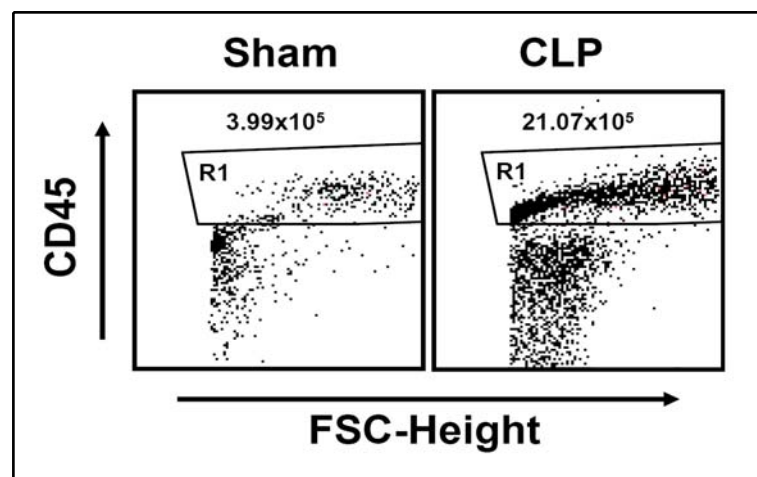


**Figure 34. Leukocyte count in the blood 24 h post CLP.**

Blood was collected 24 h post CLP or sham operation and 50  $\mu$ l of blood was used for the staining of CD45 expression on blood cells in TruCount Tubes as described in Material and Methods (**Section 2.3.7.2**). The cells were gated for CD45 against FSC channel (R1). Leukocyte count was calculated per 1000  $\mu$ l of blood. The dot plots are representative of two independent experiments.

#### 3.2.3.2 Elevated dendritic cell count during polymicrobial sepsis

Next, the blood was analyzed for the myeloid cell composition after 24 h of sham and CLP operation. Blood was stained with CD11c, dendritic cell surface marker in combination with MHC class II surface marker, a marker for the maturation status of the dendritic cells. Sepsis led to an increase of  $38.5 \pm 2.5\%$  more dendritic cells in the blood as compared to DC from sham blood (**Figure 35B vs. A, R1**). Although the total dendritic cell (CD11c<sup>+</sup>, **Figure 35A, R1**) number was found to be more in septic blood, the differentiated dendritic cells (CD11c<sup>+</sup>MHC II<sup>+</sup>) were less by  $34 \pm 8\%$  (**Figure 35D vs. C, R2**) in the same septic blood. Thus, during sepsis, the number of immature DC but

not the differentiated DC with an overall total CD11c<sup>+</sup> cell number was increased in the blood.

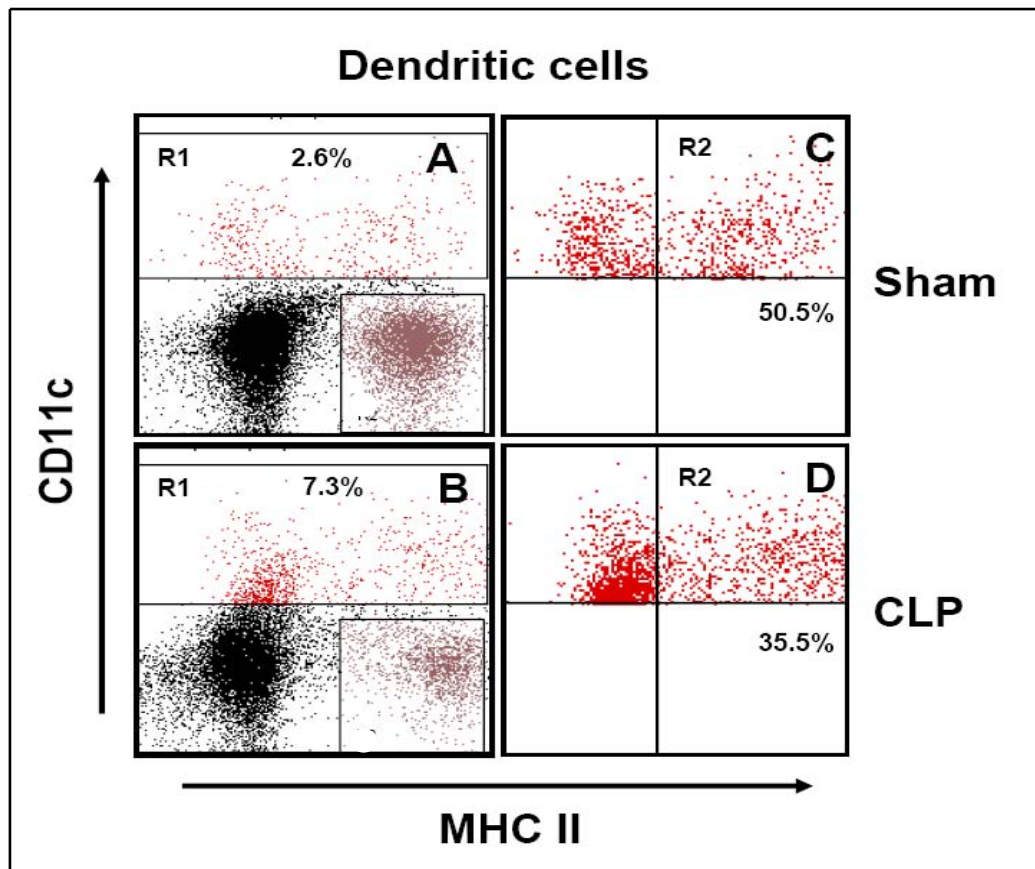


**Figure 35. Dendritic cell count in the blood during sepsis.**

Blood was collected 24 h post CLP or sham operation and stained for CD11c in combination with MHC class II. CD11c<sup>+</sup> cells were used for the gating. (A and B) Dot plots from the gated DC in the region R1 from blood cells of sham and septic mice. (C and D) MHC class II expression on gated DC is shown and CD11c<sup>+</sup>MHC<sup>+</sup> cells are shown in region R2. Quadrant lines were set where isotype controls showed less than 2% false-positive cells. Data show representative dot plots of two independent experiments.

### 3.2.3.3 Increased granulocyte and monocyte release during polymicrobial sepsis

Further, the blood was analyzed for other myeloid cells such as granulocytes and monocytes after 24 h of sham and CLP operation. Blood staining was performed with CD11c in combination with Gr1 and CD11b markers. Granulocytes were analyzed using granulocyte antigen, Gr1 and monocytes were studied by taking the cell population devoid of dendritic cells and granulocytes (CD11c<sup>-</sup>Gr<sup>-</sup>) and then gating this negative population for CD11b in a combination with Gr1, a marker to characterize monocytes and macrophages (CD11b<sup>+</sup>Gr1<sup>+</sup>). An increase in granulocyte (58.6%, **Figure 36B vs. A, R1**) and monocyte (33.33%, **Figure 36D vs. C, R2**) percentage was found in the blood of septic mice compared to the same from the blood of sham mice. This clearly stated the release of granulocytes and monocytes from bone marrow to blood.

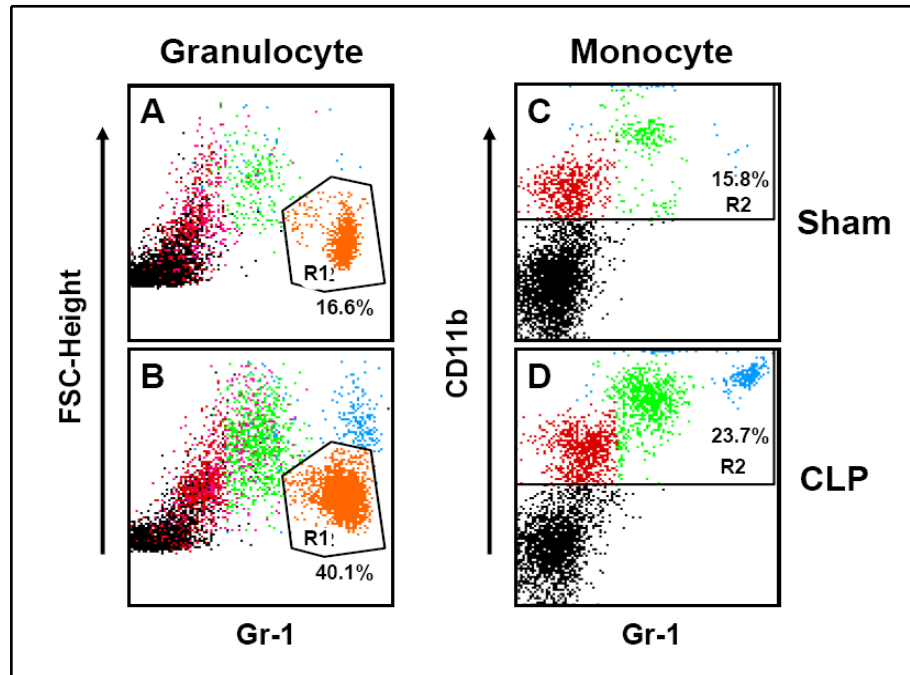


**Figure 36. Granulocyte and monocyte count in the blood during sepsis.**

Blood was collected 24 h post CLP or sham operation and stained for CD11c in combination with Gr1 and CD11b and MHC class II. (A) Granulocytes (Gr1<sup>+</sup>) cells were gated against FSC channel. (B) The cells other than the granulocytes (CD11c<sup>-</sup>Gr1<sup>+</sup>) were gated and used for analyzing monocyte population using CD11b<sup>+</sup> against Gr1<sup>+</sup> cells. Data show representative dot plots of two independent experiments.

### 3.2.4 Cell proliferation and DC composition during sepsis

#### 3.2.4.1 Enhanced bone marrow cell proliferation during polymicrobial sepsis

To further understand the mechanisms leading to the reduced BMC number during sepsis, the proliferation capacity of BMC was investigated. Therefore, 24 h post CLP or sham operation, bone marrow cells were prepared. An equal number of CFSE-labeled or unlabeled BMC were cultured and the proliferation of labeled cells was analyzed by means of FACS on d 3 and unlabeled cells were counted for proliferation on d 3 and 7. After every cell division, CFSE labeling was distributed equally between the daughter cells distinguishing consequently, each successive generation by decreased CFSE labeling of the cells. Twenty-four hours after CLP, percentage of non-dividing-CFSE-labeled cells was decreased by 54.2% (**Figure 37A, CLP vs. sham, M2 population**) indicating that there was an increased proliferation (**Figure 37A, CLP**) of these cells during sepsis. The increase in BMC proliferation after sepsis was further confirmed by the counting of the cells from d 3 and d 7 cultures (**Figure 37B**). During culture, BMC from septic mice strongly proliferated and generated up to 2.0-fold and 2.3- fold more cells after d 3 and d 7 respectively, than BMC from sham mice. The increased proliferation from septic cells was more prominent on d 7 as compared to d 3. Thus,

sepsis resulted into a strong proliferation of bone marrow cells which started as early as d 3 of culture and continued further through d 7.

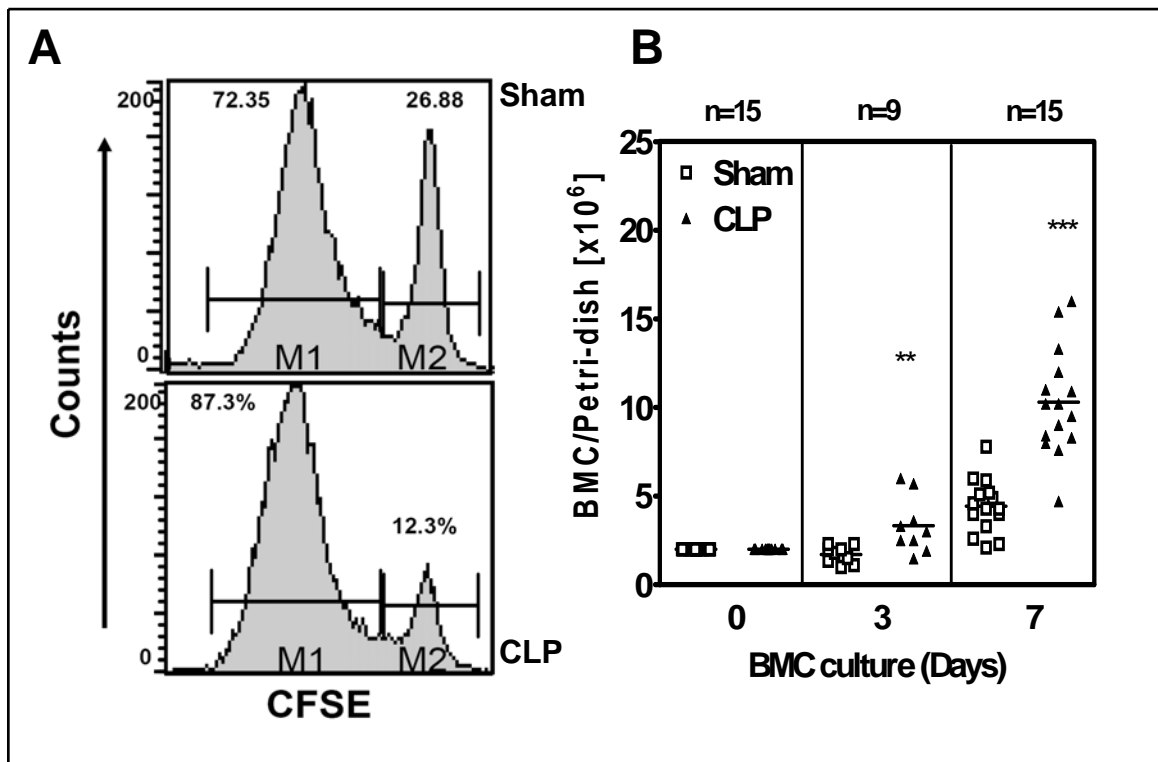


**Figure 37. BMC proliferation during polymicrobial sepsis.**

Twenty four hours post CLP, total BMC were pooled (n=2-3 per group).  $2 \times 10^6$  CFSE-labeled (A) or unlabeled (B) BMC from sham and CLP mice were cultured in Petri-dishes. (A) Proliferation of sham and septic CFSE-labeled CD11c<sup>-</sup> BMC after d 3 culture. CFSE positive cells were gated on the basis of dividing (M1) and non dividing (M2) populations. Dot plot shown are representative of two independent experiments. (B) Cell count of unlabeled BMC from sham (open squares) and septic mice (filled triangles) on d 0, 3 and 7. Data show absolute counts  $\pm$  mean of BMC/Petri-dish of all the individual experiments. n: Number of total experiments as indicated. Asterisks indicate statistically significant difference between CLP and sham group. \*\*,  $P < 0.005$ ; \*\*\*,  $P < 0.0005$ .

### 3.2.4.2 DC population during polymicrobial sepsis

Next, the possible explanation for the enhanced proliferation of bone marrow cells after sepsis was evaluated. BMC were analyzed for the content of dendritic cells and its progenitors to know whether these show any change which could give rise to increased proliferation during polymicrobial sepsis. Twenty-four hours after sham or CLP operation, BMC were prepared and studied for differentiated DC (CD11c<sup>+</sup>MHC class II<sup>+</sup>) and DC progenitor cells (CD11c<sup>+</sup>MHC class II<sup>-</sup>) by means of FACS. There was a consistent but slight elevation in the DC number from septic mice as compared to DC from sham mice (**Figure 38A**). However, BMC from septic mice contained a 1.6 to 2.6-fold higher number of differentiated DC (Cd11c<sup>+</sup>MHC class II<sup>+</sup>, **Figure 38B, IA**<sup>+</sup>) but

CD11c<sup>+</sup>MHC class II<sup>-</sup> progenitor cell count remained unchanged (**Figure 38B, IA<sup>-</sup>**). DC number did not change after CLP operation during the culture over d 7 and was akin to the sham DC proliferation tested on d 3 and then d 7 (**Figure 38C**).

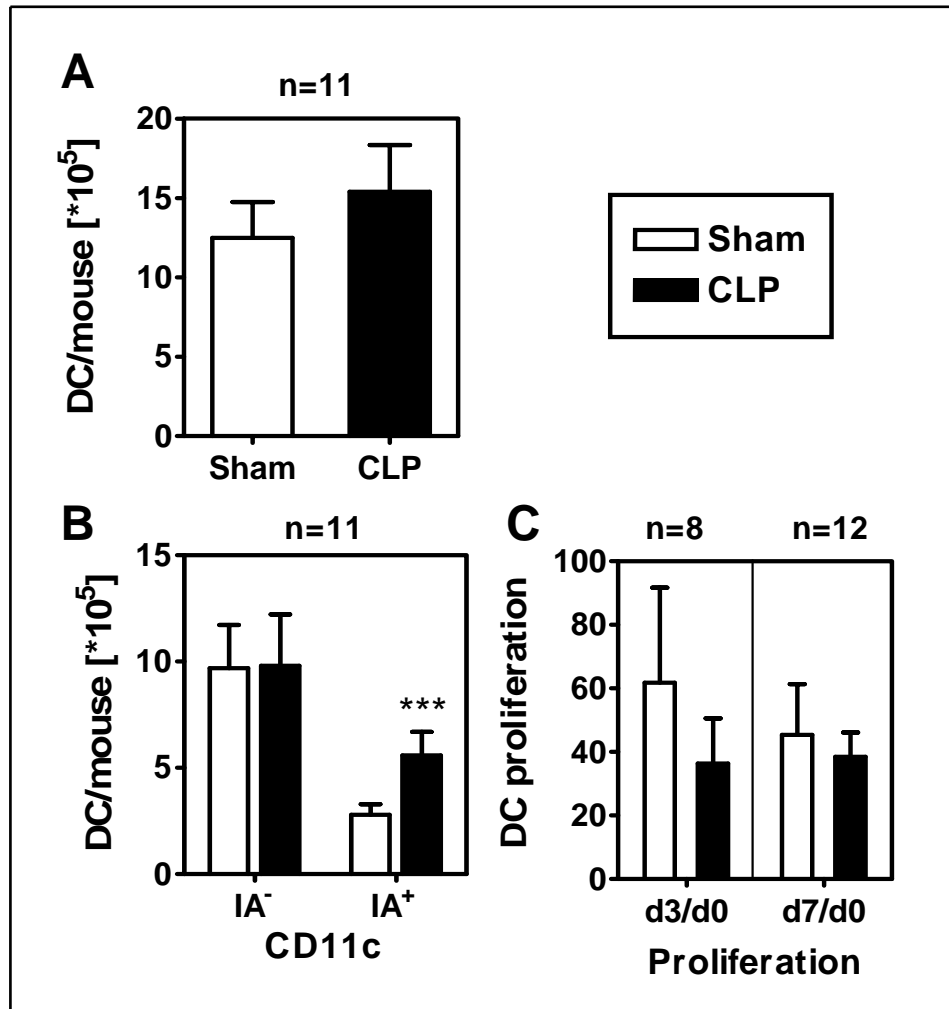


**Figure 38. DC proliferation during polymicrobial sepsis.**

Twenty-four hours after sham or CLP, total BMC were pooled (n=2-3 per group) and stained for CD11c in combination with MHC class II surface marker. CD11c<sup>+</sup> cells were gated and MHC II expression was analyzed on these cells. (A) The total number of DC per mouse after sham (open bars) and CLP operation (black bars) were calculated. BMDC number per mouse was calculated as % gated CD11c<sup>+</sup> cells x total number of cells per bone marrow/10. (B) The total numbers of CD11c<sup>+</sup>MHCII<sup>-</sup> (IA<sup>-</sup>) and CD11c<sup>+</sup>MHCII<sup>+</sup> (IA<sup>+</sup>) per mouse of sham (open bars) and septic mice (black bars) were calculated. The calculations were done as follows: CD11c<sup>+</sup>MHCII<sup>-</sup> (IA<sup>-</sup>) = number of BMDC per mouse x MHCII<sup>-</sup> DC<sup>S</sup>/100; CD11c<sup>+</sup>MHCII<sup>+</sup> (IA<sup>+</sup>) = number of BMDC per mouse - CD11c<sup>+</sup>MHCII<sup>-</sup> (IA<sup>-</sup>). (C) Proliferation of d 3 and d 7 CD11c<sup>+</sup> cells from sham (open bars) and septic (black bars) BMC was compared to the proliferation on d 0 to get the effective proliferation of dendritic cells. Data show mean  $\pm$  SEM of the pooled number of experiments as indicated. Asterisks indicate statistically significant difference between CLP and sham group. \*\*\*,  $P < 0.0005$ . <sup>S</sup> was calculated by subtracting the percentage of gated CD11c<sup>+</sup>MHCII<sup>+</sup> cells from 100.

### **3.2.5 Cytokine secretion pattern during polymicrobial sepsis**

#### **3.2.5.1 Aberrant cytokine secretion pattern of BMDC during sepsis**

A number of functional defects in dendritic cells during sepsis have been characterized. These defects include dysregulated cytokine production, changed expression of important cell surface antigens and reduced T cell activation capacity. Therefore, the capacity of BMDC to produce various pivotal cytokines such as IL-10 (**Figure 39A**), IL-12p70 (**Figure 39B**), IL-12p40 (**Figure 39C**) and TNF- $\alpha$  (**Figure 39D**) which are the key mediators for inflammatory response were analyzed. BMDC on d 7, were stimulated with or without LPS, LPS+CD40L, CpG oligonucleotides, PGN or bacteria for 18 h and the supernatants were analyzed for the above stated cytokines. Unstimulated BMDC served as control (Med) and from both sham and septic mice produced very low levels of IL-10, IL-12 (both IL-12p70 and IL-12p40) and TNF- $\alpha$ . BMDC from septic mice secreted more IL-10 but not IL-12p70 upon LPS stimulation than BMDC from sham mice. However, both IL-10 and IL-12p70 production were enhanced by stimulating the cells with CD40L along with LPS. While IL-12p70 production after sepsis was comparable, IL-12p40 showed a decreased secretion in response to LPS. The levels of IL-10 as well as IL-12p70 from septic BMDC were elevated upon CpG or bacterial stimulations when compared with BMDC from sham treated mice. However, the increased levels of IL-12p70 production was not consistent in all the experiments and sometimes a slight increase or no change was observed for septic BMDC upon CpG or bacterial stimulation when compared to sham BMDC. Upon LPS treatment, septic BMDC produced reduced levels of IL-12p40 in response to CpG and bacterial stimulations. Low levels of IL-10 and IL-12 were released in PGN-stimulated BMDC and the levels were comparable after sham or CLP operation. TNF- $\alpha$  secretion was unchanged from septic BMDC regardless of any stimulation as compared to sham BMDC. Taken together, during sepsis, BMDC develop an aberrant cytokine secretion pattern in response to bacterial stimuli associated with a predominance of IL-10.

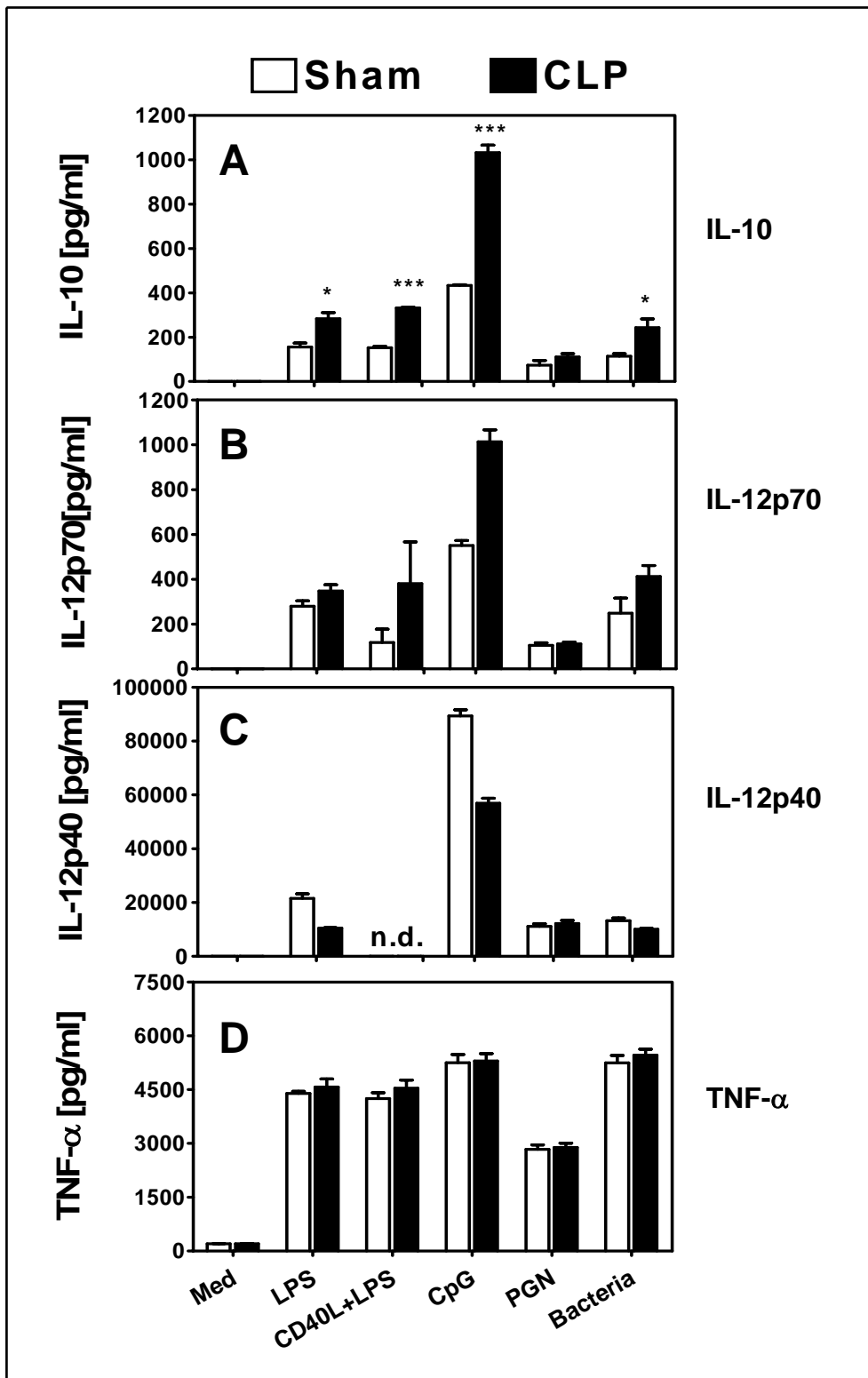


**Figure 39. Cytokine pattern of BMDC in response to bacterial components.**

BMC after 24 h CLP or sham operation, were cultured for d 7 to generate BMDC and then stimulated in the absence or presence of 100 ng/ml LPS alone or in combination with 2.5  $\mu$ g/ml CD40L, or with 5  $\mu$ g/ml CpG, 3  $\mu$ g/ml PGN or bacterial preparation for 18 h. Supernatants of BMDC from septic mice (black bars) and from sham mice (open bars) were analyzed for IL-10 (A), IL-12p70 (B), IL-12p40 (C) and TNF- $\alpha$  (D). Data show mean  $\pm$  SD of triplicate cultures and are representative of a minimum of four experiments. Asterisks indicate significant differences between cultures of sham and CLP groups. \*,  $P < 0.05$ ; \*\*\*,  $P < 0.0005$ . n.d., not determined.

### 3.2.5.1.1 Unchanged CD40, CD86 and MHC class II expression of BMDC during polymicrobial sepsis

Next, the effect of sepsis on the maturation status of BMDC in response to different bacterial components was investigated. Therefore, CD40, CD86 and MHC class II expression on CD11c BMDC was determined after sham and CLP operation. The non-stimulated-BMDC from both sham and septic mice showed low expression of surface molecules and the expression of these CD40, CD86 and MHC class II markers was strongly upregulated in response to LPS, CpG, PGN and bacteria as expected. However, neither upregulation nor down regulation of any of the surface markers was seen after 24 h sepsis clearly indicating no effect of sepsis on the expression of these surface markers (Figure 40).

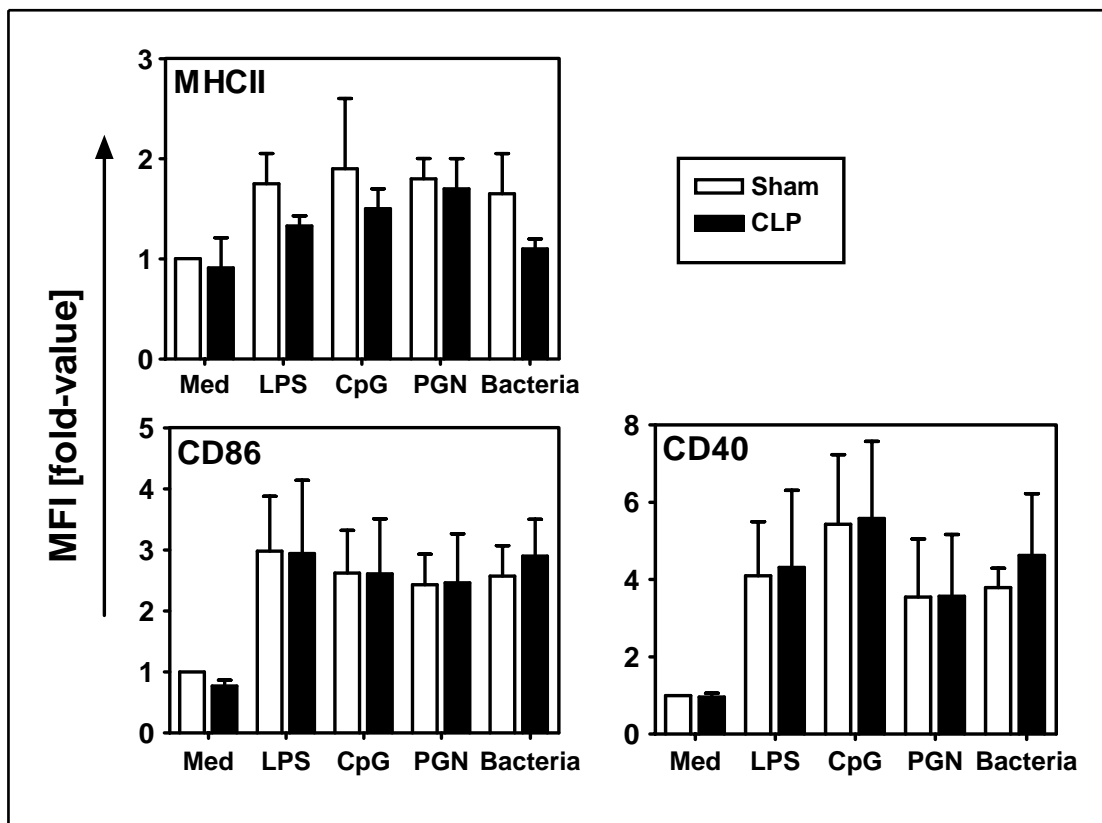


**Figure 40. Maturation of BMDC during polymicrobial sepsis.**

BMC after 24 h CLP or sham operation were cultured for 7 d to generate BMDC and then stimulated in the absence or presence of LPS, CpG, PGN or bacterial preparation for 18 h. Non-adherent cells were pooled and stained for CD11c<sup>+</sup> in combination with MHC class II, CD40 and CD86. CD11c<sup>+</sup> cells were used for the gating and MHC class II, CD86 and CD40 were then analyzed on CD11c<sup>+</sup> gated cells of sham (open bars) and septic mice (black bars). MFI-fold-values of the indicated surface markers for all the given stimuli were normalized on sham medium taking that as 1. Data show mean  $\pm$  SD of three to four independent experiments.

### 3.2.5.2 Reduced cytokine secretion pattern of BMC during sepsis

In order to test whether any cytokine that would promote the enhanced IL-10 release is present in the BMC cultures, the cytokine secretion of BMC prepared 24 h after CLP or sham operation was investigated. The cytokine pattern from BMC was analyzed for IL-10 (**Figure 41A**), IL-12 (**Figure 41B**) and TNF- $\alpha$  release (**Figure 41C**). BMC were prepared 24 h post CLP and sham operation and cultured with or without LPS, CpG, PGN or bacteria. In the absence of any stimulation (Med), neither IL-10 nor IL-12p70 was synthesized by BMC from both sham and septic mice, though very low level of TNF- $\alpha$  was secreted by BMC from both the groups. BMC from sham mice responded strongly to CpG as compared to other stimulations i.e. LPS, PGN and bacteria for the production of IL-10 and IL-12. However, during sepsis, BMC showed a drastic decline in the production of IL-10 and IL-12 upon stimulation with any bacterial stimuli, but the reduction was more prominent in CpG-stimulated BMC. There was a considerably higher secretion of TNF- $\alpha$  in response to all the given stimuli from both sham and septic BMC, but when compared between sham and septic BMC, TNF- $\alpha$  production was significantly low from septic BMC. Thus, IL-10, IL-12p70 cytokine levels were undetectable and TNF- $\alpha$  secretion was in very low amounts from both sham and septic BMC under nonstimulated conditions. There was a drastic decline in the production of all the stated cytokines upon stimulation with any bacterial component e.g. LPS, CpG, PGN or bacterial preparation.

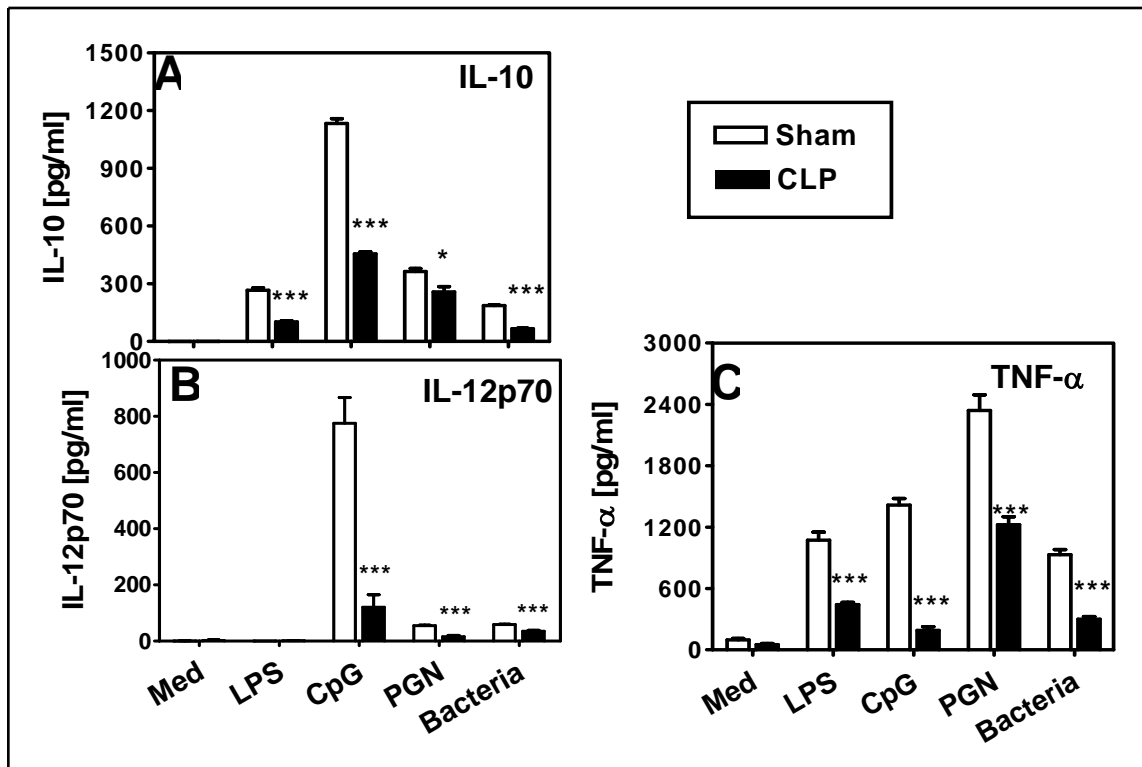


**Figure 41. Cytokine pattern of BMC in response to bacterial components.**

BMC after 24 h CLP or sham operation were cultured in the absence or presence of LPS or with CpG, PGN or bacterial preparation for 18 h. Supernatants of DC from sham (black bars) and septic mice (open bars) were analyzed for IL-10 (A), IL-12p70 (B) and TNF- $\alpha$  (C). Data show mean  $\pm$  SD of triplicate cultures and are representative of a minimum of four experiments. Asterisks indicate significant differences between cultures of sham and CLP groups. \*,  $P < 0.05$ ; \*\*\*,  $P < 0.0005$ .

### 3.2.6 T cell activation during polymicrobial sepsis

#### 3.2.6.1 *In vitro* T cell-stimulatory capacity of BMDC during sepsis

To investigate the capacity of BMDC to induce T cell activation, CpG-induced T cell proliferation and cytokine production in sham and septic mice was examined. Titrated numbers of purified BMDC from sham and septic mice, in the presence or absence of CpG (5  $\mu$ g/ml) were cocultured with allogenic CFSE-labeled T cells. After d 3, the non-adherent cells were checked for proliferating T cells by gating CFSE-positive CD4<sup>+</sup> viable and proliferating T cells using FACS (Figure 42A). BMDC from both sham and septic mice showed similar T cell proliferation capacity in the absence (Med. Figure 42B and C vs. D) or presence of stimulation (CpG, Figure 42B and E vs. F). The proliferation capacity was found to be same with all the titrated numbers of BMDC (Figure 42G). However, an enhanced T cell proliferation in response to CpG-stimulated BMDC as compared to non-stimulated BMDC (Figure 42B and C, D vs. E, F and G) was found for both the groups of mice.

IFN- $\gamma$ , a pivotal cytokine produced by T cells during the proliferation indicating the polarization of Th cells towards Th1, was analyzed in BMDC/T cell coculture supernatants after d 3. Non-stimulated BMDC from both sham and CLP operated mice induced the T cells to secrete low levels of IFN- $\gamma$  and septic BMDC induced the T cells to release even lower amounts of IFN- $\gamma$  when compared with BMDC from sham mice. IFN- $\gamma$  synthesis was increased many-fold from the T cells cocultured with BMDC upon CpG stimulation (**Figure 42H**). T cells cultured with BMDC from septic mice in spite of having the same proliferation as that of sham BMDC/T cell cocultures, produced up to two-fold less IFN- $\gamma$  upon CpG stimulation (**Figure 42H**). Thus, BMDC from septic mice showed same T cell proliferative capacity but were less effective in inducing T cell derived IFN- $\gamma$  synthesis than BMDC from sham mice.

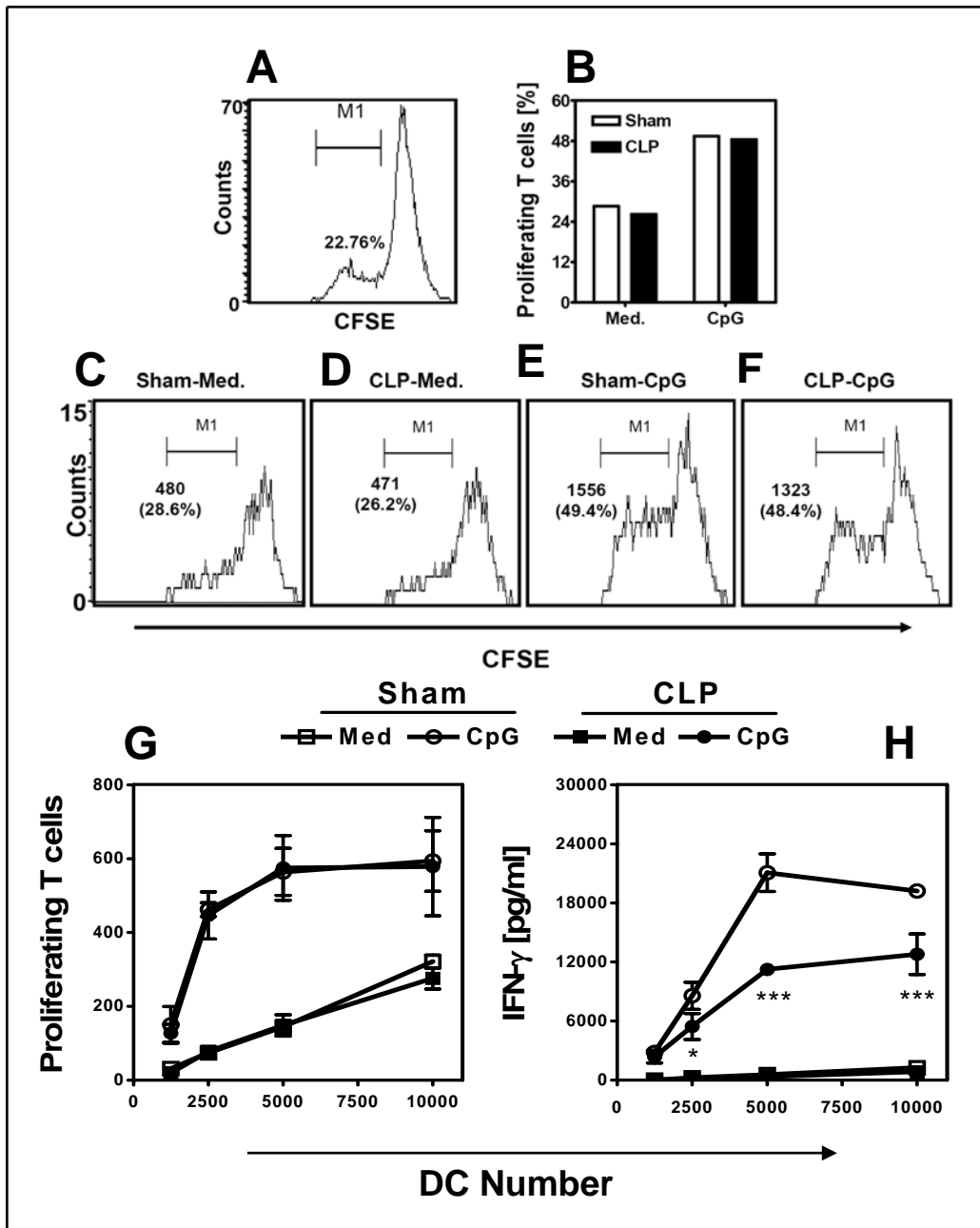


**Figure 42. *In vitro* T cell proliferation and IFN- $\gamma$  synthesis during sepsis.**

BMC after 24 h CLP or sham operation, were cultured for d 7 to generate BMDC. Titrated numbers of BMDC were cultured in the absence and presence of CpG in 96-well plates for 18 h and then CFSE-labeled, allogenic T cells were added to it. After d 3, non-adherent cells were analyzed for proliferation (A-G) as described in Materials and Methods (Section 2.3.7.3) and the supernatants were tested for IFN- $\gamma$  by ELISA (42H). (A) Histogram showing M1 population along with the mother population of proliferating T cells. (B) Representative graph from one of the BMDC titrated cells with or without CpG stimulation. (C-F) Histograms only with M1 population of proliferating T cells with or without CpG stimulation. (G) Graphical representation for all the titrations of BMDC/T cell cocultures in the absence or presence of CpG. (H) IFN- $\gamma$  ELISA from the supernatants of BMDC/T cell cocultures collected after d 3. Data show mean  $\pm$  SEM of triplicate cultures of BMDC with medium (open squares), and after CpG stimulation (open circles) from sham mice and with medium (solid squares), and after CpG stimulation (solid circles) from septic mice and are representative of three experiments. Asterisks indicate significant differences between cultures of sham and CLP groups. \*,  $P < 0.05$ ; \*\*\*,  $P < 0.0005$ .

### 3.2.6.1.1 Increased IFN- $\gamma$ secretion through neutralization of IL-10

To address the question whether the increased IL-10 after d 7 of BMDC culture was responsible for the reduced T cell proliferation and IFN- $\gamma$  production, endogenous IL-10 was neutralized using anti-IL-10 antibody. Titrated numbers of BMDC were cultured with or without CpG and then CpG-stimulated cells were incubated with anti-IL-10 antibody before the addition of allogenic, CFSE-labeled T cells. After d 3, the supernatants were collected from BMDC/T cell cocultures and analyzed for IFN- $\gamma$  production. Though, BMDC upon CpG stimulation from both sham and septic mice induced T cells derived higher levels of IFN- $\gamma$  (**Figure 42H**), the latter was much lower from the septic BMDC/ T cell cocultures as compared to that from sham mice (**Figure 42H**). Anti-IL-10 had no effect on non-stimulated cells (Data not shown), but further increased the T cell derived IFN- $\gamma$  release in response to CpG-stimulated BMDC/T cell cocultures from both sham as well as septic mice. However, T cells induced by septic BMDC produced significantly more IFN- $\gamma$  (**Figure 43**). Therefore, neutralization of endogenous IL-10 using anti-IL-10 antibody restored the T cells derived IFN- $\gamma$  production induced by septic BMDC even above levels induced by sham BMDC.

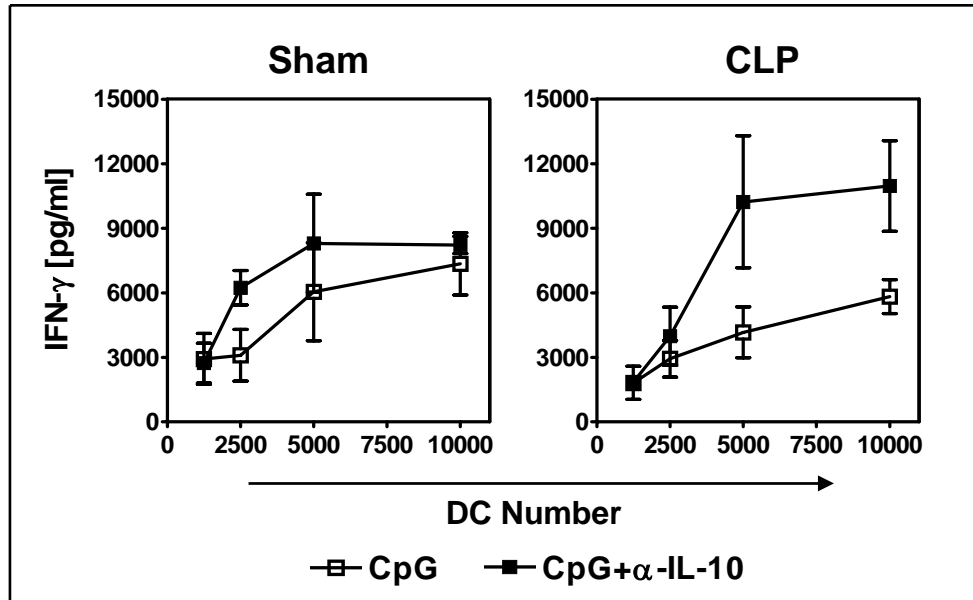


**Figure 43. Effect of  $\alpha$ -IL-10 on IFN- $\gamma$  production.**

BMC after 24 h CLP or sham operation, were cultured for 7 d to generate BMDC. Titrated numbers of BMDC were cultured in the absence and presence of 5  $\mu$ g/ml CpG in 96-well plates for 18 h and then incubated with a dose of 10  $\mu$ g/ml of anti-IL-10 antibody for an hour before the addition of CFSE-labeled, allogenic T cells. After d 3, the supernatants were tested for IFN- $\gamma$  by ELISA. Data show mean  $\pm$  SEM of triplicate cultures of BMDC with CpG (open squares), and after CpG plus anti-IL-10 incubation (filled squares) from sham and septic mice and are representative of two experiments.

### 3.2.6.2 *In vivo* T cell-stimulatory capacity of BMDC during sepsis

Furthermore, the capacity of BMDC to induce T cell activation was analyzed *in vivo*. DO11.10 TCR transgenic mice encoding a T cell receptor specific for ovalbumin (OVA) peptide (amino acids, 323-339) presented by the MHC class II molecule were used to determine *in vivo* T cell activation. T cells from DO11.10 TCR transgenic mice were purified and labeled with CFSE and then injected i.v. into the tail vein of healthy BALB/c mice. One day later, these mice were treated with BMDC stimulated with ovalbumin alone (Ova) or in combination with CpG (Ova + CpG) from both sham and septic mice. After d 3, LNCs were prepared and checked for proliferating T cells by gating CFSE-positive CD4<sup>+</sup> and DO11.10<sup>+</sup> viable and proliferating T cells using FACS (**Figure 44A**). In line with the *in vitro* pattern of proliferation, BMDC from both septic and sham mice showed similar *in vivo* T cell proliferation capacity to Ova (**Figure 44B and C vs. D**) and also to Ova in presence of CpG (Ova + CpG, **Figure 44B and E vs. F**). Further, the isolated LNCs were cultured and restimulated with Ova or ova-peptide for three days and the supernatants were assessed for IL-2 and IFN- $\gamma$ , produced by T cells during the proliferation. IL-2, a cytokine for proliferation was found similar in the restimulated-LNCs-cultures (restimulation with Ova or ova-peptide) from both the groups of mice receiving either Ova (**Figure 44G**) or Ova + CpG (**Figure 44H**) BMDC. The capacity for IFN- $\gamma$  production was significantly reduced by these restimulated-LNC-cultures (Med, Ova and ova-peptide restimulation) from the mice that received Ova + CpG-stimulated (**Figure 44J**) BMDC from the septic mice when compared with stimulated-BMDC from the sham mice. IFN- $\gamma$  secretion from the same restimulated LNCs from the mice injected with only ova-stimulated BMDC from both sham and septic mice did not show any change (Med. **Figure 44I**). Therefore, BMDC from septic mice had same T cell proliferative capacity but were less potent in inducing T cell derived IFN- $\gamma$  synthesis than BMDC from sham mice.

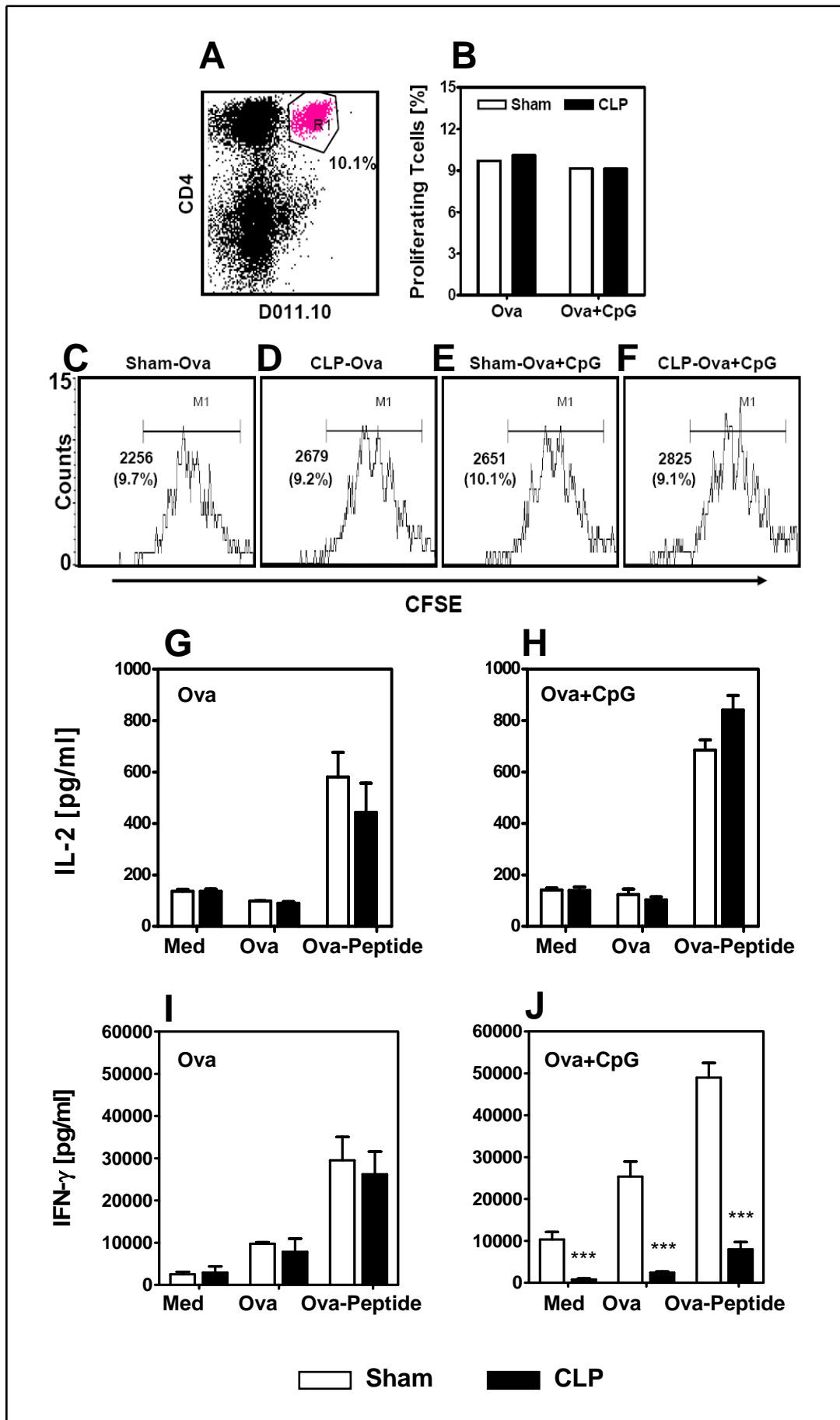


**Figure 44. *In vivo* T cell proliferation and IFN- $\gamma$  production during sepsis.**

Purified and labeled splenic T cells isolated from D011.10 TCR transgenic mice were injected i.v. into the tail vein of a healthy BALB/c mouse. After 24 h, 7 d-BMDC ( $2 \times 10^6/2$  ml/well) were stimulated with 100  $\mu\text{g/ml}$  ovalbumin (Ova) alone or in the presence of 5  $\mu\text{g/ml}$  CpG (Ova + CpG) for 7 h and  $0.5 \times 10^6$  BMDC/30  $\mu\text{l}$  PBS were then injected into the foot pad of BALB/c mice which had received the T cells, one day before. Three days later, draining LNCs were prepared and stained for CFSE-positive CD4<sup>+</sup> and D011.10<sup>+</sup> T cells. (A) One of the dot plot showing the CFSE-positive CD4<sup>+</sup> and D011.10<sup>+</sup> T cells. (B) Representative graph out of four independent experiments showing *in vivo* proliferation of CFSE-positive CD4<sup>+</sup> and D011.10<sup>+</sup> T cells gated in figure 26A from LNCs isolated from the mice injected with sham or septic Ova-stimulated and Ova + CpG-stimulated BMDC. (C, D, E and F) Histogram only with the M1 population of proliferating T cells with or without CpG stimulation from sham or septic BMDC. (G, H, I and J) Further, the isolated LNCs were cultured and restimulated in the absence (Med) or presence of 50  $\mu\text{g/ml}$  Ova and 1  $\mu\text{g/ml}$  ova peptide (Ova-peptide) in triplicates. After 3 d, the supernatants were collected and used for IL-2 (G and H) and IFN- $\gamma$  (I and J) cytokine ELISA. Data show mean  $\pm$  SD of triplicate co-cultures of T cells with BMDC from sham (open bars) and septic (black bars) mice each stimulated with Ova (G and I) or Ova + CpG stimulation (H and J). Asterisks indicate significant differences between cultures of sham and CLP groups. \*\*\*,  $P < 0.0005$ .

### 3.2.7 Different myeloid DC Progenitor during polymicrobial sepsis

The role of myeloid CD4<sup>+</sup> DC progenitors was investigated after 24 h of sham or CLP operation in order to test whether these progenitors could be associated with the enhanced IL-10 release by the dendritic cells. BMC were prepared 24 h post CLP or sham operation and stained for CD11c in combination with CD4 and MHC class II surface molecules. Total CD11c<sup>+</sup> DC were gated and selected for MHCII<sup>-</sup> surface marker to have the DC progenitors. CD4<sup>+</sup> expression was studied on these DC progenitors to analyze the CD4<sup>+</sup> myeloid progenitors (CD11c<sup>+</sup>MHCII<sup>-</sup>CD4<sup>+</sup>; **Figure 45A**). The percentage of the CD4<sup>+</sup> DC progenitors was high (**Figure 45A and B**) from both sham ( $22.38 \pm 6.77\%$ ) as well as septic mice ( $9.76 \pm 1.94\%$ ). However, the percentage of these myeloid progenitors after 24 h of sepsis was drastically and significantly reduced up to 56% (**Figure 45A and B**). Taken together, the decrease in the percentage of these specific progenitors might be responsible for the observed aberration in the cytokine response.

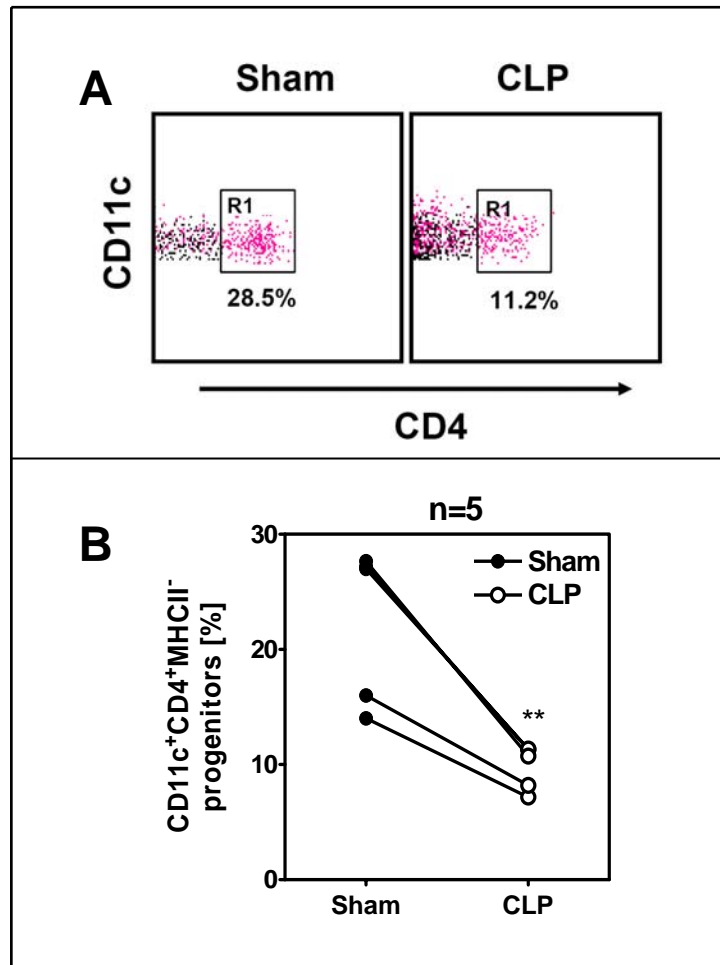


**Figure 45. CD4<sup>+</sup> myeloid progenitors during polymicrobial sepsis.**

Twenty-four hours after sham or CLP operation, total BMC were pooled (n=2-3 per group) and stained for CD11c<sup>+</sup> in combination with CD4<sup>+</sup> and MHC class II surface markers. (A) CD11c cells were gated and next MHC class II<sup>+</sup> dendritic cells were selected out of total DC. CD4<sup>+</sup> expression was analyzed on these CD11c<sup>+</sup>MHC II<sup>+</sup> cells (CD4<sup>+</sup> myeloid progenitors, **Region R1**). FACS data shown are representative of five independent experiments. (B) The percentage of CD4<sup>+</sup> DC progenitors (CD11c<sup>+</sup>CD4<sup>+</sup>MHC II<sup>+</sup>) of individual mouse from sham (filled circles) and septic (open circles). Asterisks indicate significant differences between cultures of sham and CLP groups. \*\*,  $P < 0.005$ .

# DISCUSSION

---

## 4. Discussion

The present work analyzed the effect of GM-CSF as a potential immunostimulator. Several different aspects were investigated. First, we determined the effect of an *in vitro* treatment with GM-CSF in a hemorrhagic shock model. In this context, it could be demonstrated that GM-CSF as an immunostimulator could partly reinstate the suppressed LPS-induced TNF- $\alpha$  response of peritoneal macrophages following hemorrhagic shock. As an additional pathophysiological model we utilized cecal ligation and puncture (CLP), a commonly used animal experimental model for severe polymicrobial sepsis [13, 14, 147, 152, 153]. In this model, we demonstrated that GM-CSF could partly augment the extremely suppressed IL-12 production of dendritic cells. However, in this model the effect of GM-CSF was not adequate to reach normal levels.

In order to gather a better understanding of the underlying mechanisms of GM-CSF activation of the TNF- $\alpha$  response, we analyzed the interaction between GM-CSF and LPS-signaling cascades. The priming effect of GM-CSF in terms of LPS-induced TNF- $\alpha$ -production was accompanied by a corresponding increase in I $\kappa$ B $\alpha$  phosphorylation and the activation of P38MAPK and the phosphorylation of ERK1/2 which could be shown for isolated human monocytes, the monocytic cell line THP-1 and murine peritoneal macrophages. An involvement of MAPK activity [154] was suggested and will be discussed later. To further understand the possibly involved signaling pathways, the analyses were extended to the pathophysiological situation of a hemorrhagic shock. In this context, we observed that hemorrhagic shock suppressed I $\kappa$ B $\alpha$  phosphorylation and ERK1/2 activation, but enhanced P38 phosphorylation in peritoneal macrophages. *In vitro* treatment with GM-CSF could partly, but not completely restore this alternated peritoneal macrophage response also on the basis of the investigated intracellular signaling molecules.

Since GM-CSF therapy has been suggested in clinical trials, especially for neutropenic septic patients, which suggest a predominant effect of GM-CSF on the bone marrow, further studies dealt with the role of the bone marrow during sepsis. Polymicrobial sepsis showed a significant loss of bone marrow cells. The cell loss could not be attributed to

the increased apoptosis as the percentage of apoptotic cells was very low. In addition, an elevated count of dendritic cells together with monocytes and granulocyte in the blood was observed during sepsis suggesting increased release of these cell populations from the bone marrow into the blood.

In spite of a diminished number of BMC during sepsis, septic mice demonstrated a higher percentage of total CD11c<sup>+</sup> cells. However, similar numbers of MHC II progenitors were found after CLP. During culture, BMC from septic mice proliferated strongly and generated up to double the number of cells after d 7 than the corresponding cultures of BMC from sham-operated mice. The number of bone marrow derived dendritic cells was found akin in both the group of mice after d 7 of culture. In addition, BMDC from septic mice, when cultured in the presence of different bacterial stimuli produced significantly higher levels of IL-10 but an unchanged amount of TNF- $\alpha$  and IL-12. Further, these septic BMDC are less potent in inducing the T cell activation observed by the low IFN- $\gamma$  synthesis by BMDC-induced T cells. Neutralization of endogenous IL-10 using anti-IL-10 antibodies could restore the reduced IFN- $\gamma$  producing capacity of Th cells induced by septic BDMC indicating a Th2 promoting IL-10 in this sepsis model.

In order to appraise the possible explanation for the elevated IL-10 cytokine level, participation of CD4<sup>+</sup> myeloid progenitors was examined. It could be demonstrated that twenty-four hours post CLP BMC demonstrated significantly lower number of the CD4<sup>+</sup>MHCII<sup>+</sup> myeloid progenitor cells. The decreased progenitors could be responsible for the enhanced IL-10 level which polarized the Th cells towards Th2 phenotype.

A reduced cytokine-producing capacity of LPS-stimulated peritoneal macrophages has been reported in several experimental settings associated with hemorrhagic shock, which are mostly in line with the results of the present study. Sublethal haemorrhage has been reported to cause a blunted cytokine response of human circulating monocytes, murine peritoneal and splenic macrophages [94]. In alignment with previously reported results [94, 155], we also found a reduced LPS-stimulated TNF- $\alpha$  response in peritoneal macrophages after hemorrhagic shock. In a similar experimental setting of sublethal hemorrhage performed in rats, a depression of LPS-induced TNF- $\alpha$  synthesis of peritoneal macrophages has been reported [156]. Also, in sublethal hemorrhage in rats, a reduced TNF- $\alpha$  production to subsequent LPS-challenge has been reported for

mononuclear cells derived from the intestinal mucosa [20], spleen cells [18, 19] and bone marrow cells [19].

A diminution in LPS-dependent TNF- $\alpha$  synthesis was also observed after cecal ligation and puncture (CLP), a model for polymicrobial sepsis. In the presented study, we observed a strong reduction in TNF- $\alpha$  producing capacity of splenic macrophages collected 24 h after CLP. These data comply with studies performed by various other groups. In a recently reported piece of work, a significant suppression of TNF- $\alpha$  in LPS-stimulated splenic macrophages has been documented in rats receiving a combined insult of trauma-hemorrhage and CLP [157]. Also, a significant depression of TNF- $\alpha$  from macrophages harvested from either peritoneal cavity or spleen has been suggested during late sepsis [158]. In addition, diminished TNF- $\alpha$  production of splenic macrophages has been demonstrated numerously after hemorrhagic shock [18, 19, 94].

Next, the capacity of splenic dendritic cells was examined in terms of IL-12 cytokine production. In alignment with a recently reported study [159], we also found a reduced CpG-stimulated IL-12 response in splenic dendritic cells during sepsis. We could show that DC became unable to secrete bioactive IL-12 in response to CpG, a well known inducer of IL-12. A state of impaired IL-12 secretion by splenic DC upon restimulation with microbial components has been reported in other models of infectious diseases also [160]. The impaired capacity of DC to release IL-12 during sepsis might contribute to the inappropriate polarization of Th cells toward Th2 phenotype. Indeed, it has been documented that after severe injury or sepsis CD4<sup>+</sup> T cell polarization is altered and that there develops a later phase of immunosuppression mediated by a predominance of the Th2-type cytokines (IL-4 and IL-10;[80] and a depression in the production of IL-2, and IFN- $\gamma$  [80, 161, 162].

GM-CSF possesses an immunostimulatory capacity and is revealed to boost the activation aptitude of monocytes in diverse pathophysiological conditions having monocyte dysfunctions [96, 99, 163-166]. The augmenting property of GM-CSF is also recognized on mature monocytes and macrophages enhancing their potential to release various cytokines such as TNF- $\alpha$ , IL-1 $\beta$  and IL-12 after LPS stimulation, a phenomenon commonly referred to as “priming” [87, 88, 99, 165, 167].

GM-CSF has been suggested as a therapeutic approach for trauma-, shock- or sepsis-induced immunosuppression [95-97] and when administered *in vitro*, could restore the impaired cytokine response and MHC-class II molecule expression of monocytes from

trauma patients [168]. In sepsis-associated immune dysfunction the administration of GM-CSF was able to counteract the reduced HLA-DR expression on monocytes as well as the reduced TNF- $\alpha$  producing capacity of whole blood cultures [95]. In another similar study, blood samples from severely injured patients or patients after major surgery show a diminished LPS-induced TNF- $\alpha$  synthesis which can be at least *in vitro* antagonized by GM-CSF [169]. In an uncontrolled clinical trial GM-CSF was given in severely injured patients with low granulocyte counts [170]. The study showed that GM-CSF rapidly elevated granulocyte counts and an increased HLA-DR expression on granulocytes was found. Further, no adverse side effects were observed so that the treatment approach was considered as safe. *In vivo* treatment with GM-CSF of mice after hemorrhage improved survival and controlled bacterial spreading after secondary septic challenge by cecal ligation and puncture [171]. Concerning hemorrhagic shock, GM-CSF application *in vivo* in mice after hemorrhage could counteract the downregulation of MHC class II molecules on peritoneal macrophages [172]. In addition, it has been demonstrated, that GM-CSF given immediately after reperfusion could restore the diminished TNF- $\alpha$  response of spleen and peritoneal cells [94]. A diminished synthesis of pro-inflammatory mediators can be induced *in vitro* by preincubation with endotoxin [173]. The status of endotoxin tolerance resembles the situation of the immune response observed after hemorrhage. GM-CSF addition to *in vitro* endotoxin-tolerized human monocytes can antagonize this tolerance and restore TNF- $\alpha$  production [164].

When GM-CSF is given *in vivo*, the restoration of the cytokine response may be explained by the generation of new macrophages population from the bone marrow, which of course is activated by the haematopoietic growth factor GM-CSF. In order to rule out a bone marrow dependent effect of GM-CSF, the stimulation with the compound in the presented study was performed *in vitro*. However, also *in vitro* treatment with GM-CSF could at least restore the TNF- $\alpha$  response of peritoneal macrophages after shock and polymicrobial sepsis.

Principally, the priming effect of GM-CSF was also evident in dendritic cells after 24 h of polymicrobial sepsis. However, the effect of GM-CSF *in vitro* on CpG-induced IL-12 production in DC from septic mice was only minimal. GM-CSF could only partially counteract the depressed CpG-dependent IL-12 production of dendritic cells from septic mice. The stimulatory effect of GM-CSF in DC was not appropriate to reach to the normal control level. For the lower responsiveness of GM-CSF towards dendritic cells,

one might suggest the downregulation of GM-CSF receptor on dendritic cells but not on macrophages during sepsis. We did not study these specific receptors in our experiments. It is known that GM-CSF receptor remain unchanged on human monocytes after trauma and septic trauma patients [97]. No data is available for dendritic cells and GM-CSF receptor expression in sepsis. However, it is known that DC mature during sepsis [80]. Kampgen et al has described abundant GM-CSF receptors on mature DC [174]. Therefore, a downregulation of the GM-CSF-receptor probably does not explain the reduced response of DC to GM-CSF in sepsis.

Alternatively, DC during sepsis could become “exhausted” and cannot respond to further stimuli e.g. GM-CSF. Indeed, we showed that during sepsis, DC expressed high percentage of CD40 and CD86, the surface markers for DC maturation as compared to the normal levels indicating that the DC are already matured during sepsis. Although, GM-CSF could further enhance the CD86 expression, no change in CD40 was recognized after GM-CSF treatment. Therefore, one can speculate that DC could respond to GM-CSF in terms of CD86 expression but not CD40, and the overall response is not sufficient to compensate the suppressed system during sepsis.

It is not evident from the present literature on GM-CSF that this cytokine in itself is able to activate the NF $\kappa$ B system or induce TNF- $\alpha$  formation in monocytes or macrophage. The presented data are in line with the literature since neither TNF- $\alpha$  release nor I $\kappa$ B phosphorylation was observed in GM-CSF-stimulated monocytes and macrophages. However, GM-CSF preincubation enhanced the LPS-induced TNF- $\alpha$  production without inducing this cytokine on its own- a phenomenon commonly referred to as “priming”. The underlying mechanism of GM-CSF priming could be sought to be an interaction between signaling cascades typical for GM-CSF and LPS. Therefore, we analyzed the signaling events activated by GM-CSF and LPS to gain a better perspective of the basic mechanisms involved in the GM-CSF effect.

We confirmed the priming effect of GM-CSF on LPS-induced TNF- $\alpha$  production in normal human circulating monocytes and the human monocytic cell line, THP-1 as well as in mouse peritoneal macrophages. The elevated TNF- $\alpha$  response was accompanied by a corresponding increase of I $\kappa$ B $\alpha$  and MAPKinase activation [87, 164, 168]. GM-CSF enhanced the TNF- $\alpha$  release of LPS-induced human monocytes, THP-1 cells and normal mouse peritoneal macrophages. The enhanced TNF- $\alpha$  production in both primed monocytes and THP-1 cells could be attributed to the immunostimulatory effect of GM-

CSF since the increased NF $\kappa$ B binding was accompanied by an increase in cytosolic I $\kappa$ B $\alpha$  phosphorylation as shown by electrophoretic mobility shift assay and Western blotting of NF $\kappa$ B components in the nuclear extracts.

GM-CSF also enhanced the ERK1/2 and P38 MAPKinases of LPS-induced human monocytes, THP-1 cells and normal mice peritoneal macrophages for the production of TNF- $\alpha$ . This effect of GM-CSF for ERK1/2 complies with the study of others where they have shown GM-CSF to induce phosphorylation of MEK1/2 and ERK1/2 in isolated monocytes [175]. Although, GM-CSF primes the phosphorylation of both ERK1/2 and P38 signaling, the priming for LPS-induced TNF- $\alpha$  synthesis seems to be primarily due to phosphorylation exerted by ERK1/2 as proved by the inhibitor studies done by our own group [154]. PD98059, an inhibitor of ERK1/2 is shown to completely abrogate the GM-CSF priming of TNF- $\alpha$  synthesis. In addition, SB203580, that has been used to demonstrate the essentiality of P38MAPK for maximum LPS-induced TNF- $\alpha$  synthesis [176] did not at all decrease GM-CSF-induced priming for TNF- $\alpha$  synthesis [154].

Next, we continued the investigation of these I $\kappa$ B $\alpha$  and MAPK signaling for the pathophysiological condition of hemorrhagic shock. Alterations in MAPK (P42/44, P38 and SAPK/JNK) and NF $\kappa$ B activation and subsequently, a diminished cytokine response of murine peritoneal macrophages has been reported following sublethal hemorrhage [94].

As described earlier, we found a reduction in LPS-stimulated TNF- $\alpha$  production in peritoneal macrophages after hemorrhagic shock as shown by others as well as our own research group [94, 155]. This seems to be accompanied by a lower NF $\kappa$ B activation in these cells since we found a lower degree of I $\kappa$ B $\alpha$  phosphorylation. Indeed, NF $\kappa$ B is known as one of the predominant transcription factors involved in TNF- $\alpha$  gene activation [177, 178]. Suppression of LPS-induced TNF- $\alpha$  synthesis of peritoneal macrophages has been reported in an experimental study of sublethal hemorrhage [156], which was also accompanied by a diminished activation of the intracellular NF $\kappa$ B signaling pathway [179]. The experimental results in animal studies are in line with clinical observation in patients with severe injury. Suppression of various cytokines and a long-term-impaired expression of NF $\kappa$ B and I $\kappa$ B $\alpha$  have been observed in peripheral blood mononuclear cells of major trauma and septic patients [58, 59]. NF $\kappa$ B transcription factor is involved in the regulation of immune and acute-phase response at the transcriptional level [180]. NF $\kappa$ B regulation may be critical for cytokine gene expression in trauma, because of its presence

in the enhancer and promoter regions of proinflammatory cytokine (for example, TNF- $\alpha$ , IL-1 $\beta$ , IL-6 and IL-8) genes and its inducibility by several extracellular signals known to be present in trauma patients, such as reactive oxygen species, cytokines and endotoxin [181, 182].

It has also been shown that maximal TNF- $\alpha$  response in macrophages also depends on the activation of P38 and P42/44 (ERK1/2) MAPK [155, 183]. Correspondingly, in our experimental setting lower TNF- $\alpha$  response was also paralleled by a dampened activation of ERK1/2.

Decreased activation of ERK1/2 as well as Jun-Kinase after LPS stimulation has been described in lung and liver tissue 24 h after hemorrhagic shock in rats [57]. On the other hand, ERK1/2 activation by hemorrhagic shock on its own has been observed as early as 1 h after hemorrhage in alveolar macrophages [56] and liver tissue [184]. Therefore, ERK1/2 activation seems to be involved in both the early stress response after shock and thereafter undergoes a counter regulation with a diminished reactivity. This response pattern resembles the production of various cytokines such as TNF- $\alpha$  and IL-6 after hemorrhagic shock.

The other investigated MAPK family member P38MAPK surprisingly shows an opposite pattern of activation. In spite of the fact that P38 activation is also necessary for a maximal TNF- $\alpha$  production [185-188], the impairment of peritoneal macrophages' TNF- $\alpha$  synthesis after haemorrhage was accompanied by an enhanced phosphorylation of P38 signal. Similar observations have been reported by Angele et al., who found an increased LPS-induced P38 phosphorylation in peritoneal macrophages isolated 2 h after haemorrhage from male but not female mice [189]. These observations may lead to the speculation that P38 activation evokes macrophages' impaired cytokine response or tolerance induction. Indeed, there exists some evidence for this hypothesis. P38MAPK seems to be involved in IL-10 secretion, which is in turn a central anti-inflammatory mediator dampening TNF- $\alpha$  response also after hemorrhagic shock [190]. Besides the possible involvement of P38 in IL-10 regulation, there does not exist any clear experimental proof for a shock-induced cytokine response suppression mediated by P38 activation.

Summarizing this part of the study, the present work investigated the innate immune response after hemorrhagic shock as well as in polymicrobial sepsis. Defects in the primary response of macrophages and DC were described on the basis of cytokine

response, surface marker expression and intracellular signaling cascade. GM-CSF as a potential immunostimulating compound was able to counteract most of these deteriorations of the immune response levels. Therefore, this substance may be of interest as an immunomodulator in this context.

In addition to the above described role of GM-CSF as immunomodulator the function of GM-CSF as growth factor during polymicrobial sepsis was addressed. During sepsis, a large part of DC is lost in lymphoid organs and the remaining DC display an aberrant cytokine secretion pattern. Therefore, it is conceivable that there exists a failure of the DC generation in the bone marrow that is dependent on GM-CSF. This defect might result in an impaired “refill” of the DC pool in lymphoid organs and/or in the release of DC with an aberrant cytokine response to bacterial products.

First, the generation of myeloid cells from the bone marrow during sepsis was analyzed. We showed that polymicrobial sepsis induced a strong reduction of total bone marrow cells, isolated 24 h post CLP. The percentage of reduction of BMC was found up to 40% which is indeed a significant loss of cells to the body’s defense system to combat the infection. One might speculate two possibilities for the explanation of this cell loss during sepsis. First, there could be enhanced apoptosis and second, there could be an increase in the release of different bone marrow cells into the blood during sepsis.

Apoptosis, the programmed cell death (PCD), plays an important role in the pathology of sepsis [191]. A substantial loss of dendritic cells [75], as well as of B and T-helper cells due to PCD has been observed in the spleen [192] and thymus [193]. Increased apoptosis has also been shown for circulating lymphocytes, particularly CD4 and CD8 T cells, B cells and NK cells [194] in case of septic patients. Although, there does exist an ample amount of information regarding apoptosis of different cell types in different organs and in the circulation, there is paucity of data showing apoptosis of total bone marrow cells during sepsis. In the present study, an increased apoptosis of BMC after 24 h of CLP was investigated which is in alignment with the studies performed by Chung et al who also mentioned an increase in apoptosis in the similar experimental conditions [193]. However, the increase in apoptosis could not argue for the reduced number of total BMC during sepsis, since, the total percentage of apoptotic cells found during sham as well as sepsis was too low to account for this effect. The percentage of both dying and dead cells was 6% maximum as confirmed by Annexin V and 7-AAD, respectively.

Concerning the second parameter of cell loss during sepsis, increased release of bone marrow cells into the blood could be another responsible mechanism. Indeed, an

enhancement in total leukocyte count was found 24 h after CLP. A significant increase for the release of other myeloid cells such as dendritic cells, granulocytes and monocytes from the bone marrow into the blood was also observed. There was an increase in the release of total CD11c<sup>+</sup> cells which showed specially the phenotype of MHC II<sup>-</sup> DC progenitors. It cannot be excluded that the CD11c<sup>+</sup> MHCII<sup>-</sup> population also contain some NK cells although at a lesser extend than DC [195, 196]. Furthermore, analysis of the generation of myeloid cells from bone marrow *in vitro* showed that DC progenitors in the bone marrow of septic mice have the same sensitivity to GM-CSF and proliferate in the same manner as DC progenitors from sham mice.

Despite an increased number of DC in the circulation during sepsis, the sepsis-associated loss of DC in lymphoid organs cannot be compensated. This suggests that either the homing of newly released DC to the lymphoid organs is deregulated or that these cells undergo apoptosis after reaching these organs. However, it can not be told for sure about the deregulation of homing to different organs since no experiments were performed to track the migration of the cells from bone marrow to different organs such as spleen. Thus, the failure of the immune system to replace the sepsis-associated loss of DC in the lymphoid organs seems not to be mediated by an impaired generation and release of DC into the circulation.

Not only the depletion of dendritic cells was found during sepsis but also the remaining DC showed a deviated cytokine production at least in the spleen [80]. This altered cytokine production might be the consequence of a sepsis-mediated modulation of splenic DC or it might represent the phenotype of DC after homing into the spleen. The possibility of a “new” DC population was supported by the finding that DC generated from bone marrow of septic mice *in vitro* display an altered cytokine secretion pattern in comparison to BMDC from sham mice. TNF- $\alpha$ , IL-10, IL-12 were selected to study the cytokines behavior of BMDC during sepsis. Among the pro-inflammatory cytokines, TNF- $\alpha$  was selected since it is recognized as a key cytokine mediating the pro-inflammatory response [197-201]. Next, we studied IL-12, a heterodimeric cytokine consisting of p35 and p40 subunits [1, 202]. It is known that IL-12 is produced by phagocytes, B lymphocytes and dendritic cells in response to bacteria or bacterial products [203-205]. In addition, IL-12 is required for the production of IFN- $\gamma$  by T lymphocytes and supports the development of the Th1 phenotype of CD4<sup>+</sup> T cells [162]. Concerning IL-10, during the last decade, several studies indicate that among the anti-

inflammatory cytokines, it plays an important role in sepsis response [36, 206] and the expression of IL-10 may contribute to sepsis-induced immunosuppression [36, 80]. In the present work, we showed that the secretion of TNF- $\alpha$  from both sham and septic mice was found to be similar. We observed that 24 h after CLP, DC were unable to secrete bioactive IL-12 in the absence of any stimulation. Cytokine synthesis of untreated BMDC might represent the activity of BMDC in situ. However, BMDC from both sham as well as septic mice could secrete IL-12 in response to LPS + CD40L or CpG, both well known inducers of IL-12 and also in the presence of other stimuli such as PGN or bacteria. Although, BMDC could secrete IL-12 in response to different stimuli, we found no change among both the groups of mice. Instead, BMDC from septic mice secreted prominent levels of IL-10 *ex vivo*, which were further enhanced upon stimulation with otherwise IL-12-inducing agents. The reason for this abnormal cytokines secretion remains unclear. IL-12, the counter-regulatory cytokine for IL-10 seems not to be responsible for this enhanced IL-10 as no change was observed during sepsis concerning IL-12. In addition to test the functional characteristic of BMDC, the DC were also investigated for their phenotypic expression of surface co-stimulatory molecules such as CD40 and CD86, the maturation markers of dendritic cells. BMDC did not enhance the expression of CD40 or CD86 upon sepsis within 24. Thus, In spite of no change in terms of BMDC surface marker expression, sepsis modulated the bone marrow derived dendritic cells in terms of cytokine secretion. BMDC mirror in part phenotype of splenic DC during sepsis. This supports the hypothesis of “new” population in the spleen. Further, the question whether altered DC behavior could be relevant for T cell polarization, was addressed. The capacity of BMDC to induce T cell activation was evaluated both *in vitro* and *in vivo*. *In vitro* T cell proliferative capacity of BMDC was found unchanged after 24 h of CLP operation. BMDC from septic mice induced a similar proliferation of T cells as did BMDC from sham mice. However, in spite of having the same proliferation potential, T cells stimulated with BMDC from septic mice released less IFN- $\gamma$  than T cells stimulated with BMDC from sham mice. The results from *in vitro* studies complied with the *in vivo* BMDC-induced T cell activation studies. The predominance of IL-10 released from BMDC during sepsis as shown here might polarize Th cells towards Th2 and in parallel might inhibit the development of a Th1 response that is required for the effective clearance of bacterial infections [207]. The finding that BMDC from septic mice secreted elevated levels of Th2 cytokines upon different

stimulation with bacterial components further supported this conjecture. The suppressive activity of IL-10 on Th1 cell polarization and proliferation might explain the finding that DC from septic mice were inferior to DC from controls in T cell activation. Taking the fact of IL-10 into consideration, endogenous IL-10 was neutralized using anti-IL-10 antibody which interestingly restored the decreased IFN- $\gamma$  production induced by BMDC from septic mice. This further added the proof that IL-10 might be responsible for skewing the system towards Th2 type of phenotype and on other hand inhibiting the Th1 system.

The mechanisms underlying the reduced capacity of BMDC from septic mice to polarize T cells towards Th1 remain unclear. Th1 cell proliferation is impaired by the activity of Th2 cells or by regulatory T cells. BMDC-induced T cells were not tested for the release of Th2 cytokines like IL-13, IL-10 or IL-5. On the other hand, BMDC were shown to induce the expansion of naturally occurring CD4<sup>+</sup>CD25<sup>+</sup> regulatory T cells which suppressed the activation of DC mediated activation of CD4<sup>+</sup>CD25<sup>-</sup> T cells [208]. These Treg cells inhibit the proliferation and cytokine release of antigen-specific Th1 cells. Therefore, it might be possible that BMDC expand and activate Treg cells that prevent the induction of a protective Th1 immune response. Further characterization of BMDC-activated T cells is needed to clarify the mechanisms of impaired Th1-polarization.

DC progenitors in the bone marrow from septic mice underwent several rounds of proliferation during the seven-day-lasting culture. The finding that during this long-lasting 7 d culture BMDC from septic mice differentiate to an altered phenotype than DC progenitor from sham mice is remarkable. This altered differentiation might originate from an altered composition of the environment or from a changed subtype composition of DC progenitors. It is shown that the presence of IL-10 or high amounts of LPS during the culture and BMC development generate DC characterized by enhanced IL-10 which favors Th2 polarization. However, in this study, no IL-10 was detected in the supernatants from untreated bone marrow cells from septic mice representing the cytokines milieu in situ. Also, no LPS was observed in the bone marrow cell cultures. This suggests that neither LPS nor IL-10 because of their absence during the culture of bone marrow cells can explain the increased Th2 polarization during sepsis.

The other possibility of different subtype composition might explain the enhanced IL-10 and induction of Th cells towards Th2 phenotype. Therefore, we looked for different subsets as the explanation for the enhanced IL-10 level and developed Th2 pattern. DC

are known to be heterogeneous which can be distinguished by a variety of cell surface markers and functional attributes [209]. It is of great interest to know whether differential immune responses are mediated by distinct subsets or simply reflect a functional stage of all DC. There is therefore great development in delineating more precisely the developmental pathways between immediate DC precursors and their progeny. CD11c<sup>+</sup>MHC II<sup>-</sup> precursor DC population in mouse bone marrow like CD11c<sup>+</sup>MHC II<sup>-</sup> blood cells has been identified to possess the capacity to generate various mature DC populations *in vivo*. CD11c<sup>+</sup>MHC II<sup>-</sup> precursor DC in bone marrow was shown to have two different B220<sup>+</sup> and B220<sup>-</sup> subpopulations, which are morphologically, immunophenotypically, and functionally distinct [210].

However, the presence of GM-CSF expands the bone marrow progenitors to develop preferentially into myeloid DC [62, 63]. So far there is not present enough literature for myeloid progenitors. Myeloid DC are characterized by CD11c<sup>+</sup>MHC II<sup>+</sup> surface markers that also originate from CD11c<sup>+</sup>MHC II<sup>-</sup> DC progenitors. We investigated the CD4<sup>+</sup> DC progenitors (CD4<sup>+</sup>CD11c<sup>+</sup>MHC II<sup>-</sup>) in the bone marrow cells after 24 h of CLP operation. Interestingly, we found a strong reduction in the percentage of these progenitors in septic BMC as compared to sham BMC. It might be speculated that this progenitor population might be the responsible factor for the enhanced IL-10 release by BMDC during sepsis and for the polarization towards Th2 like phenotype. Although, it was not proved in the present study but it can be investigated by deleting the CD4<sup>+</sup> progenitor population out of bone marrow cells and then looking for the effect upon their depletion for IL-10 release by dendritic cells.

Taken together, GM-CSF mediates the generation of bone marrow-derived DC that display a Th2-promoting phenotype in case of bone marrow cells from septic mice. Generation of such Th2-polarizing DC during sepsis *in vivo* might explain the altered phenotype of DC in lymphoid organs during sepsis.

# SUMMARY

---

## 5. Summary

After hemorrhagic shock and during sepsis, antigen-presenting cells lose the capacity to respond to bacteria or bacterial products with the secretion of pro-inflammatory cytokines. This malfunction of antigen-presenting cells like macrophages and dendritic cells is associated with the development of immunosuppression and might lead to multi-organ failure and death. GM-CSF is a cytokine that is known to modulate the cytokine secretion of antigen-presenting cells and additionally acts as growth factor on myeloid cells. In the present study, the capacity of GM-CSF to restore the secretion of pro-inflammatory cytokines by macrophages and dendritic cells was investigated in animal models for hemorrhagic shock and polymicrobial sepsis. Additionally, it was tested *in vitro*, whether GM-CSF might mediate the differentiation of competent dendritic cells from bone marrow during sepsis.

GM-CSF restored the suppressed LPS-induced TNF- $\alpha$  release from the splenic macrophages after hemorrhagic shock and during sepsis up to levels observed for the respective LPS-stimulated cells from sham mice. GM-CSF partially but not completely restored the suppressed LPS-induced TNF- $\alpha$  production from the peritoneal macrophages after hemorrhagic shock. The GM-CSF-mediated restoration of the LPS-induced TNF- $\alpha$  secretion by peritoneal macrophages was verified on the level of I $\kappa$ B $\alpha$  phosphorylation. In addition GM-CSF effects were also associated with increased levels of the activated forms of the signaling molecules P38MAPK and ERK1/2, possibly suggesting an involvement of one of these MAPK in the stimulatory effects of GM-CSF. In contrast, GM-CSF was inefficient in restoring the LPS-induced cytokine response by dendritic cells from septic animals. Analyses of the phenotype of dendritic cells that differentiated from bone marrow progenitors of septic mice in the presence of GM-CSF showed that these dendritic cells display an aberrant cytokine response and fail to polarize Th lymphocytes towards Th1. This malfunction of *in vitro* generated dendritic cells from septic mice is associated with an increased secretion of IL-10 in response to immunostimulatory bacterial oligonucleotides and resembles the deviated cytokine response from splenic dendritic cells during sepsis. The absence of IL-10 or LPS during

the GM-CSF-dependent differentiation of dendritic cells suggests that another mechanism was responsible for the development of the abnormal phenotype from BMDC from septic mice. A reduced population of CD4<sup>+</sup> dendritic cell progenitors with so far unknown function was found in the bone marrow of septic mice and might play a role in the aberrant differentiation of dendritic cells during sepsis. In summary, GM-CSF therapy might reinforce the macrophages' antibacterial defence mechanisms during hemorrhagic shock and sepsis-associated immunosuppression. However, differentiation of dendritic cells from bone marrow during sepsis might result in an aberrant phenotype of dendritic cells that prevent the development of a protective Th1 response and, thereby, further aggravates immunosuppression.

# REFERENCES

---

## 6. Rererences

1. Abdi K. IL-12: the role of p40 versus p75. *Scand J Immunol* 2002; 56:1-11.
2. Gutierrez G, Reines HD, Wulf-Gutierrez ME. Clinical review: hemorrhagic shock. *Crit Care* 2004; 8:373-81.
3. Martel MJ, MacKinnon KJ, Arsenault MY, Bartellas E, Klein MC, Lane CA, et al. Hemorrhagic shock. *J Obstet Gynaecol Can* 2002; 24:504-20; quiz 521-4.
4. Falk JL, O'Brien JF, Kerr R. Fluid resuscitation in traumatic hemorrhagic shock. *Crit Care Clin* 1992; 8:323-40.
5. Marzi I. Hemorrhagic shock: update in pathophysiology and therapy. *Acta Anaesthesiol Scand Suppl* 1997; 111:42-4.
6. Boontham P, Chandran P, Rowlands B, Eremin O. Surgical sepsis: dysregulation of immune function and therapeutic implications. *Surgeon* 2003; 1:187-206.
7. Payen D, Faivre V, Lukaszewicz AC, Losser MR. Assessment of immunological status in the critically ill. *Minerva Anesthesiol* 2000; 66:757-63.
8. Glauser MP. Pathophysiologic basis of sepsis: considerations for future strategies of intervention. *Crit Care Med* 2000; 28:S4-8.
9. Cohen J. The immunopathogenesis of sepsis. *Nature* 2002; 420:885-91.
10. Vincent JL. Microvascular endothelial dysfunction: a renewed appreciation of sepsis pathophysiology. *Crit Care* 2001; 5:S1-5.
11. Hotchkiss RS, Karl IE. The pathophysiology and treatment of sepsis. *N Engl J Med* 2003; 348:138-50.
12. Angele MK, Chaudry IH. Surgical trauma and immunosuppression: pathophysiology and potential immunomodulatory approaches. *Langenbecks Arch Surg* 2005; 390:333-41.
13. Deitch EA. Animal models of sepsis and shock: a review and lessons learned. *Shock* 1998; 9:1-11.
14. Wichterman KA, Baue AE, Chaudry IH. Sepsis and septic shock--a review of laboratory models and a proposal. *J Surg Res* 1980; 29:189-201.
15. Ertel W, Keel M, Neidhardt R, Steckholzer U, Kremer JP, Ungethuen U, et al. Inhibition of the defense system stimulating interleukin-12 interferon-gamma pathway during critical illness. *Blood* 1997; 89:1612-20.
16. Majetschak M, Flach R, Heukamp T, Jennissen V, Obertacke U, Neudeck F, et al. Regulation of whole blood tumor necrosis factor production upon endotoxin stimulation after severe blunt trauma. *J Trauma* 1997; 43:880-7.
17. Ertel W, Morrison MH, Ayala A, Dean RE, Chaudry IH. Interferon-gamma attenuates hemorrhage-induced suppression of macrophage and splenocyte functions and decreases susceptibility to sepsis. *Surgery* 1992; 111:177-87.
18. Zervos EE, Kramer AA, Salhab KF, Norman JG, Carey LC, Rosemurgy AS. Sublethal hemorrhage blunts the inflammatory cytokine response to endotoxin in a rat model. *J Trauma* 1999; 46:145-9.
19. Flohe S, Ackermann M, Reuter M, Nast-Kolb D, Schade FU. Sublethal hemorrhagic shock reduces tumor necrosis factor-alpha-producing capacity in different cell compartments. *Eur Cytokine Netw* 2000; 11:420-6.

20. Schroder J, Kahlke V, Fandrich F, Zabel P, Kremer B. Tumor necrosis factor-alpha hyporesponsiveness of rat intestinal mononuclear cells and whole portal venous blood after hemorrhagic shock. *Crit Care Med* 1998; 26:526-32.
21. Khadaroo RG, Fan J, Powers KA, Fann B, Kapus A, Rotstein OD. Impaired induction of IL-10 expression in the lung following hemorrhagic shock. *Shock* 2004; 22:333-9.
22. Ayala A, Perrin MM, Ertel W, Chaudry IH. Differential effects of hemorrhage on Kupffer cells: decreased antigen presentation despite increased inflammatory cytokine (IL-1, IL-6 and TNF) release. *Cytokine* 1992; 4:66-75.
23. Ayala A, Perrin MM, Wang P, Ertel W, Chaudry IH. Hemorrhage induces enhanced Kupffer cell cytotoxicity while decreasing peritoneal or splenic macrophage capacity. Involvement of cell-associated tumor necrosis factor and reactive nitrogen. *J Immunol* 1991; 147:4147-54.
24. Zanotti S, Kumar A. Cytokine modulation in sepsis and septic shock. *Expert Opin Investig Drugs* 2002; 11:1061-75.
25. van der Poll T, van Deventer SJ. Cytokines and anticytokines in the pathogenesis of sepsis. *Infect Dis Clin North Am* 1999; 13:413-26, ix.
26. Suffredini AF, Reda D, Banks SM, Tropea M, Agosti JM, Miller R. Effects of recombinant dimeric TNF receptor on human inflammatory responses following intravenous endotoxin administration. *J Immunol* 1995; 155:5038-45.
27. Hinshaw LB, Tekamp-Olson P, Chang AC, Lee PA, Taylor FB, Jr., Murray CK, et al. Survival of primates in LD100 septic shock following therapy with antibody to tumor necrosis factor (TNF alpha). *Circ Shock* 1990; 30:279-92.
28. Beutler B, Milsark IW, Cerami AC. Passive immunization against cachectin/tumor necrosis factor protects mice from lethal effect of endotoxin. *Science* 1985; 229:869-71.
29. Tracey KJ, Fong Y, Hesse DG, Manogue KR, Lee AT, Kuo GC, et al. Anti-cachectin/TNF monoclonal antibodies prevent septic shock during lethal bacteraemia. *Nature* 1987; 330:662-4.
30. Bahrami S, Yao YM, Leichtfried G, Redl H, Marzi I, Schlag G. Significance of TNF in hemorrhage-related hemodynamic alterations, organ injury, and mortality in rats. *Am J Physiol* 1997; 272:H2219-26.
31. Marshall JC. Such stuff as dreams are made on: mediator-directed therapy in sepsis. *Nat Rev Drug Discov* 2003; 2:391-405.
32. Zentella A, Manogue K, Cerami A. The role of cachectin/TNF and other cytokines in sepsis. *Prog Clin Biol Res* 1991; 367:9-24.
33. Vassalli P. The pathophysiology of tumor necrosis factors. *Annu Rev Immunol* 1992; 10:411-52.
34. Pfeffer K, Matsuyama T, Kundig TM, Wakeham A, Kishihara K, Shahinian A, et al. Mice deficient for the 55 kd tumor necrosis factor receptor are resistant to endotoxic shock, yet succumb to *L. monocytogenes* infection. *Cell* 1993; 73:457-67.
35. Flynn JL, Goldstein MM, Chan J, Triebold KJ, Pfeffer K, Lowenstein CJ, et al. Tumor necrosis factor-alpha is required in the protective immune response against *Mycobacterium tuberculosis* in mice. *Immunity* 1995; 2:561-72.
36. Scumpia PO, Moldawer LL. Biology of interleukin-10 and its regulatory roles in sepsis syndromes. *Crit Care Med* 2005; 33:S468-71.
37. Walley KR, Lukacs NW, Standiford TJ, Strieter RM, Kunkel SL. Balance of inflammatory cytokines related to severity and mortality of murine sepsis. *Infect Immun* 1996; 64:4733-8.

38. Echtenacher B, Freudenberg MA, Jack RS, Mannel DN. Differences in innate defense mechanisms in endotoxemia and polymicrobial septic peritonitis. *Infect Immun* 2001; 69:7271-6.
39. Latifi SQ, O'Riordan MA, Levine AD. Interleukin-10 controls the onset of irreversible septic shock. *Infect Immun* 2002; 70:4441-6.
40. Song GY, Chung CS, Chaudry IH, Ayala A. What is the role of interleukin 10 in polymicrobial sepsis: anti-inflammatory agent or immunosuppressant? *Surgery* 1999; 126:378-83.
41. Ayala A, Chung CS, Song GY, Chaudry IH. IL-10 mediation of activation-induced TH1 cell apoptosis and lymphoid dysfunction in polymicrobial sepsis. *Cytokine* 2001; 14:37-48.
42. Manley MO, O'Riordan MA, Levine AD, Latifi SQ. Interleukin 10 extends the effectiveness of standard therapy during late sepsis with serum interleukin 6 levels predicting outcome. *Shock* 2005; 23:521-6.
43. Laudanski K, Wyczechowska D. Monocyte-related immunopathologies in trauma patients. *Arch Immunol Ther Exp (Warsz)* 2005; 53:321-8.
44. Cavaillon JM, Adib-Conquy M. Monocytes/macrophages and sepsis. *Crit Care Med* 2005; 33:S506-9.
45. Munoz C, Carlet J, Fitting C, Misset B, Bleriot JP, Cavaillon JM. Dysregulation of in vitro cytokine production by monocytes during sepsis. *J Clin Invest* 1991; 88:1747-54.
46. Meldrum DR, Ayala A, Perrin MM, Ertel W, Chaudry IH. Diltiazem restores IL-2, IL-3, IL-6, and IFN-gamma synthesis and decreases host susceptibility to sepsis following hemorrhage. *J Surg Res* 1991; 51:158-64.
47. Ditschkowski M, Kreuzfelder E, Rebmann V, Ferencik S, Majetschak M, Schmid EN, et al. HLA-DR expression and soluble HLA-DR levels in septic patients after trauma. *Ann Surg* 1999; 229:246-54.
48. Pangault C, Le Tulzo Y, Tattevin P, Guilloux V, Bescher N, Drenou B. Down-modulation of granulocyte macrophage-colony stimulating factor receptor on monocytes during human septic shock. *Crit Care Med* 2006; 34:1193-201.
49. Monneret G, Finck ME, Venet F, Debard AL, Bohe J, Biennvenu J, et al. The anti-inflammatory response dominates after septic shock: association of low monocyte HLA-DR expression and high interleukin-10 concentration. *Immunol Lett* 2004; 95:193-8.
50. Muller Kobold AC, Tulleken JE, Zijlstra JG, Sluiter W, Hermans J, Kallenberg CG, et al. Leukocyte activation in sepsis; correlations with disease state and mortality. *Intensive Care Med* 2000; 26:883-92.
51. van der Bruggen T, Nijenhuis S, van Raaij E, Verhoef J, van Asbeck BS. Lipopolysaccharide-induced tumor necrosis factor alpha production by human monocytes involves the raf-1/MEK1-MEK2/ERK1-ERK2 pathway. *Infect Immun* 1999; 67:3824-9.
52. Karin M, Ben-Neriah Y. Phosphorylation meets ubiquitination: the control of NF-[kappa]B activity. *Annu Rev Immunol* 2000; 18:621-63.
53. Li N, Karin M. Signaling pathways leading to nuclear factor-kappa B activation. *Methods Enzymol* 2000; 319:273-9.
54. Senftleben U, Karin M. The IKK/NF-kappa B pathway. *Crit Care Med* 2002; 30:S18-26.
55. Hagemann C, Blank JL. The ups and downs of MEK kinase interactions. *Cell Signal* 2001; 13:863-75.

56. Abraham E, Arcaroli J, Shenkar R. Activation of extracellular signal-regulated kinases, NF-kappa B, and cyclic adenosine 5'-monophosphate response element-binding protein in lung neutrophils occurs by differing mechanisms after hemorrhage or endotoxemia. *J Immunol* 2001; 166:522-30.
57. Carter Y, Liu G, Fier A, Mendez C. Effects of tolerizing sublethal hemorrhage on p44/42 and SAPK/JNK Map-kinase activation. *Shock* 2002; 18:132-7.
58. Adib-Conquy M, Adrie C, Moine P, Asehnoune K, Fitting C, Pinsky MR, et al. NF-kappaB expression in mononuclear cells of patients with sepsis resembles that observed in lipopolysaccharide tolerance. *Am J Respir Crit Care Med* 2000; 162:1877-83.
59. Adib-Conquy M, Asehnoune K, Moine P, Cavaillon JM. Long-term-impaired expression of nuclear factor-kappa B and I kappa B alpha in peripheral blood mononuclear cells of trauma patients. *J Leukoc Biol* 2001; 70:30-8.
60. Knoferl MW, Liener UC, Perl M, Bruckner UB, Kinzl L, Gebhard F. Blunt chest trauma induces delayed splenic immunosuppression. *Shock* 2004; 22:51-6.
61. Beutler B, Rietschel ET. Innate immune sensing and its roots: the story of endotoxin. *Nat Rev Immunol* 2003; 3:169-76.
62. Banchereau J, Briere F, Caux C, Davoust J, Lebecque S, Liu YJ, et al. Immunobiology of dendritic cells. *Annu Rev Immunol* 2000; 18:767-811.
63. Pulendran B, Smith JL, Caspary G, Brasel K, Pettit D, Maraskovsky E, et al. Distinct dendritic cell subsets differentially regulate the class of immune response in vivo. *Proc Natl Acad Sci U S A* 1999; 96:1036-41.
64. Banchereau J, Steinman RM. Dendritic cells and the control of immunity. *Nature* 1998; 392:245-52.
65. Boes M, Cerny J, Massol R, Op den Brouw M, Kirchhausen T, Chen J, et al. T-cell engagement of dendritic cells rapidly rearranges MHC class II transport. *Nature* 2002; 418:983-8.
66. Guery JC, Adorini L. Dendritic cells are the most efficient in presenting endogenous naturally processed self-epitopes to class II-restricted T cells. *J Immunol* 1995; 154:536-44.
67. Steinman RM, Nussenzweig MC. Avoiding horror autotoxicus: the importance of dendritic cells in peripheral T cell tolerance. *Proc Natl Acad Sci U S A* 2002; 99:351-8.
68. Lutz MB, Schuler G. Immature, semi-mature and fully mature dendritic cells: which signals induce tolerance or immunity? *Trends Immunol* 2002; 23:445-9.
69. Morelli AE, Zahorchak AF, Larregina AT, Colvin BL, Logar AJ, Takayama T, et al. Cytokine production by mouse myeloid dendritic cells in relation to differentiation and terminal maturation induced by lipopolysaccharide or CD40 ligation. *Blood* 2001; 98:1512-23.
70. Lanzavecchia A, Sallusto F. From synapses to immunological memory: the role of sustained T cell stimulation. *Curr Opin Immunol* 2000; 12:92-8.
71. Jacob J, Baltimore D. Modelling T-cell memory by genetic marking of memory T cells in vivo. *Nature* 1999; 399:593-7.
72. Reis e Sousa C, Edwards AD, Manickasingham SP, Schulz O. Conditioning of dendritic cells by pathogen-derived stimuli. *Immunobiology* 2001; 204:595-7.
73. Galley HF, Webster NR. The immuno-inflammatory cascade. *Br J Anaesth* 1996; 77:11-6.
74. Ria F, Penna G, Adorini L. Th1 cells induce and Th2 inhibit antigen-dependent IL-12 secretion by dendritic cells. *Eur J Immunol* 1998; 28:2003-16.

75. Hotchkiss RS, Tinsley KW, Swanson PE, Grayson MH, Osborne DF, Wagner TH, et al. Depletion of dendritic cells, but not macrophages, in patients with sepsis. *J Immunol* 2002; 168:2493-500.
76. Tinsley KW, Grayson MH, Swanson PE, Drewry AM, Chang KC, Karl IE, et al. Sepsis induces apoptosis and profound depletion of splenic interdigitating and follicular dendritic cells. *J Immunol* 2003; 171:909-14.
77. Efron PA, Martins A, Minnich D, Tinsley K, Ungaro R, Bahjat FR, et al. Characterization of the systemic loss of dendritic cells in murine lymph nodes during polymicrobial sepsis. *J Immunol* 2004; 173:3035-43.
78. Chung CS. *Year Book of Intensive Care and Emergency Medicine*: Berlin, Springer-Verlag, 2000:27-40.
79. Scumpia PO, McAuliffe PF, O'Malley KA, Ungaro R, Uchida T, Matsumoto T, et al. CD11c+ dendritic cells are required for survival in murine polymicrobial sepsis. *J Immunol* 2005; 175:3282-6.
80. Flohe SB, Agrawal H, Schmitz D, Gertz M, Flohe S, Schade FU. Dendritic cells during polymicrobial sepsis rapidly mature but fail to initiate a protective Th1-type immune response. *J Leukoc Biol* 2006; 79:473-81.
81. Wen H, Hogaboam CM, Gauldie J, Kunkel SL. Severe sepsis exacerbates cell-mediated immunity in the lung due to an altered dendritic cell cytokine profile. *Am J Pathol* 2006; 168:1940-50.
82. Miyatake S, Otsuka T, Yokota T, Lee F, Arai K. Structure of the chromosomal gene for granulocyte-macrophage colony stimulating factor: comparison of the mouse and human genes. *Embo J* 1985; 4:2561-8.
83. Cousins DJ, Staynov DZ, Lee TH. Regulation of interleukin-5 and granulocyte-macrophage colony-stimulating factor expression. *Am J Respir Crit Care Med* 1994; 150:S50-3.
84. Nimer SD, Uchida H. Regulation of granulocyte-macrophage colony-stimulating factor and interleukin 3 expression. *Stem Cells* 1995; 13:324-35.
85. Arai KI, Lee F, Miyajima A, Miyatake S, Arai N, Yokota T. Cytokines: coordinators of immune and inflammatory responses. *Annu Rev Biochem* 1990; 59:783-836.
86. Paul CC, Baumann MA. Modulation of spontaneous outgrowth of Epstein-Barr virus immortalized B-cell clones by granulocyte-macrophage colony-stimulating factor and interleukin-3. *Blood* 1990; 75:54-8.
87. Hayes MP, Zoon KC. Priming of human monocytes for enhanced lipopolysaccharide responses: expression of alpha interferon, interferon regulatory factors, and tumor necrosis factor. *Infect Immun* 1993; 61:3222-7.
88. Sisson SD, Dinarello CA. Production of interleukin-1 alpha, interleukin-1 beta and tumor necrosis factor by human mononuclear cells stimulated with granulocyte-macrophage colony-stimulating factor. *Blood* 1988; 72:1368-74.
89. Saarinen-Pihkala UM, Lanning M, Perkkio M, Makiperna A, Salmi TT, Hovi L, et al. Granulocyte-macrophage colony-stimulating factor support in therapy of high-risk acute lymphoblastic leukemia in children. *Med Pediatr Oncol* 2000; 34:319-27.
90. Trigg ME, Peters C, Zimmerman MB. Administration of recombinant human granulocyte-macrophage colony-stimulating factor to children undergoing allogeneic marrow transplantation: a prospective, randomized, double-masked, placebo-controlled trial. *Pediatr Transplant* 2000; 4:123-31.

91. Bilgin K, Yaramis A, Haspolat K, Tas MA, Gunbey S, Derman O. A randomized trial of granulocyte-macrophage colony-stimulating factor in neonates with sepsis and neutropenia. *Pediatrics* 2001; 107:36-41.
92. Paine R, 3rd, Wilcoxon SE, Morris SB, Sartori C, Baleeiro CE, Matthay MA, et al. Transgenic overexpression of granulocyte macrophage-colony stimulating factor in the lung prevents hyperoxic lung injury. *Am J Pathol* 2003; 163:2397-406.
93. Malik IA, Zahid M, Haq S, Syed S, Moid I, Waheed I. Effect of subcutaneous injection of granulocyte-macrophage colony stimulating factor (GM-CSF) on healing of chronic refractory wounds. *Eur J Surg* 1998; 164:737-44.
94. Husain B, Lendemans S, Ackermann M, Wendel A, Schade FU, Flohe S. GM-CSF counteracts hemorrhage-induced suppression of cytokine-producing capacity. *Inflamm Res* 2004; 53:13-21.
95. Nierhaus A, Montag B, Timmler N, Frings DP, Gutensohn K, Jung R, et al. Reversal of immunoparalysis by recombinant human granulocyte-macrophage colony-stimulating factor in patients with severe sepsis. *Intensive Care Med* 2003; 29:646-51.
96. Williams MA, White SA, Miller JJ, Toner C, Withington S, Newland AC, et al. Granulocyte-macrophage colony-stimulating factor induces activation and restores respiratory burst activity in monocytes from septic patients. *J Infect Dis* 1998; 177:107-15.
97. Flohe S, Lendemans S, Selbach C, Waydhas C, Ackermann M, Schade FU, et al. Effect of granulocyte-macrophage colony-stimulating factor on the immune response of circulating monocytes after severe trauma. *Crit Care Med* 2003; 31:2462-9.
98. Ferguson TA, Green DR. T cells are just dying to accept grafts. *Nat Med* 1999; 5:1231-2.
99. Xu J, Lucas R, Schuchmann M, Kuhnle S, Meergans T, Barreiros AP, et al. GM-CSF restores innate, but not adaptive, immune responses in glucocorticoid-immunosuppressed human blood in vitro. *J Immunol* 2003; 171:938-47.
100. Goodall GJ, Bagley CJ, Vadas MA, Lopez AF. A model for the interaction of the GM-CSF, IL-3 and IL-5 receptors with their ligands. *Growth Factors* 1993; 8:87-97.
101. Watanabe S, Itoh T, Arai K. Roles of JAK kinase in human GM-CSF receptor signals. *Leukemia* 1997; 11 Suppl 3:76-8.
102. Sakamoto KM, Mignacca RC, Gasson JC. Signal transduction by granulocyte-macrophage colony-stimulating factor and interleukin-3 receptors. *Receptors Channels* 1994; 2:175-81.
103. de Groot RP, Coffey PJ, Koenderman L. Regulation of proliferation, differentiation and survival by the IL-3/IL-5/GM-CSF receptor family. *Cell Signal* 1998; 10:619-28.
104. Quelle FW, Sato N, Witthuhn BA, Inhorn RC, Eder M, Miyajima A, et al. JAK2 associates with the beta c chain of the receptor for granulocyte-macrophage colony-stimulating factor, and its activation requires the membrane-proximal region. *Mol Cell Biol* 1994; 14:4335-41.
105. Matsuguchi T, Zhao Y, Lilly MB, Kraft AS. The cytoplasmic domain of granulocyte-macrophage colony-stimulating factor (GM-CSF) receptor alpha subunit is essential for both GM-CSF-mediated growth and differentiation. *J Biol Chem* 1997; 272:17450-9.

106. Duronio V, Clark-Lewis I, Schrader JW. Two polypeptides identified by interleukin 3 cross-linking represent distinct components of the interleukin 3 receptor. *Exp Hematol* 1992; 20:505-11.
107. Sakamaki K, Miyajima I, Kitamura T, Miyajima A. Critical cytoplasmic domains of the common beta subunit of the human GM-CSF, IL-3 and IL-5 receptors for growth signal transduction and tyrosine phosphorylation. *Embo J* 1992; 11:3541-9.
108. Plataniias LC. The p38 mitogen-activated protein kinase pathway and its role in interferon signaling. *Pharmacol Ther* 2003; 98:129-42.
109. Plataniias LC. Map kinase signaling pathways and hematologic malignancies. *Blood* 2003; 101:4667-79.
110. Dijkers PF, van Dijk TB, de Groot RP, Raaijmakers JA, Lammers JW, Koenderman L, et al. Regulation and function of protein kinase B and MAP kinase activation by the IL-5/GM-CSF/IL-3 receptor. *Oncogene* 1999; 18:3334-42.
111. Al-Shami A, Mahanna W, Naccache PH. Granulocyte-macrophage colony-stimulating factor-activated signaling pathways in human neutrophils. Selective activation of Jak2, Stat3, and Stat5b. *J Biol Chem* 1998; 273:1058-63.
112. Satoh T, Nakafuku M, Miyajima A, Kaziro Y. Involvement of ras p21 protein in signal-transduction pathways from interleukin 2, interleukin 3, and granulocyte/macrophage colony-stimulating factor, but not from interleukin 4. *Proc Natl Acad Sci U S A* 1991; 88:3314-8.
113. Sato N, Sakamaki K, Terada N, Arai K, Miyajima A. Signal transduction by the high-affinity GM-CSF receptor: two distinct cytoplasmic regions of the common beta subunit responsible for different signaling. *Embo J* 1993; 12:4181-9.
114. Waterman WH, Sha'afi RI. Effects of granulocyte-macrophage colony-stimulating factor and tumour necrosis factor-alpha on tyrosine phosphorylation and activation of mitogen-activated protein kinases in human neutrophils. *Biochem J* 1995; 307 ( Pt 1):39-45.
115. Waterman WH, Sha'afi RI. A mitogen-activated protein kinase independent pathway involved in the phosphorylation and activation of cytosolic phospholipase A2 in human neutrophils stimulated with tumor necrosis factor-alpha. *Biochem Biophys Res Commun* 1995; 209:271-8.
116. Yuo A, Okuma E, Kitagawa S, Takaku F. Tyrosine phosphorylation of p38 but not extracellular signal-regulated kinase in normal human neutrophils stimulated by tumor necrosis factor: comparative study with granulocyte-macrophage colony-stimulating factor. *Biochem Biophys Res Commun* 1997; 235:42-6.
117. Nahas N, Molski TF, Fernandez GA, Sha'afi RI. Tyrosine phosphorylation and activation of a new mitogen-activated protein (MAP)-kinase cascade in human neutrophils stimulated with various agonists. *Biochem J* 1996; 318 ( Pt 1):247-53.
118. de Groot RP, van Dijk TB, Caldenhoven E, Coffey PJ, Raaijmakers JA, Lammers JW, et al. Activation of 12-O-tetradecanoylphorbol-13-acetate response element-and dyad symmetry element-dependent transcription by interleukin-5 is mediated by Jun N-terminal kinase/stress-activated protein kinase kinases. *J Biol Chem* 1997; 272:2319-25.
119. Terada K, Kaziro Y, Satoh T. Ras-dependent activation of c-Jun N-terminal kinase/stress-activated protein kinase in response to interleukin-3 stimulation in hematopoietic BaF3 cells. *J Biol Chem* 1997; 272:4544-8.
120. Nagata Y, Nishida E, Todokoro K. Activation of JNK signaling pathway by erythropoietin, thrombopoietin, and interleukin-3. *Blood* 1997; 89:2664-9.

121. Foltz IN, Schrader JW. Activation of the stress-activated protein kinases by multiple hematopoietic growth factors with the exception of interleukin-4. *Blood* 1997; 89:3092-6.
122. Sato S, Katagiri T, Takaki S, Kikuchi Y, Hitoshi Y, Yonehara S, et al. IL-5 receptor-mediated tyrosine phosphorylation of SH2/SH3-containing proteins and activation of Bruton's tyrosine and Janus 2 kinases. *J Exp Med* 1994; 180:2101-11.
123. Coffey PJ, Schweizer RC, Dubois GR, Maikoe T, Lammers JW, Koenderman L. Analysis of signal transduction pathways in human eosinophils activated by chemoattractants and the T-helper 2-derived cytokines interleukin-4 and interleukin-5. *Blood* 1998; 91:2547-57.
124. Corey S, Eguinoa A, Puyana-Theall K, Bolen JB, Cantley L, Mollinedo F, et al. Granulocyte macrophage-colony stimulating factor stimulates both association and activation of phosphoinositide 3OH-kinase and src-related tyrosine kinase(s) in human myeloid derived cells. *Embo J* 1993; 12:2681-90.
125. Gold MR, Duronio V, Saxena SP, Schrader JW, Aebersold R. Multiple cytokines activate phosphatidylinositol 3-kinase in hemopoietic cells. Association of the enzyme with various tyrosine-phosphorylated proteins. *J Biol Chem* 1994; 269:5403-12.
126. al-Shami A, Bourgoin SG, Naccache PH. Granulocyte-macrophage colony-stimulating factor-activated signaling pathways in human neutrophils. I. Tyrosine phosphorylation-dependent stimulation of phosphatidylinositol 3-kinase and inhibition by phorbol esters. *Blood* 1997; 89:1035-44.
127. Tilton B, Andjelkovic M, Didichenko SA, Hemmings BA, Thelen M. G-Protein-coupled receptors and Fcγ-receptors mediate activation of Akt/protein kinase B in human phagocytes. *J Biol Chem* 1997; 272:28096-101.
128. Brisette WH, Baker DA, Stam EJ, Umland JP, Griffiths RJ. GM-CSF rapidly primes mice for enhanced cytokine production in response to LPS and TNF. *Cytokine* 1995; 7:291-5.
129. Tiegs G, Barsig J, Matiba B, Uhlig S, Wendel A. Potentiation by granulocyte macrophage colony-stimulating factor of lipopolysaccharide toxicity in mice. *J Clin Invest* 1994; 93:2616-22.
130. Hoflich C, Volk HD. [Immunomodulation in sepsis]. *Chirurg* 2002; 73:1100-4.
131. Kox WJ, Volk T, Kox SN, Volk HD. Immunomodulatory therapies in sepsis. *Intensive Care Med* 2000; 26 Suppl 1:S124-8.
132. Gotzinger P, Wamser P, Barlan M, Sautner T, Jakesz R, Fugger R. Candida infection of local necrosis in severe acute pancreatitis is associated with increased mortality. *Shock* 2000; 14:320-3; discussion 323-4.
133. Torre D, Tambini R, Manfredi M, Mangani V, Livi P, Maldifassi V, et al. Circulating levels of granulocyte macrophage colony-stimulating factor in patients with the systemic inflammatory response syndrome. *J Infect* 2003; 47:296-9.
134. Perry SE, Mostafa SM, Wenstone R, McLaughlin PJ. Low plasma granulocyte-macrophage colony stimulating factor is an indicator of poor prognosis in sepsis. *Intensive Care Med* 2002; 28:981-4.
135. Bundschuh DS, Barsig J, Hartung T, Randow F, Docke WD, Volk HD, et al. Granulocyte-macrophage colony-stimulating factor and IFN-gamma restore the systemic TNF-alpha response to endotoxin in lipopolysaccharide-desensitized mice. *J Immunol* 1997; 158:2862-71.

136. Riikonen P, Saarinen UM, Maki-pernaa A, Hovi L, Komulainen A, Pihkala J, et al. Recombinant human granulocyte-macrophage colony-stimulating factor in the treatment of febrile neutropenia: a double blind placebo-controlled study in children. *Pediatr Infect Dis J* 1994; 13:197-202.
137. Devereaux S, Linch DC, Gribben JG, McMillan A, Patterson K, Goldstone AH. GM-CSF accelerates neutrophil recovery after autologous bone marrow transplantation for Hodgkin's disease. *Bone Marrow Transplant* 1989; 4:49-54.
138. Klingemann HG, Barnett MJ, Phillips GL. Use of an immunoglobulin preparation enriched for IgA to treat recurrent sinopulmonary infections in a patient with chronic GVHD. *Bone Marrow Transplant* 1990; 5:205.
139. Greenberg P, Advani R, Keating A, Gulati SC, Nimer S, Champlin R, et al. GM-CSF accelerates neutrophil recovery after autologous hematopoietic stem cell transplantation. *Bone Marrow Transplant* 1996; 18:1057-64.
140. Banerjea MC, Speer CP. The current role of colony-stimulating factors in prevention and treatment of neonatal sepsis. *Semin Neonatol* 2002; 7:335-49.
141. Wolach B, Gavrieli R, Pomeranz A. Effect of granulocyte and granulocyte macrophage colony stimulating factors (G-CSF and GM-CSF) on neonatal neutrophil functions. *Pediatr Res* 2000; 48:369-73.
142. Hubel K, Carter RA, Liles WC, Dale DC, Price TH, Bowden RA, et al. Granulocyte transfusion therapy for infections in candidates and recipients of HPC transplantation: a comparative analysis of feasibility and outcome for community donors versus related donors. *Transfusion* 2002; 42:1414-21.
143. Root RK, Dale DC. Granulocyte colony-stimulating factor and granulocyte-macrophage colony-stimulating factor: comparisons and potential for use in the treatment of infections in nonneutropenic patients. *J Infect Dis* 1999; 179 Suppl 2:S342-52.
144. Leitch IO, Kucukcelebi A, Robson MC. Inhibition of wound contraction by topical antimicrobials. *Aust N Z J Surg* 1993; 63:289-93.
145. Sparwasser T, Miethke T, Lipford G, Borschert K, Hacker H, Heeg K, et al. Bacterial DNA causes septic shock. *Nature* 1997; 386:336-7.
146. Chaudry IH, Wichterman KA, Baue AE. Effect of sepsis on tissue adenine nucleotide levels. *Surgery* 1979; 85:205-11.
147. Hubbard WJ, Choudhry M, Schwacha MG, Kerby JD, Rue LW, 3rd, Bland KI, et al. Cecal ligation and puncture. *Shock* 2005; 24 Suppl 1:52-7.
148. Lutz MB, Kukutsch N, Ogilvie AL, Rossner S, Koch F, Romani N, et al. An advanced culture method for generating large quantities of highly pure dendritic cells from mouse bone marrow. *J Immunol Methods* 1999; 223:77-92.
149. Heidenreich S, Gong JH, Schmidt A, Nain M, Gemsa D. Macrophage activation by granulocyte/macrophage colony-stimulating factor. Priming for enhanced release of tumor necrosis factor-alpha and prostaglandin E2. *J Immunol* 1989; 143:1198-205.
150. Suzuki K, Hino M, Hato F, Tatsumi N, Kitagawa S. Cytokine-specific activation of distinct mitogen-activated protein kinase subtype cascades in human neutrophils stimulated by granulocyte colony-stimulating factor, granulocyte-macrophage colony-stimulating factor, and tumor necrosis factor-alpha. *Blood* 1999; 93:341-9.
151. Trapnell BC, Whitsett JA. Gm-CSF regulates pulmonary surfactant homeostasis and alveolar macrophage-mediated innate host defense. *Annu Rev Physiol* 2002; 64:775-802.

152. Baker CC, Chaudry IH, Gaines HO, Baue AE. Evaluation of factors affecting mortality rate after sepsis in a murine cecal ligation and puncture model. *Surgery* 1983; 94:331-5.
153. Otero-Anton E, Gonzalez-Quintela A, Lopez-Soto A, Lopez-Ben S, Llovo J, Perez LF. Cecal ligation and puncture as a model of sepsis in the rat: influence of the puncture size on mortality, bacteremia, endotoxemia and tumor necrosis factor alpha levels. *Eur Surg Res* 2001; 33:77-9.
154. Lendemans S, Rani M, Selbach C, Kreuzfelder E, Schade FU, Flohe S. GM-CSF priming of human monocytes is dependent on ERK1/2 activation. *J Endotoxin Res* 2006; 12:10-20.
155. Jarrar D, Kuebler JF, Rue LW, 3rd, Matalon S, Wang P, Bland KI, et al. Alveolar macrophage activation after trauma-hemorrhage and sepsis is dependent on NF-kappaB and MAPK/ERK mechanisms. *Am J Physiol Lung Cell Mol Physiol* 2002; 283:L799-805.
156. Mendez C, Jaffray C, Wong V, Salhab KF, Kramer AA, Carey LC, et al. Involvement of p38 mitogen-activated protein kinase in the induction of tolerance to hemorrhagic and endotoxic shock. *J Surg Res* 2000; 91:165-70.
157. Suzuki T, Shimizu T, Szalay L, Choudhry MA, Rue LW, 3rd, Bland KI, et al. Androstenediol ameliorates alterations in immune cells cytokine production capacity in a two-hit model of trauma-hemorrhage and sepsis. *Cytokine* 2006; 34:76-84.
158. Zhu XH, Zellweger R, Wichmann MW, Ayala A, Chaudry IH. Effects of prolactin and metoclopramide on macrophage cytokine gene expression in late sepsis. *Cytokine* 1997; 9:437-46.
159. Ding Y, Chung CS, Newton S, Chen Y, Carlton S, Albina JE, et al. Polymicrobial sepsis induces divergent effects on splenic and peritoneal dendritic cell function in mice. *Shock* 2004; 22:137-44.
160. Andrews DM, Andoniou CE, Granucci F, Ricciardi-Castagnoli P, Degli-Esposti MA. Infection of dendritic cells by murine cytomegalovirus induces functional paralysis. *Nat Immunol* 2001; 2:1077-84.
161. O'Sullivan ST, Lederer JA, Horgan AF, Chin DH, Mannick JA, Rodrick ML. Major injury leads to predominance of the T helper-2 lymphocyte phenotype and diminished interleukin-12 production associated with decreased resistance to infection. *Ann Surg* 1995; 222:482-90; discussion 490-2.
162. Hensler T, Heidecke CD, Hecker H, Heeg K, Bartels H, Zantl N, et al. Increased susceptibility to postoperative sepsis in patients with impaired monocyte IL-12 production. *J Immunol* 1998; 161:2655-9.
163. Williams MA, Withington S, Newland AC, Kelsey SM. Monocyte anergy in septic shock is associated with a predilection to apoptosis and is reversed by granulocyte-macrophage colony-stimulating factor ex vivo. *J Infect Dis* 1998; 178:1421-33.
164. Randow F, Docke WD, Bundschuh DS, Hartung T, Wendel A, Volk HD. In vitro prevention and reversal of lipopolysaccharide desensitization by IFN-gamma, IL-12, and granulocyte-macrophage colony-stimulating factor. *J Immunol* 1997; 158:2911-8.
165. Xu J, Lucas R, Wendel A. The potential of GM-CSF to improve resistance against infections in organ transplantation. *Trends Pharmacol Sci* 2004; 25:254-8.
166. Roilides E, Holmes A, Blake C, Venzon D, Pizzo PA, Walsh TJ. Antifungal activity of elutriated human monocytes against *Aspergillus fumigatus* hyphae:

- enhancement by granulocyte-macrophage colony-stimulating factor and interferon-gamma. *J Infect Dis* 1994; 170:894-9.
167. Hartung T. Immunomodulation by colony-stimulating factors. *Rev Physiol Biochem Pharmacol* 1999; 136:1-164.
  168. Flohe S, Borgermann J, Dominguez FE, Majetschak M, Lim L, Kreuzfelder E, et al. Influence of granulocyte-macrophage colony-stimulating factor (GM-CSF) on whole blood endotoxin responsiveness following trauma, cardiopulmonary bypass, and severe sepsis. *Shock* 1999; 12:17-24.
  169. Presneill JJ, Harris T, Stewart AG, Cade JF, Wilson JW. A randomized phase II trial of granulocyte-macrophage colony-stimulating factor therapy in severe sepsis with respiratory dysfunction. *Am J Respir Crit Care Med* 2002; 166:138-43.
  170. Spagnoli GC, Juretic A, Rosso R, Van Bree J, Harder F, Heberer M. Expression of HLA-DR in granulocytes of polytraumatized patients treated with recombinant human granulocyte macrophage-colony-stimulating factor. *Hum Immunol* 1995; 43:45-50.
  171. Austin OM, Redmond HP, Watson WG, Cunney RJ, Grace PA, Bouchier-Hayes D. The beneficial effects of immunostimulation in posttraumatic sepsis. *J Surg Res* 1995; 59:446-9.
  172. Sun H, Wu X, Qian X, Qi X, Tang W, Xu J, et al. Posttraumatic expression of MHC II molecules: an experimental and clinical study. *Chin J Traumatol* 2000; 3:50-52.
  173. Randow F, Syrbe U, Meisel C, Krausch D, Zuckermann H, Platzer C, et al. Mechanism of endotoxin desensitization: involvement of interleukin 10 and transforming growth factor beta. *J Exp Med* 1995; 181:1887-92.
  174. Kampgen E, Koch F, Heufler C, Eggert A, Gill LL, Gillis S, et al. Understanding the dendritic cell lineage through a study of cytokine receptors. *J Exp Med* 1994; 179:1767-76.
  175. McLeish KR, Knall C, Ward RA, Gerwins P, Coxon PY, Klein JB, et al. Activation of mitogen-activated protein kinase cascades during priming of human neutrophils by TNF-alpha and GM-CSF. *J Leukoc Biol* 1998; 64:537-45.
  176. Carter AB, Monick MM, Hunninghake GW. Both Erk and p38 kinases are necessary for cytokine gene transcription. *Am J Respir Cell Mol Biol* 1999; 20:751-8.
  177. Liu ZG. Molecular mechanism of TNF signaling and beyond. *Cell Res* 2005; 15:24-7.
  178. Hawiger J. Innate immunity and inflammation: a transcriptional paradigm. *Immunol Res* 2001; 23:99-109.
  179. Kramer AA, Salhab KF, Shafii AE, Norman J, Carey LC, Mendez C. Induction of tolerance to hemorrhagic or endotoxic shock involves activation of NF-kappaB. *J Surg Res* 1999; 83:89-94.
  180. Baldwin AS, Jr. The NF-kappa B and I kappa B proteins: new discoveries and insights. *Annu Rev Immunol* 1996; 14:649-83.
  181. Baeuerle PA, Henkel T. Function and activation of NF-kappa B in the immune system. *Annu Rev Immunol* 1994; 12:141-79.
  182. Moine P, Shenkar R, Kaneko D, Le Tulzo Y, Abraham E. Systemic blood loss affects NF-kappa B regulatory mechanisms in the lungs. *Am J Physiol* 1997; 273:L185-92.
  183. Carter Y, Liu G, Yang J, Fier A, Mendez C. Sublethal hemorrhage induces tolerance in animals exposed to cecal ligation and puncture by altering p38,

- p44/42, and SAPK/JNK MAP kinase activation. *Surg Infect (Larchmt)* 2003; 4:17-27.
184. McKillop IH, Schmidt CM, Cahill PA, Sitzmann JV. Altered expression of mitogen-activated protein kinases in a rat model of experimental hepatocellular carcinoma. *Hepatology* 1997; 26:1484-91.
  185. Paul A, Wilson S, Belham CM, Robinson CJ, Scott PH, Gould GW, et al. Stress-activated protein kinases: activation, regulation and function. *Cell Signal* 1997; 9:403-10.
  186. Lee JC, Laydon JT, McDonnell PC, Gallagher TF, Kumar S, Green D, et al. A protein kinase involved in the regulation of inflammatory cytokine biosynthesis. *Nature* 1994; 372:739-46.
  187. Kumar S, Boehm J, Lee JC. p38 MAP kinases: key signalling molecules as therapeutic targets for inflammatory diseases. *Nat Rev Drug Discov* 2003; 2:717-26.
  188. Adams JL, Badger AM, Kumar S, Lee JC. p38 MAP kinase: molecular target for the inhibition of pro-inflammatory cytokines. *Prog Med Chem* 2001; 38:1-60.
  189. Angele MK, Nitsch S, Knoferl MW, Ayala A, Angele P, Schildberg FW, et al. Sex-specific p38 MAP kinase activation following trauma-hemorrhage: involvement of testosterone and estradiol. *Am J Physiol Endocrinol Metab* 2003; 285:E189-96.
  190. Schwacha MG, Chaudry IH, Alexander M. Regulation of macrophage IL-10 production postinjury via beta2 integrin signaling and the P38 MAP kinase pathway. *Shock* 2003; 20:529-35.
  191. Perl M, Chung CS, Ayala A. Apoptosis. *Crit Care Med* 2005; 33:S526-9.
  192. Hotchkiss RS, Tinsley KW, Swanson PE, Schmiege RE, Jr., Hui JJ, Chang KC, et al. Sepsis-induced apoptosis causes progressive profound depletion of B and CD4+ T lymphocytes in humans. *J Immunol* 2001; 166:6952-63.
  193. Chung CS, Song GY, Moldawer LL, Chaudry IH, Ayala A. Neither Fas ligand nor endotoxin is responsible for inducible peritoneal phagocyte apoptosis during sepsis/peritonitis. *J Surg Res* 2000; 91:147-53.
  194. Hotchkiss RS, Coopersmith CM, Karl IE. Prevention of lymphocyte apoptosis--a potential treatment of sepsis? *Clin Infect Dis* 2005; 41 Suppl 7:S465-9.
  195. Schleicher U, Hesse A, Bogdan C. Minute numbers of contaminant CD8+ T cells or CD11b+CD11c+ NK cells are the source of IFN-gamma in IL-12/IL-18-stimulated mouse macrophage populations. *Blood* 2005; 105:1319-28.
  196. Kamath AT, Sheasby CE, Tough DF. Dendritic cells and NK cells stimulate bystander T cell activation in response to TLR agonists through secretion of IFN-alpha beta and IFN-gamma. *J Immunol* 2005; 174:767-76.
  197. Calandra T, Baumgartner JD, Glauser MP. Anti-lipopolysaccharide and anti-tumor necrosis factor/cachectin antibodies for the treatment of gram-negative bacteremia and septic shock. *Prog Clin Biol Res* 1991; 367:141-59.
  198. Eichacker PQ, Hoffman WD, Farese A, Banks SM, Kuo GC, MacVittie TJ, et al. TNF but not IL-1 in dogs causes lethal lung injury and multiple organ dysfunction similar to human sepsis. *J Appl Physiol* 1991; 71:1979-89.
  199. Mozes T, Zijlstra FJ, Heiligers JP, Tak CJ, Ben-Efraim S, Bonta IL, et al. Sequential release of tumour necrosis factor, platelet activating factor and eicosanoids during endotoxin shock in anaesthetized pigs: protective effects of indomethacin. *Br J Pharmacol* 1991; 104:691-9.

200. Ashkenazi A, Marsters SA, Capon DJ, Chamow SM, Figari IS, Pennica D, et al. Protection against endotoxic shock by a tumor necrosis factor receptor immunoadhesin. *Proc Natl Acad Sci U S A* 1991; 88:10535-9.
201. Cohen J, Exley AR. Treatment of septic shock with antibodies to tumour necrosis factor. *Schweiz Med Wochenschr* 1993; 123:492-6.
202. Kobayashi M, Fitz L, Ryan M, Hewick RM, Clark SC, Chan S, et al. Identification and purification of natural killer cell stimulatory factor (NKSF), a cytokine with multiple biologic effects on human lymphocytes. *J Exp Med* 1989; 170:827-45.
203. Haraguchi S, Day NK, Nelson RP, Jr., Emmanuel P, Duplantier JE, Christodoulou CS, et al. Interleukin 12 deficiency associated with recurrent infections. *Proc Natl Acad Sci U S A* 1998; 95:13125-9.
204. Ozmen L, Pericin M, Hakimi J, Chizzonite RA, Wysocka M, Trinchieri G, et al. Interleukin 12, interferon gamma, and tumor necrosis factor alpha are the key cytokines of the generalized Shwartzman reaction. *J Exp Med* 1994; 180:907-15.
205. Lauw FN, Dekkers PE, te Velde AA, Speelman P, Levi M, Kurimoto M, et al. Interleukin-12 induces sustained activation of multiple host inflammatory mediator systems in chimpanzees. *J Infect Dis* 1999; 179:646-52.
206. Steinhauser ML, Hogaboam CM, Kunkel SL, Lukacs NW, Strieter RM, Standiford TJ. IL-10 is a major mediator of sepsis-induced impairment in lung antibacterial host defense. *J Immunol* 1999; 162:392-9.
207. Corinti S, Albanesi C, la Sala A, Pastore S, Girolomoni G. Regulatory activity of autocrine IL-10 on dendritic cell functions. *J Immunol* 2001; 166:4312-8.
208. Brinster C, Shevach EM. Bone marrow-derived dendritic cells reverse the anergic state of CD4+CD25+ T cells without reversing their suppressive function. *J Immunol* 2005; 175:7332-40.
209. Shortman K, Liu YJ. Mouse and human dendritic cell subtypes. *Nat Rev Immunol* 2002; 2:151-61.
210. Diao J, Winter E, Chen W, Cantin C, Cattral MS. Characterization of distinct conventional and plasmacytoid dendritic cell-committed precursors in murine bone marrow. *J Immunol* 2004; 173:1826-33.

## 7. Curriculum Vitae

**Family name:** Rani  
**Given name:** Meenakshi  
**Date of birth:** Jan. 26, 1978  
**Place of birth:** Haryana, India  
**Marriage status:** Married

### Education:

Feb, 2003-present  
Ph.D. candidate  
Department of Trauma Surgery, University of Duisburg-  
Essen, University Hospital Essen, Essen-45147, Germany.

2000-2002  
Pre-PhD course, Jawaharlal Nehru University (JNU), New  
Delhi-110067, India

1998-2000  
Master of Biotechnology, All India Institute of Medical  
Sciences (AIIMS), New Delhi-110029, India

1995-1998  
Bachelor of Science, Maharishi Dayanand University,  
Rohtak, Haryana, India

### Research experience:

Feb 2003-Till date  
Prof. Dr. Rer. Nat. FU Shade  
Department of Trauma Surgery, University Hospital Essen,  
Essen-45147, Germany.

Aug 2002-Feb 2003  
Dr. Med. Elke Cario  
Department of Gastroenterology, University Hospital  
Essen, Essen, Germany

Aug 2001 - Aug 2002  
Prof. S. K. Kar  
Centre for Biotechnology, Jawaharlal Nehru University  
(JNU), New Delhi-110067, India

Apr 1999 - Apr 2000  
Prof. S. N. Das  
Department of Biotechnology, All India Institute of  
Medical Sciences, New Delhi-110029 India.

May 2001-Jun 2001  
Prof. Dr. T. P. Singh  
Department of Biophysics, All India Institute of Medical  
Sciences, New Delhi-110029 India.

## 8. Publications

1. **Rani, Meenakshi**; Agrawal, H, Gertz, Michaela; Schade, U. F; Flohé, Stefanie B.  
Reprogramming of Dendritic cell progenitors in the bone marrow during polymicrobial sepsis.  
(Communicated to *J Immunology*).
2. **Rani, Meenakshi**; Husain, Baher; Schade, F. Ulirich; Flohé, Sascha.  
Haemorrhagic shock in mice - Intracellular signalling and immunomodulation of peritoneal macrophages' LPS response.  
*Immunobiology*, 2006; 211 (9): 711-9.
3. Lendemans S, **Rani M**, Selbach C, Kreuzfelder E, Schade FU, Flohe S.  
GM-CSF priming of human Monocytes is dependent on ERK 1/2 activation.  
*J End Res.* 2006; 12(1):10-20.
4. H. Agrawal; **M. Rani**; M. Gertz; D. Schmitz; F. U. Schade; S. B. Flohé.  
Dendritic cells develop an aberrant cytokine response during polymicrobial sepsis.  
(Communicated to *Cytokine*).
5. S. Lendemans; E. Kreuzdelder; **M. Rani**; E. Bayeeh; F. Ulrich Schade; S. B. Flohe;  
C. Waydhas; S. Flohe.  
Monocytic expression of TLR2 is decreased and B lymphocytic TLR6 expression increased in injured patients with sepsis.  
(*J Trauma.* 2006; Jul. Accepted for Publication).
6. Agarwal A, **Rani M**, Saha GK, Valarmathi TM, Bahadur S, Mohanti BK, Das SN.  
Disregulated expression of the Th2 cytokine gene in patients with intraoral squamous cell carcinoma.  
*Immunol Invest.* 2003 Feb; 32 (1-2):17-30.

7. Das SN, Agarwal A, **Rani M**, Saha GK, Mohanti BK.  
Polarization of cytokine response in patients with intraoral squamous cell carcinoma.  
*Clin. Cancer. Res.* 2001; 7 (Suppl): 3758s.

## **Abstracts and Posters in Conferences/Workshops**

1. **M. Rani**; F. U. Schade; S. Flohé.  
Priming of LPS-induced human monocytic THP-1 cells by GM-CSF.  
*Shock* 2005; 23, Supplement 2: Abstract 197, 73.
2. **M. Rani**; H. Agrawal; M. Gertz; F. U. Schade; S. B. Flohé.  
Reprogramming of dendritic cell progenitors in the bone marrow during polymicrobial sepsis.  
*Immunobiology* 2005; 210 (6-8): H.33: 435-436.
3. **Rani, Meenakshi**; Husain, Baher; Schade, F. Ulirich; Flohé, Sascha.  
Alternation of murine peritoneal macrophages' LPS response after hemorrhage stimulation by GM-CSF.  
*Immunobiology* 2004; 209 (4-6): E.50: 339.
4. S. Flohe; **M. Rani**; B. Husain; F. U. Schade.  
Alternation of murine peritoneal macrophages' LPS response after hemorrhage – stimulation by GM-CSF.  
*Shock* 2005; 23, Supplement 2: Abstract 69, 23.
5. H. Agrawal; **M. Rani**; M. Gertz; D. Schmitz; F. U. Schade; S. B. Flohé.  
Dendritic cells develop an aberrant cytokine response during polymicrobial sepsis.  
*Immunobiology* 2005; 210 (6-8): H.11: 428.
6. E. Cario; **M. Rani**; S. Sankarnarayanan; C. Kirschning; G. Gerken; D. Podolsky.  
Characterization of a novel Toll like receptor- 2 dependent pathway regulating intestinal epithelial barrier functions via protein kinase C (PKC).  
*DDW* 2003, Publishing ID: 180; Abstract ID 100656.

7. E. Baiyee; B. Nyadu; S. Flohe; **M. Rani**; S. Lendemans; E. Kreuzdelder.

Monocytic expression of TLR2 is decreased and B lymphocytic TLR6 expression increased in injured patients with sepsis.

*Immunobiology* 2004; 209 (4-6): Abstract J.22: 339.

Erklärung:

Hiermit erkläre ich, gem. §6 Abs.2, Nr.7 der Promotionsordnung der Fachbereiche 6 bis 9 zur Erlangung des Dr. rer. nat., dass ich das Arbeitsgebiet, dem das Thema „**Modulation of Monocyte, Macrophages and Dendritic Cells by GM-CSF after Hemorrhagic Shock and during Polymicrobial Sepsis**“ zuzuordnen ist, in Forschung und Lehre vertrete und den Antrag von Frau Meenakshi Rani befürworte.

Essen, den 26.06.2006

-----  
Prof. Ulrich F. Schade  
(Betreuer der Arbeit)

Erklärung:

Hiermit erkläre ich, gem. §6 Abs.2, Nr.6 der Promotionsordnung der Fachbereiche 6 bis 9 zur Erlangung des Dr. rer. nat., dass ich die vorliegende Dissertation selbstständig verfasst und mich keiner anderen als der angegebenen Hilfsmittel bedient habe.

Essen, den 26.06.2006

-----  
Meenakshi Rani  
(Doktorand)

Erklärung:

Hiermit erkläre ich, gem. §6 Abs.2, Nr.8 der Promotionsordnung der Fachbereiche 6 bis 9 zur Erlangung des Dr. rer. nat., dass ich keine anderen Promotionen bzw. Promotionsversuche in der Vergangenheit durchgeführt habe und dass diese Arbeit von keiner Fakultät abgelehnt worden ist.

Essen, den 26.06.2006

-----  
Meenakshi Rani  
(Doktorand)